



January 2019

Per- And Polyfluoroalkyl Substances In The Soil Environment: Sorption, Bioaccumulation And Biotransformation

Bosen Jin

Follow this and additional works at: <https://commons.und.edu/theses>

Recommended Citation

Jin, Bosen, "Per- And Polyfluoroalkyl Substances In The Soil Environment: Sorption, Bioaccumulation And Biotransformation" (2019). *Theses and Dissertations*. 2464.
<https://commons.und.edu/theses/2464>

This Thesis is brought to you for free and open access by the Theses, Dissertations, and Senior Projects at UND Scholarly Commons. It has been accepted for inclusion in Theses and Dissertations by an authorized administrator of UND Scholarly Commons. For more information, please contact zeinebyousif@library.und.edu.

PER- AND POLYFLUOROALKYL SUBSTANCES IN THE SOIL ENVIRONMENT:
SORPTION, BIOACCUMULATION AND BIOTRANSFORMATION

by

Bosen Jin

Bachelor of Science, Environmental Science, Wuhan University, 2016

A Thesis

Submitted to the Graduate Faculty

of the

University of North Dakota

in partial fulfillment of the requirements

for the degree of

Master of Science, Environmental Engineering

Grand Forks, North Dakota

May 2019

Copyright 2019 Bosen Jin

This thesis, submitted by Bosen Jin in partial fulfillment of the requirements for the Degree of Master of Science from the University of North Dakota, has been read by the Faculty Advisory Committee under whom the work has been done and is hereby approved.



Dr. Feng Xiao (Committee Chairperson)



Dr. Michael Mann (Committee Member)



Dr. Gautham Krishnamoorthy (Committee Member)

This thesis is being submitted by the appointed advisory committee as having met all of the requirements of the School of Graduate Studies at the University of North Dakota and is hereby approved.



Dr. Chris Nelson, Associate Dean
School of Graduate Studies

4/26/19

Date

PERMISSION

Title Per- and Polyfluoroalkyl Substances in the Soil Environment: Sorption,
Bioaccumulation and Biotransformation

Department Civil Engineering

Degree Master of Science in Environmental Engineering

In presenting this thesis in partial fulfillment of the requirements for a graduate degree from the University of North Dakota, I agree that the library of this University shall make it freely available for inspection. I further agree that permission for extensive copying for scholarly purposes may be granted by the professor who supervised my thesis work or, in his absence, by the Chairperson of the department or the dean of the School of Graduate Studies. It is understood that any copying or publication or other use of this dissertation or part thereof for financial gain shall not be allowed without my written permission. It is also understood that due recognition shall be given to me and to the University of North Dakota in any scholarly use which may be made of any material in my thesis.

Bosen Jin
5/2/2019

TABLE OF CONTENTS

LIST OF FIGURES	VIII
LIST OF TABLES	XII
ACKNOWLEDGMENTS	XIV
ABSTRACT.....	XV
CHAPTER 1: INTRODUCTION AND OVERVIEW	1
1.1. AN OVERVIEW OF PER- AND POLY-FLUOROALKYL SUBSTANCES (PFASs).....	1
1.2. SOURCES, TRANSPORT AND FATE OF PFASs	3
1.3. TOXICOLOGY AND HEALTH CONCERNS.....	6
1.4. LEGACY AND EMERGING PFASs	6
CHAPTER 2: SORPTION BEHAVIOR OF PERFLUOROOCCTANOIC ACID (PFOA) AND ITS PRECURSOR COMPOUNDS, A ZWITTERIONIC AND A CATIONIC POLY- PFAS ON FIVE SOILS	9
2.1. INTRODUCTION.....	9
2.2. EXPERIMENTAL SECTION	10
2.2.1. <i>Chemicals</i>	10
2.2.2. <i>Sorbents preparation and their characterization</i>	11
2.2.3. <i>Batch test setup</i>	13
2.2.4. <i>Instrumental analysis of PFASs and soils</i>	14
2.2.5. <i>Zeta potential measurement</i>	15

2.2.6. Determination of the monovalent cationic effect.....	16
2.2.7. QA/QC.....	16
2.3. RESULT AND DISCUSSION	18
2.3.1. QA/QC.....	18
2.3.2. Adsorption and desorption kinetics	18
2.3.2. Adsorption and desorption isotherms	20
2.3.3. Effect of soil properties on PFAS adsorption	24
2.3.5. Desorption hysteresis.....	31
2.3.6. Zeta potential (ζ) analysis.....	37
2.3.7. The effect of the monovalent cation (Na^+)	40
CHAPTER 3: BIOACCUMULATION AND BIOTRANSFORMATION OF CATIONIC AND ZWITTERIONIC POLY-PFASs BY EARTHWORMS (<i>LUMBRICUS TERRESTRIS</i>) IN SOIL.....	43
3.1. INTRODUCTION.....	43
3.2. EXPERIMENTAL SECTION.....	44
3.2.1. Chemicals.....	44
3.2.2. Soil and earthworm preparation.....	45
3.2.3. Bioaccumulation experimental setup.....	46
3.2.4. Bioconcentration experimental setup	50
3.2.5. Extraction and analysis of PFASs.....	50
3.2.6. QA/QC.....	51
3.2.7. Data analysis	52
3.3. RESULTS AND DISCUSSION	54

3.3.1. QA/QC.....	54
3.3.2. Earthworm mortality and health.....	56
3.3.3. Uptake and elimination kinetics of PFASs in earthworms	59
3.3.4. Bioaccumulation of poly-PFASs in earthworms.....	65
3.3.5. Bioconcentration of PFASs in earthworms.....	70
3.3.6. Generation of PFOA and PFOS from the precursor compounds in earthworms.....	72
CHAPTER 4: CONCLUSIONS AND RECOMMENDATIONS TO FUTURE WORK	84
REFERENCES.....	86
APPENDICES.....	96
APPENDIX A.....	96
APPENDIX B.....	102

LIST OF FIGURES

Figure 1.1. Source, transport and fate of per- and polyfluoroalkyl substances (PFASs) into the environment: the main pathways. Adapted from Ahrens and Bundschuh (2014).....	4
Figure 1.2. PFASs included in this thesis: #1, perfluorooctanoic acid (PFOA); #2, perfluorooctaneamido betaine (PFOAB); #3, perfluorooctaneamido ammonium salt (PFOAAmS); #4, perfluorooctanesulfonic acid (PFOS); #5, perfluorooctanesulfonamido betaine (PFOSB); and #6, perfluorooctanesulfonamido ammonium salt (PFOSAmS).	8
Figure 2.1. Adsorption and desorption kinetics of PFOAB on SW soil.	20
Figure 2.2. Adsorption and desorption isotherms of PFOA, PFOAB and PFOAAmS on five soils.	22
Figure 2.3. Dependence of distribution coefficient (K_d) of PFOA (0.4 μM and 10 μM) on the fraction of soil organic matter (f_{om}) and soil organic carbon (f_{oc}).	26
Figure 2.4. Dependence of distribution coefficient (K_d) of PFOA (0.4 μM and 10 μM) on the aluminum concentrations in soil.	27
Figure 2.5. Dependence of distribution coefficient (K_d) of PFOA (0.4 μM and 10 μM) on the iron concentrations in soil.	27
Figure 2.6. Dependence of distribution coefficient (K_d) of PFOA (0.4 μM and 10 μM) on the soil pore volumes.	28
Figure 2.7. Dependence of distribution coefficient (K_d) of PFOA (0.4 μM and 10 μM) on the N_2 BET surface area of soils.	28
Figure 2.8. Correlation between sorption of PFOAAmS and f_{oc} (left) or CEC (right) of soils. The K_d was calculated using the Freundlich model at four concentrations (0.001, 0.01, 0.1, and 1 $\mu\text{mol/L}$).	30
Figure 2.9. Correlation between sorption of PFOAB and f_{oc} of soils. The K_d was calculated using the Freundlich model at four concentrations (0.001, 0.01, 0.1, and 1 $\mu\text{mol/L}$).	31
Figure 2.10. The desorption hysteresis index of PFOAB at 10 μM versus the fraction of soil organic matter.	34
Figure 2.11. N_2 BET surface area of soils (raw, adsorption of PFOAB at 20 μM , and desorption of PFOAB at 20 μM).	36

Figure 2.12. Pore volume of soils (raw, adsorption of PFOAB at 20 μ M, and desorption of PFOAB at 20 μ M).....	36
Figure 2.13. Pore size distributions of soils (adsorption and desorption of PFOAB at 20 μ M)...	37
Figure 2.14. The zeta potential versus the different initial concentration of PFOAB in selected batch experiments for the UND, SW and NF soil.	39
Figure 2.15. The zeta potential versus the different initial concentration of PFOAAmS in selected batch experiments for the UND, SW and NF soil.	39
Figure 2.16. Effects of cationic concentration (Na^+) on the adsorption of PFOAB and PFOAAmS by UND soil based on the distribution coefficient (K_d).	42
Figure 3.1. Earthworm morphology. (Lee, 1985).....	49
Figure 3.2. A typical “head” part of a lumbricid earthworm. (Lee, 1985)	49
Figure 3.3. Extraction efficiency of PFAS in soil by using two extractants: pure methanol and methanol with 0.5 M HCl.	56
Figure 3.4. Extraction efficiency of PFAS in earthworm by using two extractants: pure methanol and methanol with 0.5 M HCl.....	56
Figure 3.5. Tumors in dead earthworms.	58
Figure 3.6. Uptake and elimination of four poly-PFASs in earthworm in the first bioaccumulation experiment.	60
Figure 3.7. Uptake and elimination of four poly-PFASs in earthworm in the second bioaccumulation experiment.	61
Figure 3.8. Uptake and elimination of PFOA and PFOS in earthworm in the second bioaccumulation experiment.	62
Figure 3.9. Uptake rates of six PFASs in the first and the second experiments.	63
Figure 3.10. Observed bioaccumulation factors (BAF) of four poly-PFASs.	67
Figure 3.11. Comparison between observed and kinetic BAF values in the first experiment. ...	68
Figure 3.12. Comparison between observed and kinetic BAF values in the second experiment.	69
Figure 3.13. Bioconcentration of six PFASs in water experiments.....	71
Figure 3.14. Concentration of four poly-PFASs in earthworm on Day 14.....	72

Figure 3.15. PFOA and PFOS were generated from four poly-PFASs in the first bioaccumulation experiment.....	73
Figure 3.16. PFOA and PFOS were generated from four poly-PFASs in the second bioaccumulation experiment.	74
Figure 3.17. BAF values of PFOA from bioaccumulation experiments of PFOA and its precursor compounds.	76
Figure 3.18. BAF values of PFOS from bioaccumulation experiments of PFOS and its precursor compounds.	76
Figure 3.19. Mass spectrum of an intermediate PFAS (labeled as b) in PFOAB group in earthworm.	78
Figure 3.20. Predicted biotransformation pathway of PFOAB and PFOAAmS.	79
Figure 3.21. Predicted biotransformation pathway of PFOSB and PFOSAmS.....	80
Figure 3.22. Intermediate PFASs in PFOAB group in earthworm and soil.	81
Figure 3.23. Intermediate PFASs in PFOAAmS group in earthworm and soil.....	82
Figure 3.24. Intermediate PFASs in PFOSAmS group in earthworm and soil.....	82
Figure 3.25. Intermediate PFASs in PFOSB group in earthworm and soil.	83
Figure A-1. Relationships for PFOAAmS concentrations between Group 1 and Group 2 (the equation in the figure was used to correct concentrations of PFOAAmS control group).	97
Figure A-2. Dependence of distribution coefficient (K_d) of PFOAAmS at 20 μM on the N_2 BET surface area and pore volume of soils.....	97
Figure A-3. Dependence of distribution coefficient (K_d) of PFOAB (4 μM and 15 μM) on the N_2 BET surface area of soils.	98
Figure A-4. Dependence of distribution coefficient (K_d) of PFOAB (4 μM and 15 μM) on the soil pore volumes.	99
Figure A-5. FT-IR result of raw SW soil.....	100
Figure A-6. FT-IR result of post-adsorption SW soil for PFOAAmS.....	100
Figure A-7. The desorption hysteresis index of PFOAB at 10 μM versus the fraction of soil organic matter, CEC, Iron, and Aluminum, respectively.	102

Figure B-1. Uptake fitting curves of PFOA and PFOS in the second experiment.	103
Figure B-2. Uptake fitting curves of four poly-PFASs in the first experiment.	104
Figure B-3. Uptake fitting curves of four poly-PFASs in the second experiment.....	105
Figure B-4. Elimination fitting curves of four poly-PFASs in the first experiment.	106
Figure B-5. Elimination fitting curves of four poly-PFASs in the second experiment.	107
Figure B-6. Elimination fitting curves of PFOAB and PFOSAmS in the additional experiment.	107
Figure B-7. Kinetic BAF values in the first and the second bioaccumulation experiment.	108

LIST OF TABLES

Table 2.1. Properties of soils.....	13
Table 2.2. Soil pH.....	13
Table 2.3. Results modeled by biexponential decay function	20
Table 2.4. Fitting parameters of Freundlich model for the sorption of PFOA, PFOAB and PFOAAmS onto five soils.	23
Table 2.5. Distribution coefficients (K_d) between solid phase and liquid phase	24
Table 2.6. Desorption hysteresis indices (HI).....	33
Table 2.7. N_2 BET surface area and pore volume of soils (raw, adsorption of PFOAB at 20 μ M, and desorption of PFOAB at 20 μ M).....	35
Table 2.8. Zeta potential and pH in selected batch experiments of PFOAB and PFOAAmS adsorption.....	40
Table 2.9. The distribution coefficient (K_d) of PFOAB and PFOAAmS adsorption on UND at the different concentration of sodium ion.....	42
Table 3.1. Earthworm mortality.....	57
Table 3.2. Computed values of uptake kinetic rate (k_u), elimination kinetic rate (k_e) in the uptake phase, elimination half-life ($t_{1/2}$) and kinetic bioaccumulation factor ($BAF_{kinetic}$) in the first and the second experiment for six PFASs.....	63
Table 3.3. Computed value of depuration kinetic rate (ke') in the elimination phase for four poly-PFASs.....	65
Table 3.4. BAF values of four poly-PFASs in the first, second and third experiments	66
Table 3.5. Concentration of six PFASs in earthworm on Day 14.....	71
Table 3.6. Mass information of PFOA, PFOS, PFOA precursor compounds, PFOS precursor compounds, and the intermediate poly-PFASs in earthworm	79
Table A-1. Filter adsorption study of PFOA, PFOAB and PFOAAmS	96
Table A-2. Predicted PFAS concentrations in the solid phase for adsorption (q_e^s).....	101

Table A-3. Predicted PFAS concentrations in the solid phase for desorption (q_e^d).....	101
Table B-1. Paired Samples t-Test for all six PFASs.....	102
Table B-2. Paired Samples t-Test for four poly-PFASs	102

ACKNOWLEDGMENTS

I wish to first express my utmost appreciation to my advisor Dr. Feng “Frank” Xiao for his guidance and support during my time in the master’s program at the University of North Dakota. I am also grateful to Dr. Michael Mann (Institute of Energy Studies) and Dr. Gautham Krishnamoorthy (Department of Chemical Engineering) for being my committee members and for their advice and inspiration throughout my graduate education. In addition to my committee members, I would like to thank Dr. Mikhail Golovko and Mrs. Svetlana Golovko for the sample analysis work at UND School of Medicine and Health Sciences and would also like to thank Dr. Julia Zhao for allowing me to use instruments at UND Department of Chemistry. Moreover, I could not accomplish my research without the support of the faculties and staff members of the University of North Dakota. Finally, I am deeply grateful to my parents, who encouraged and sponsored me for the master’s program.

To my mom Jing Wang and my dad Zuqiang Jin,
The great parents in the world!

ABSTRACT

Per- and polyfluoroalkyl substances (PFASs) are man-made chemicals, widely used in both industries and daily lives, such as in non-stick cookware, waterproof clothing, and painting materials. Researchers have investigated PFASs for about two decades, but most of the studies focus on perfluoroalkyl substances with very limited information available on polyfluoroalkyl substances. In this research, we investigated the sorption/desorption mechanisms perfluorooctanoic acid (PFOA) and its two cationic and zwitterionic precursor compounds, perfluorooctanesulfonamido ammonium salt (PFOSAmS) and perfluorooctaneamido betaine (PFOAB) in a group of soil. We also studied the bioaccumulation and bioconcentration of these chemicals along with perfluorooctane sulfonate (PFOS) and its cationic and zwitterionic precursor compounds, perfluorooctanesulfonamido ammonium salt (PFOSAmS) and perfluorooctanesulfonamido betaine (PFOSB), in earthworm (*Lumbricus terrestris*).

Chapter 2 of this thesis presents the sorption and desorption results of PFOA, PFOAB, and PFOAAmS in five soils. The Freundlich model was fitted to the sorption and desorption data. The value of the distribution coefficient (K_d) was computed and used to compare the adsorption and desorption of different PFAS compounds. The result showed that K_d values of PFOAB and PFOAAmS were much higher than PFOA, with the ranked order of PFOAAmS > PFOAB > PFOA. Soil properties, especially including the soil organic matter, the cation exchange capacity, and the BET surface area, were found to affect the adsorption of these

chemicals. The sorption-desorption hysteresis of the zwitterionic PFAS (PFOAB) was found in soils with a relatively low soil organic matter. The desorption hysteresis index was calculated and employed to assess the degree of hysteresis. The sorption study could help to understand and predict the fate and transport of cationic and zwitterionic poly-PFASs in the soil environment.

Chapter 3 presents the bioaccumulation and biotransformation results of all the six PFAS compounds in earthworm. Earthworms were exposed to a PFAS in a loamy soil for up to 28 days and in water for up to 21 days. The bioaccumulation factors were calculated, and the bioaccumulation factor (BAF) of PFOS was observed the highest one in all the experiments. The order of BAF values was PFOAB > PFOSB > PFOSAmS > PFOAAmS in the first bioaccumulation experiment. The results also demonstrate the generation of PFOA and PFOS from their cationic and zwitterionic precursor compounds in earthworm.

Chapter 1: Introduction and Overview

1.1. An overview of per- and poly-fluoroalkyl substances (PFASs)

Per- and polyfluoroalkyl substances (PFASs) refer to a large group of fluorinated organic compounds. It has been estimated that more than 3,000 PFASs have been on the market (Wang et al., 2017). There are several major classes of PFASs, including perfluoroalkyl acids (PFAAs), PFAA precursors, and fluoropolymers. All PFASs are man-made chemicals wherever used in the laboratory, or found in the environment (Giesy and Kannan, 2002). Those fluorinated organic chemicals have been manufactured for over 70 years. In 1938, the polytetrafluoroethylene (PTFE) was firstly discovered by Dr. Roy Plunkett and his colleagues at DuPont (Sperati et al., 1986). PTFE is a fluorinated polymer with a well-known brand name: Teflon. Since 3M produced the perfluoroalkyl carboxylates (PFCAs) using an electrochemical fluorination method (ECF) in 1947 (Prevedouros et al., 2006), more PFASs have been manufactured and widely utilized in both industries and daily lives, such as in aqueous film-forming foams (Kishi and Arai, 2008; Barzen-Hanson et al., 2017; Xiao et al., 2017), non-stick cookware (Thomas, 1998; Xiao et al., 2011), fast food packaging (Schaidler et al., 2017), and waterproof clothing (Harris et al., 2017).

Although many PFAS products have advanced industrial technologies and improved people's living standards, the impact on human health and ecological system were paid little

attention for many years, compared with chlorinated and brominated organic substances (Holmström et al., 2005). With the development of instrumental analysis, especially the growth of liquid chromatography and mass spectrometry, PFAS compounds were detected in human blood (Olsen et al., 2003), in aquatic environment (Taniyasu et al., 2003), in marine biota (Van de Vijver et al., 2003), and even in the Arctic (Butt et al., 2008). The toxicity of PFAS has also been intensively studied in the recent two decades. Guyton et al. (2009) reported that perfluorooctane sulfonate (PFOS) and perfluorooctanoic acid (PFOA) were harmful primarily on the liver cell in rodents. Lau et al. (2004, 2007) claimed that PFOA was an immune system toxicant, and was also able to affect thyroid hormone levels. In addition, PFOA and PFOS have been found to be carcinogens in animal tests (U.S. EPA, 2005), and PFOA was likely to be carcinogenic in humans (U.S. EPA, 2006). Furthermore, researchers have demonstrated that long-chain PFASs are bioaccumulative (Martin et al., 2003; Schultz et al., 2003; Martin et al., 2004). PFOA and PFOS are considered as persistent organic pollutants (POPs) in the environment (Nania et al., 2009) because the strong carbon-fluorine bond is hard to be broken under the environmental condition. The half-lives of PFOA and PFOS in the human body are 1-3.5 years and 8.67 years, respectively (Hekster et al., 2003).

PFASs have gained more attention among the environmental community and the public since 2009 (Wang et al., 2009). In recent years, U.S. EPA began to require the monitoring of PFOA and PFOS in public water systems based on the third Unregulated Contaminant Monitoring Rule (UCMR 3) published on May 2nd, 2012. In 2016, U.S. EPA provided the drinking-water advisory level for PFOA and PFOS at 0.07 ppb (Fang et al., 2018). Several studies have reported the decline in blood levels of PFAS in recent years, thanks to the reduction in PFAS production in the United States. Kato et al. (2011) reported that a sustained decline of

PFHxS and PFOS concentrations in the U.S. population from 1999 to 2008. Olsen et al. (2017) also found that PFHxS, PFOS, and PFOA concentrations displayed significant downward trends in American Red Cross blood donors from 2000 to 2015. However, PFAS contamination is still a great concern in many parts of the country. It is indubitably important to generate updated regulations and develop novel engineering treatments for PFASs.

1.2. Sources, transport and fate of PFASs

The total emissions of perfluorocarboxylates (PFCAs) in the past several decades were assessed to be 3,200 to 7,300 tonnes from both the direct and indirect sources with 3,200 to 6,900 tonnes from the direct sources (Prevedouros et al., 2006). In addition, Paul et al. (2009) described that the global historical releases of perfluorooctane sulfonyl fluoride (POSF) were appraised to be 9,600 tonnes from 1970 to 2002 with about 50% of emissions from the direct sources to air and water. Since perfluorocarboxylates and perfluorooctane sulfonyl fluoride were the significant parts of the PFAS family and were widely used all over the world, PFASs have become severe global pollutants.

PFASs and related products have been used in numerous products by various companies. Paul et al. (2009) estimated that 3M manufactured about 78% of the global POSF in 2000 from 15 plants (seven in North America, seven in Europe, six in Asia and one in South America). The indirect sources principally include degradable PFASs such as precursor compounds of PFOA and PFOS. For example, the PFAS-containing solid wastes may release degradable PFAS in landfills, which degrade to PFAAs (Lang et al., 2016; Benskin et al., 2012; Allred et al., 2015).

Many PFASs can undergo “long-range transport” (Ahrens and Bundschuh, 2014) from sources to remote locations. There are three main pathways for the transport of PFASs: a.)

atmospheric transport, b.) aquatic transport, and c.) biologic transport. It is still unclear with which pathway is the one for PFASs (Ahrens, 2011). Figure 1.1 shows the main transport pathways and fate of PFASs into the ecosystem.

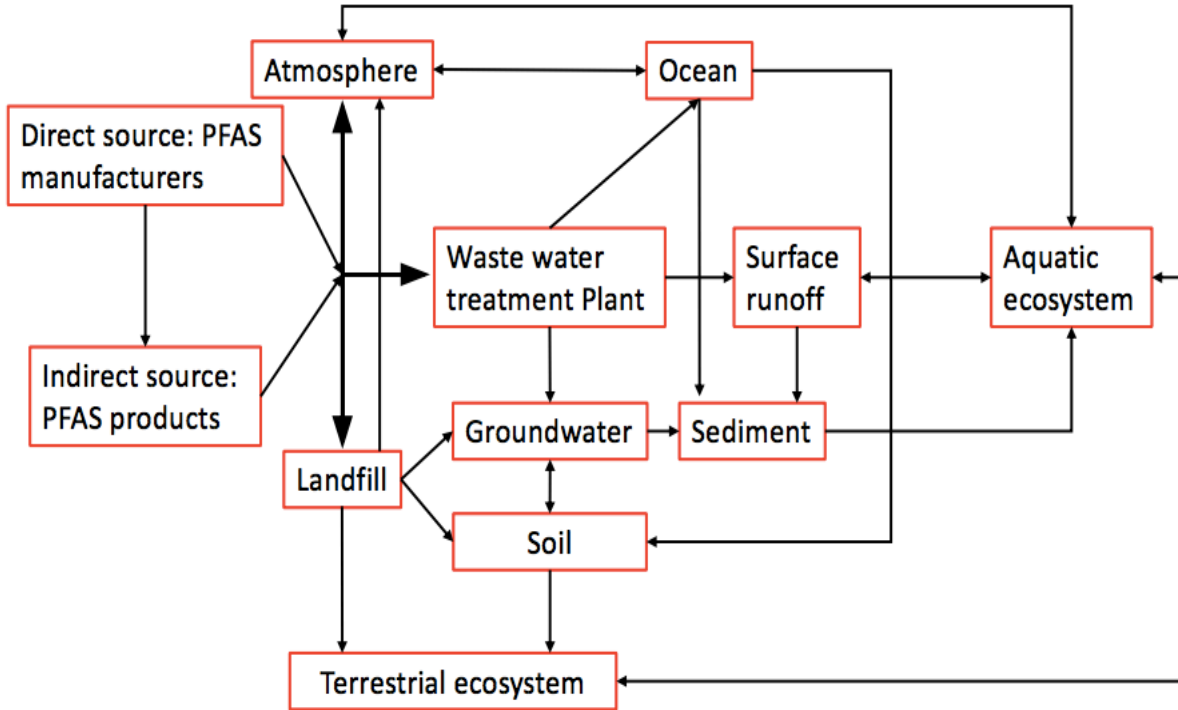


Figure 1.1. Source, transport and fate of per- and polyfluoroalkyl substances (PFASs) into the environment: the main pathways. Adapted from Ahrens and Bundschuh (2014).

Many PFASs are non-volatile, and they could not be transported through the atmosphere. However, fluorotelomer alcohols (FTOHs) were described as the typical volatile PFASs by Lei et al. (2004) with a relatively high Henry's Law constant (H). Although to estimate the volatility of an organic pollutant, the vapor pressure is usually applied to predict the possibility of its entrance into the atmosphere, it is more powerful to employ Henry's Law constant (H), calculated by the ratio of the chemical equilibrium concentrations between the gas phase and the

liquid phase (Vallero, 2014). Except for FTOHs, many short-chain PFASs ($C_{n \leq 6}$) could also evaporate into the atmosphere, but their environmental effects were slightly discussed since they cannot bioaccumulate (Conder et al., 2008). Prevedouros et al. (2006) pointed out that some PFASs could form the gas-bubble production in the ocean and be transported as marine aerosols in the atmosphere.

For the non-volatile PFASs, the most crucial transport pathway is through the aquatic environment, since many PFASs are able to dissolve in the water, especially those ionizable PFASs (Ahrens and Bundschuh, 2014). PFASs were released to waters from both direct and indirect sources. Discharged PFASs could go through the flow into groundwater (Xiao et al., 2015), surface runoff (Xiao et al., 2012a), secondary effluent (Xiao et al., 2012b), and seawater by the water cycle contaminating soil and sediment. Organisms could assimilate PFASs from both water and soil/sediment, and the chemicals start to enter the producers, such as wheat (Zhao et al., 2014), and the primary consumers, such as earthworm (Zhao et al., 2013). Through food chains and food webs, PFASs were detected in many animals, including fishes (Dassuncao et al., 2018), birds (Miller et al., 2015), and marine mammals (Gebbink et al., 2016).

From Figure 1.1, soil is one of the most critical media in the environment as the connection of PFASs in the terrestrial and aquatic ecosystems. The PFAS contamination on soil became severe in the United States due to the usage of aqueous film-forming foam (Rich et al., 2015) at over 100 military sites. Thus, it is important to understand the effect of PFAS contamination on soil environment and the transportation and fate of PFASs in the soil-water system.

1.3. Toxicology and health concerns

To study the toxicity of PFASs and the related health concerns, many toxicity tests have been conducted, including the chronic feeding tests with fishes (Jantzen et al., 2017), rodents (Li et al., 2019) and non-human primates (Butenhoff et al., 2002) and the acute toxic tests with rodents (Bhatarai et al., 2011) and earthworms (Yuan et al., 2017). The health effects of human beings (Anderson-Mahoney et al., 2008; Daly et al., 2015) and even infants (Sunderland et al., 2018; Winkens et al., 2017; Gyllenhammar et al., 2018; Papadopoulou et al., 2016) under PFAS exposures have also been investigated in several studies. There were four significant toxicological effects: hepatotoxicity (Lau et al., 2007); reproductive and developmental toxicity (Butenhoff et al., 2004); immunotoxicity (Yang et al., 2002); thyroid hormonal effects (Lau et al., 2003). Certain PFASs (e.g., PFOA) were considered as carcinogens based on animal tests (Steenland et al., 2010).

Bioaccumulation factor was an important degree to assess the environmental risk of the PFAS (Hekster et al. 2003). Researchers (Martin et al., 2003; Liu et al., 2011; Zhao et al., 2013) have performed a series of bioconcentration, bioaccumulation and bioconversion experiments for PFAAs and a few other PFASs using both aquatic organisms (e.g., rainbow trout and mussel) and terrestrial organisms (e.g., earthworm: *Lumbricus terrestris* or *Eisenia fetida*).

1.4. Legacy and emerging PFASs

Wang et al. (2017) estimated 20,000 of PFAS related peer-reviewed articles which showed that > 93% of those articles were about perfluoroalkyl substances (e.g., PFOA and PFOS) and that less than 7% were about polyfluoroalkyl substances since 2002. Those well-

studied PFASs are also called legacy PFASs, such as PFOA and PFOS. In contrast, people started to investigate emerging PFASs in the past several years with the development of high-resolution mass spectrometry (Xiao et al., 2017).

The so-called emerging PFASs have been detected in marine mammals (Gebbink et al., 2016), rivers (Gebbink et al., 2017), food (Farré and Barceló, 2013), aqueous film forming foam (Backe et al., 2013), sediments (Munoz et al., 2016) and many other media in the ecosystem. Xiao (2017) reported that 455 new PFASs were discovered from 2009 to 2017, including 45%, 29%, 17%, and 8% of which are anions, zwitterions, cations, and neutrals, respectively. Because of the charges on the nonfluorinated moiety of cationic and zwitterionic PFAS, these compounds may possess unique physicochemical properties, which would have very different effects on the environment in comparison with the legacy PFASs.

The knowledge gaps regarding behaviors of emerging PFASs in the environment need to be completed urgently. Liu et al. (2019) studied the distribution and partitioning behavior of four poly-PFASs in the water and the sediment around coastal areas. Mejia-Avendaño et al. (2016) investigated the biodegradation of several emerging poly-PFASs in soil. Xiao et al. (2018) reported that PFOA and PFOS could be generated their precursor compounds during water disinfection. Brusseau (2019) studied the influence of molecular structure on the sorption of 15 poly-PFASs to fluid-fluid interfaces.

However, studies of those emerging charged polyfluoroalkyl substances were still very limited. Thus, four precursor compounds of PFOA and PFOS (two cationic and two zwitterionic), including PFOA and PFOS were studied in this thesis to explore the sorption behaviors of those PFASs on five soils and the bioaccumulation and biotransformation behaviors

of those PFASs by earthworms in soil. Figure 1.2 displays the six PFASs used in this thesis drawn by MarvinSketch (ChemAxon, Escondido, CA), where the chemicals with a positive charge are cationic poly-PFASs (PFOAAmS and PFOSAmS), and where the chemicals with both a positive and a negative charge are zwitterionic poly-PFASs (PFOAB and PFOSB).

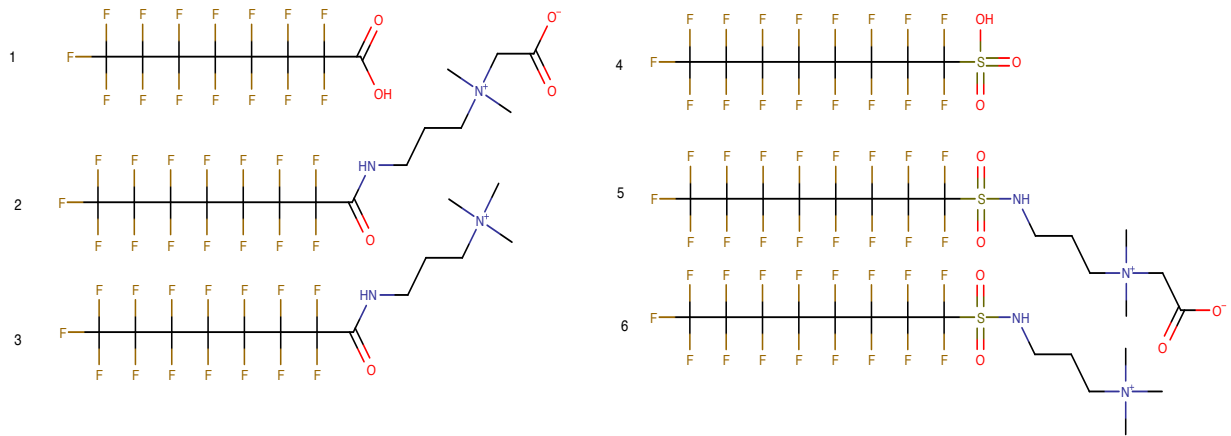


Figure 1.2. PFASs included in this thesis: #1, perfluorooctanoic acid (PFOA); #2, perfluorooctaneamido betaine (PFOAB); #3, perfluorooctaneamido ammonium salt (PFOAAmS); #4, perfluorooctanesulfonic acid (PFOS); #5, perfluorooctanesulfonamido betaine (PFOSB); and #6, perfluorooctanesulfonamido ammonium salt (PFOSAmS).

Chapter 2: Sorption behavior of perfluorooctanoic acid (PFOA) and its precursor compounds, a zwitterionic and a cationic poly-PFAS on five soils

2.1. Introduction

The sorption and desorption are a fundamental process governing the fate and transport of organic compounds where they transfer from one phase to the other phase. In many cases, a so-called “desorption hysteresis” can occur. As the most common adsorbents in the environment and the major sink of numerous organic pollutants, soil or sediment is an essential material to be tested for the sorption behavior of PFASs. Since the aquatic transport is the primary pathway for the transmission of dissolved PFASs (Ahrens and Bundschuh, 2014), it is also necessary to conduct the experiment in the water to comprehend how PFASs will be distributed between the solid phase and the liquid phase to estimate the partitioning behaviors in the environment.

Many researchers (Higgins and Luthy, 2006; Xiao et al., 2011; Pereira et al., 2018; Lee and Mabury, 2017; Li et al., 2019) have been studying the sorption behaviors of PFASs on soil or sediment. However, most of them focused on PFAAs, and the sorption study of polyfluoroalkyl substances are limited. The studies of cationic and zwitterionic poly-PFASs are much inadequate. Based on previous studies, the sorption ability of soil or sediment for PFAAs are not high. With the increase of the fluorinated carbon chain length, the adsorption behavior is enhanced (Li et al., 2019). Higgins and Luthy (2006) found that different chain length and

diverse functional groups of PFASs had effects on adsorption. Many previous researchers claimed that the soil properties are able to play an important role in sorption behaviors, especially the soil organic matter (SOM). The cationic effect for adsorption was studied as well by adjusting the concentration of sodium ions. All those parameters will be considered in the sorption studies of the emerging poly-PFASs on different soils. Moreover, the BET (Brunauer, Emmett and Teller) surface area measurement and the Fourier-transform infrared spectroscopy (FT-IR) technology were employed to understand the sorption mechanisms at the micro scale.

2.2. Experimental Section

2.2.1. Chemicals

PFOA and its two precursors, PFOAB and PFOAAmS, were studied in this research and were purchased from Fluka Chemie GmbH (Buchs, Switzerland) and Beijing FLUOBON Surfactant Institute (Beijing, China), respectively. Three stock standard solutions (1 mM) of PFOA, PFOAB and PFOAAmS were prepared in a 50/50 (v/v) solution of HPLC grade methanol (Thermo Fisher scientific, Geel, Belgium) and distilled water (UND Department of Chemical Engineering, Grand Forks, ND). Stock solutions were preserved in 125 mL HDPE wide-mouth-bottles (Thermo Fisher Scientific, Waltham, MA) and stored at 4 °C in the fridge. There was no PFASs found in both the distilled water and methanol, detected by Waters UPLC coupled with QToF-MS (Waters Corporation, Milford, MA). The buffer stock solution for sorption and desorption experiments was made by 2 mM sodium bicarbonate (Na_2CO_3) and 0.2 g L^{-1} sodium azide (NaN_3) in distilled water, and the pH of the buffer solution was ~8.2. Sodium bicarbonate and sodium azide were purchased from Fisher Scientific (Fair Lawn, NJ) and Acros

Organics (Geel, Belgium), respectively. Buffer solutions were preserved in the one-gallon Fisherbrand lightweight HDPE bottle (Thermo Fisher Scientific, Waltham, MA) at 4 °C in the fridge.

2.2.2. Sorbents preparation and their characterization

Four different soil samples (labeled as SW, CE, NF, BS) were obtained from UND Civil Engineering lab (Grand Forks, ND), and another soil sample (labeled as UND) was collected from UND campus (47°55'11.8"N, 97°04'17.4"W). Sieves (# 10, # 20, # 40, # 60 and # 80), purchased from Humboldt Mfg. Co. (Elgin, IL), were applied to each soil sample. All soil samples were then heated in the oven (Cascade TEK, Cornelius, OR) at 40 °C for 48 hours to remove moisture and stored in the desiccator (Bel-Art, Wayne, NJ) at room temperature (22.5 °C ± 0.5 °C).

Some properties of the five soils were shown in Table 2.1. The values of cation exchange capacity (CEC, meq 100 g⁻¹) and percentage of organic carbon (f_{oc}) in soil were determined by the Recommended Chemical Soil Test Procedures for the North Central Region (1988) by a commercial laboratory (Agvise Laboratories, Northwood, ND). The CEC was the summation of cations (K⁺, Ca²⁺, Mg²⁺, Na⁺, and H⁺). The cations extracted using 1 M ammonium acetate (pH 7) were determined by a Perkin 5400 Elmer ICP (Hebron, KY). The value of f_{oc} was measured by the Walkley-Black method (Qiu et al., 2010). The weight loss method (Schulte et al.; Beyer et al.) was employed to determine the percentage of soil organic matter (f_{om}). The value of f_{om} was calculated by two empirical formulas:

$$f_{om} = -0.33 + 0.973 \times f_{LOI} \text{ (Schulte et al., 1991)} \quad (2.1)$$

$$f_{om} = 0.04 + 0.66 \times f_{LOI} \text{ (Beyer et al., 1991)} \quad (2.2)$$

where f_{om} is the percentage of soil organic matter, f_{LOI} is the percentage of soil weight loss on ignition. To set up the loss on ignition test, firstly, clean and empty porcelain crucibles were heated in the oven at 375 °C for one hour and then placed in the desiccator. After cooling down at 22.5 °C ± 0.5 °C, the weight of crucible was measured and recorded. The soil sample was also heated in the oven at 105 °C for 24 hours and then placed in the desiccator to cool down at room temperature. Each soil sample (5.0 g) was weighed and put into the crucible, and subsequently heated in the oven at 360 °C for two hours. After cooling down at room temperature in the desiccator, the total weight of the sample with crucible was measured and utilized to calculate the value of f_{om} by Equation (2.1) and (2.2).

All the glassware and plastic bottles were cleaned with 0.1 mol/L hydrochloric acid (Sigma-Aldrich, St. Louis, MO) and rinsed with distilled water before measuring the concentration of iron and aluminum in the soil. According to the Hach soil extraction method for iron, 10 mL of 0.1 mol/L hydrochloric acid (Sigma-Aldrich, St. Louis, MO) was added into 5.000 g ± 0.005 g of soil sample each. The Hach DR/2000 spectrophotometer (Loveland, CO) was applied to detect the iron concentration in the extract by Method 8145. For aluminum, 10 mL of 0.5 M CuCl₂ (Sigma-Aldrich, St. Louis, MO) was added into 1.000 g ± 0.005 g of soil for extraction (Barra et al., 2001). The Hach DR/2000 spectrophotometer was applied to measure the aluminum concentration by Method 8012. In addition, soil pH, as shown in Table 2.2, was measured by the pH-meter (Denver Instruments, Bohemia, NY) in four types of solutions.

Table 2.1. Properties of soils

Soil	f_{om} , % ^a	f_{om} , % ^b	f_{oc} , % ^c	CEC, <i>meq/100g</i> ^c	Iron, <i>ppm</i>	Aluminum, <i>ppm</i>	N ₂ BET surface area, m ² g ⁻¹	Pore volume, cm ³ g ⁻¹
UND	9.86	6.95	5.3	41	10.00	29.75	13.70	0.029
SW	1.24	1.11	0.9	38.2	12.01	32.63	26.94	0.048
NF	0.29	0.46	0.1	22.5	24.01	1.92	20.49	0.039
BS	0.02	0.28	0.1	24.8	7.99	16.24	14.92	0.030
CE	1.46	1.25	1.2	41.3	10.00	26.94	22.42	0.039

- Schulte et al., 1991.
- Beyer et al., 1991.
- Agvise Laboratories.

Table 2.2. Soil pH

Soil	pH ^a	pH ^b	pH ^c	pH ^d
UND	7.8	7.33	5.54	7.93
SW	7.9	7.42	6.91	8.25
NF	7.9	7.41	6.21	8.27
BS	7.9	7.45	6.13	8.26
CE	8.0	7.25	6.77	8.06

- Soil + Adams-Evans buffer (Agvise Laboratories, Northwood, ND).
- 5.000 g ± 0.001 g Soil + 5 mL distilled water.
- 5.000 g ± 0.001 g Soil + 5 mL of 1 M CaCl₂ (Fisher Scientific, Fair Lawn, NJ).
- Soil (UND 100 mg; SW 450 mg; NF 50 mg; BS 100 mg; CE 100 mg) + buffer (2 mM Na₂CO₃ + 200 mg L⁻¹ NaN₃).

2.2.3. Batch test setup

Both adsorption/desorption kinetics and isotherms experiments were conducted by using batch tests at 22.5 °C ± 0.5 °C. PFASs and soils were added into 50-mL polypropylene centrifuge tubes (Thermo Fisher Scientific, Waltham, MA), with 50 mL buffer solution to maintain stable pH and ionic strength. Appropriate initial PFAS concentrations and soil weights were determined in preliminary tests as described in previous studies (Tang et al., 2010; Higgins and Luthy, 2006; Xiao et al., 2017; Li et al., 2018 and Pereira et al., 2018). The Glas-Col rotator (Terre Haute, IN) was used to rotate tubes at 10 revolutions per minute (rpm) for both adsorption

and desorption experiments. Also, a soil-free control group (PFAS in 50 mL of buffer solution without soil) was set up with the same PFAS concentration as the corresponding experimental sample.

Samples were taken periodically during adsorption and desorption to determine the kinetics. Based on the kinetics result, samples were allowed to equilibrate for about four days when apparent equilibrium was reached to establish isotherms. The sample tube was centrifuged by Clay Adams Dynac centrifuge (Parsippany, NJ) at 5000 rpm for 5 minutes. The supernatant was filtrated by a 0.2- μ m nylon filter (Thermo Scientific, Rockwood, TN) to a 2-mL HPLC vial (Agilent, Santa Clara, CA), and was stored in the fridge at 4 °C before analysis. The pH of the supernatant was measured by pH-meter (Denver Instruments, Bohemia, NY). Desorption experiment was conducted after adsorption. After centrifugation at 5000 rpm for 5 minutes, 25 mL of supernatant was removed and replaced with 25 mL of buffer solution to initiate desorption.

2.2.4. Instrumental analysis of PFASs and soils

Concentrations of PFASs were determined by a Waters Acquity ultrahigh-pressure liquid chromatography (UPLC) system coupled with a Waters Synapt G2-S HD QToF-MS (Waters Corporation, Milford, MA) available at Department of Biomedical Sciences, University of North Dakota. Instrumental conditions of chromatography and mass spectrometry were the same as shown in the previous study (Xiao et al., 2018). Electrospray ionization (ESI) was used in the QToF-MS. Due to the instrumental optimization, PFOA was analyzed under ESI negative mode, while PFOAB and PFOAAmS were analyzed under ESI positive mode (Table A-0). MassLynx

V4.1 software provided by Waters Corporation (Milford, MA) was utilized for instrument control, acquisition, mass analysis, and peak integrals.

Before analysis, the soil sample was dried by the Harvest Right Freeze Dryer (North Salt Lake, Utah) at 70 °F (10 hours freezing and 15 hours drying). The dried soil sample was stored in the desiccator. The pore size distribution and the BET surface area of the soil sample were measured by the N₂ porosimetry – Autosorb iQ Automated Gas Sorption Analyzer (Quantachrome Instruments, Boynton Beach, FL). At first, the soil sample was outgassed for two hours under vacuum at 293K (for the post-adsorption and the post-desorption soil sample) or 473 K (for the raw soil sample). The micro-porosities and pore size distributions of soil were measured by quenched solid density functional theory (QSDFT) from the nitrogen adsorption isotherm at 77 K (Xiao et al., 2018). The 40-point Brunauer Emmett Teller (BET) method was employed to calculate the surface area of the soil sample based on both nitrogen adsorption and desorption isotherms. Soil samples were also characterized by Fourier-transform infrared spectroscopy (FT-IR) with a Nicolet iS5 spectrometer and iD5 ATR accessory (Thermo Scientific, Madison, WI, USA). Forty scans were taken for each sample in the frequency range 4000 – 500 cm⁻¹ at 4 cm⁻¹ resolution in the transmittance mode.

2.2.5. Zeta potential measurement

Zeta potential (ζ) is the potential difference between the dispersion medium and the stationary layer of fluid attached to the dispersed particle (Lu and Gao, 2010; Gumustas et al., 2017; Pan et al., 2012). As different soil samples and PFASs with different concentrations were used in the batch test, studying the zeta potential could help understand how the concentration of

adsorbate affected the sorption process, since PFOAB and PFOAAmS are zwitterionic and cationic, respectively.

Three soils (UND, SW, and NF) with PFOAB and PFOAAmS were chosen for this experiment. After reaching the equilibrium of adsorption, the batch sample was firstly centrifuged by Clay Adams Dynac centrifuge (Parsippany, NJ) at 5000 rpm for 5 minutes. The supernatant was subsequently taken and measured by using Zetasizer Nano-Zs analyzer (Malvern Instrument Ltd., Malvern, United Kingdom) at $22.5\text{ }^{\circ}\text{C} \pm 0.5\text{ }^{\circ}\text{C}$. All samples were measured three times.

2.2.6. Determination of the monovalent cationic effect

The batch test of soil adsorption was conducted in the buffer solution ($\text{pH} = 8.16 \pm 0.02$; $[\text{Na}^+] \approx 4\text{ mM}$). However, in the environment, many soil-water systems were at high ionic strength conditions such as seawater, brackish groundwater and snowmelt containing road salts. The experiment of monovalent cationic effect (Na^+) on the soil adsorption was set up with sodium chloride, purchased from Fisher Scientific (Fair Lawn, NJ), added into the batch test to provide 0.01 M, 0.1 M and 1M of $[\text{Na}^+]$. UND soil was chosen for this experiment with $10\text{ }\mu\text{M}$ PFOAB and $20\text{ }\mu\text{M}$ PFOAAmS. The experimental procedure in this part was the same as the adsorption batch test described above.

2.2.7. QA/QC

No fluorinated material was used in this experiment, and no PFAS was found in the

distilled water and the HPLC grade Methanol. All the tubes and HPLC vials were cleaned by the distilled water and the HPLC grade Methanol to assure that there was no PFAS contamination before all experiments. Calibration standards of PFASs were used to obtain the calibration curve to calculate the PFAS concentration. Based on a signal-to-noise ratio (S/N) of 10 (Saadati et al. 2013).

The PFAS recovery test was conducted to understand the potential loss of PFASs during the batch test. When the sample reached the adsorption equilibrium and was obtained and stored in the HPLC vial, the liquid in the sample tube was carefully removed as much as it could be without the excessive loss of soil. The freeze dryer was used to remove the rest of moisture in the soil sample. The dried soil sample was extracted by the HPLC grade methanol with 0.5 M hydrochloride acid (in total 26 mL). The sample was then under the ultrasonic (Cole-Parmer, Vernon Hills, IL) for one hour at room temperature ($22.5\text{ }^{\circ}\text{C} \pm 0.5\text{ }^{\circ}\text{C}$). The supernatant was filtered by a 0.2- μm nylon filter into the HPLC vial for analysis. The recovery of PFAS in soil was calculated by mass balance using the following equation:

$$R = \frac{C_w \times V_1 + C_{s-\text{MeOH}} \times V_2 \times (m_1/m_2)}{C_i \times V_1} \times 100\% \quad (2.3)$$

where C_w is the aqueous equilibrium concentration of PFAS, μM ; C_i is the initial PFAS concentration obtained from the control group, μM ; $C_{s-\text{MeOH}}$ is the PFAS concentration in extract, μM ; V_1 is the total volume of buffer solution used in the batch test, L; V_2 is the total volume of HPLC grade Methanol used in the extraction, L; m_1 is the initial weight of sorbent, mg; m_2 is the weight of sorbent used in extraction, mg.

In case that the aqueous equilibrium concentrations of PFASs were changed during

filtration by the nylon filter, samples were taken with and without the filter used for a different range of concentrations of PFOA, PFOAB and PFOAAmS in 50 mL buffer solutions without soils to comprehend if PFASs would be adsorbed in the nylon filter (Table A-1).

2.3. Result and discussion

2.3.1. QA/QC

The recovery rates of PFOA, PFOAB, and PFOAAmS were $107.8\% \pm 3.9\%$, $106.4\% \pm 8.0\%$, and $74.6\% \pm 8.9\%$, respectively. In addition, some researchers (Lath et al., 2019; Chandramouli et al., 2015) found that during the nylon filtration, PFASs were absorbed in the filter. Lath et al. (2019) discovered that the recovery rate of PFOA using a nylon filter was only 21.2%. Chandramouli et al. (2015) stated that the nylon filter absorbed about 25% of PFOA. They also reported that some other PFASs were adsorbed significantly ($> 75\%$) on nylon filters. In this study, PFOAAmS was found to be adsorbed in the nylon filter. Nonetheless, the average adsorption rate of PFOA on the nylon filter (shown in Table A-1) was only 2%, which was neglectable. Based on the result shown in Figure A-1, the loss of PFOAAmS in nylon filter was corrected with controls.

2.3.2. Adsorption and desorption kinetics

The adsorption and desorption kinetics of PFOAB were tested on SW soil as an illustration. As shown in Figure 2.1, both adsorption and desorption processes of PFOAB on SW soil reached apparent equilibrium in approximately three days. During the first 10 or 20 hours, the soil adsorption rate (k_1) was high, while after the fast adsorption part, the rate (k_2) became

obviously much lower, compared with k_1 . This phenomenon of adsorption kinetics has been well-studied (Wu and Gschwend, 1986; Higgins and Luthy, 2006; Li et al., 2018), and was able to be expressed by the biexponential decay function,

$$F_w = F_0 + F_1 \times e^{-k_1 t} + F_2 \times e^{-k_2 t} \quad (2.4)$$

where F_w is the fraction of remaining analyte in the aqueous phase at time t ; F_0 , F_1 , and F_2 represent kinetically different fractions of analyte adsorption on the soil. The OriginPro 9.0 (Northampton, MA) was used to calculate the kinetics data with Equation (2.4). Shown in Table 2.3, k_1 was about six times higher than k_2 in adsorption kinetics. For desorption kinetics study, it showed (Table 2.3) that k_1 was almost equal to k_2 , although, in the beginning, the desorption kinetics process was assumed the same as adsorption. Nonetheless, based on the equilibrium of adsorption, the rate of desorption process should be consistently at a low level. It was better to fit the desorption kinetics result by the exponential decay function:

$$F_w = F_0 + F_1 \times e^{-k \cdot t} \quad (2.5)$$

where F_w is the fraction of remaining analyte in the aqueous phase at time t ; F_0 and F_1 represent kinetically different fractions of analyte adsorption on the soil. Although after 96 hours, it seemed that the fraction of residual analyte would still decrease, the change is less than 5%.

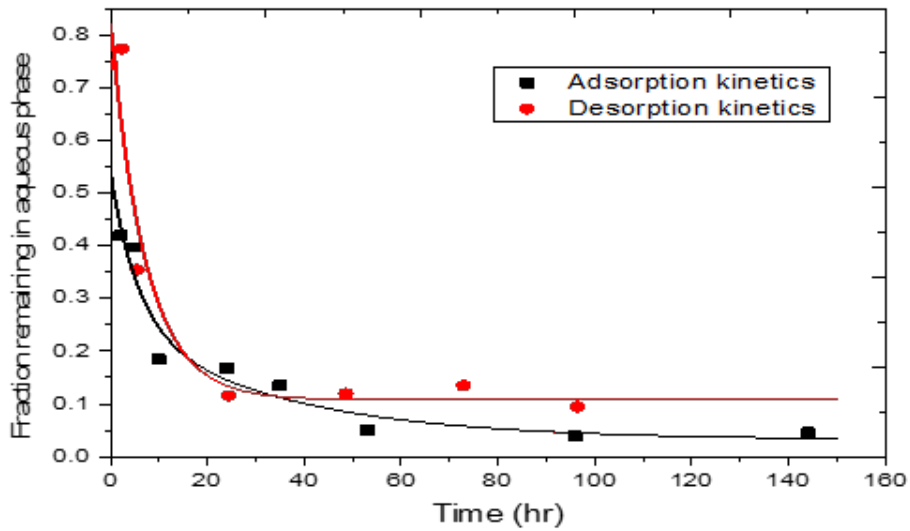


Figure 2.1. Adsorption and desorption kinetics of PFOAB on SW soil.

Table 2.3. Results modeled by biexponential decay function

Sorption type	k_1 (hr ⁻¹)	k_2 (hr ⁻¹)	R^2
Adsorption	0.180	0.029	0.87
Desorption	0.138	0.138	0.81

2.3.2. Adsorption and desorption isotherms

The Freundlich isotherm model was applied to fit the experimental data, expressed as:

$$C_s = K_F \times C_w^{1/n} \quad (2.6)$$

where C_s is the equilibrium concentration in the solid phase, $\mu\text{moles kg}^{-1}$; C_w is the aqueous equilibrium concentration, μM ; K_F and $1/n$ are constants for a given adsorbate and adsorbent at a specific temperature. The value of C_w was obtained from the sample measured by the UPLC MS/MS, while the value of C_s was calculated by the equation below:

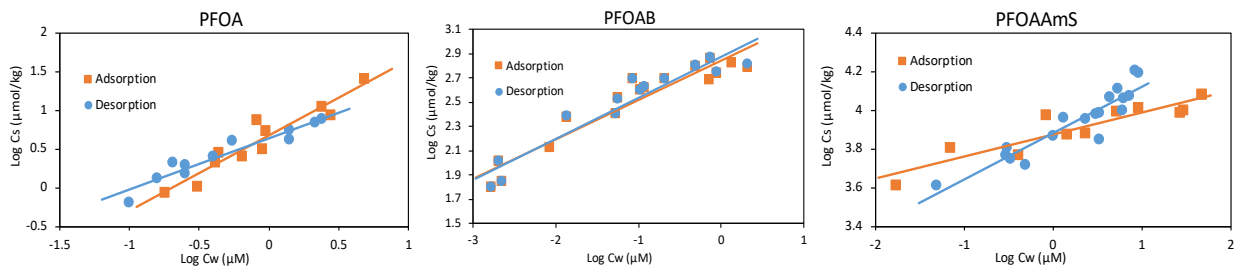
$$C_s = (C_i - C_w) \times V/m \quad (2.7)$$

where C_s is the equilibrium concentration in the solid phase, $\mu\text{moles kg}^{-1}$; C_w is the aqueous equilibrium concentration, μM ; C_i is the initial concentration obtained from the control group, μM ; V is the total volume used in the batch test, L; m is the weight of sorbent, kg. To better analyze the data, the Freundlich equation was modified as:

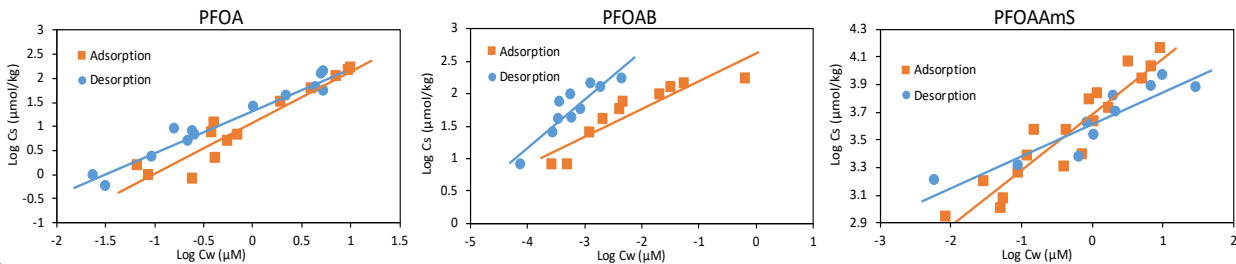
$$\log C_s = \frac{1}{n} \log C_w + \log K_F \quad (2.8)$$

to obtain a linear relationship between $\log C_s$ and $\log C_w$. The results (in the logarithmic scale) of adsorption and desorption isotherms of PFASs on five soils were shown in Figure 2.2 and Table 2.4.

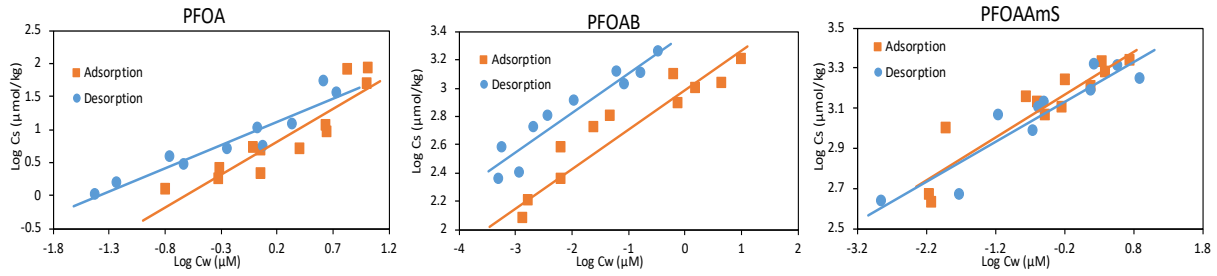
a. UND soil



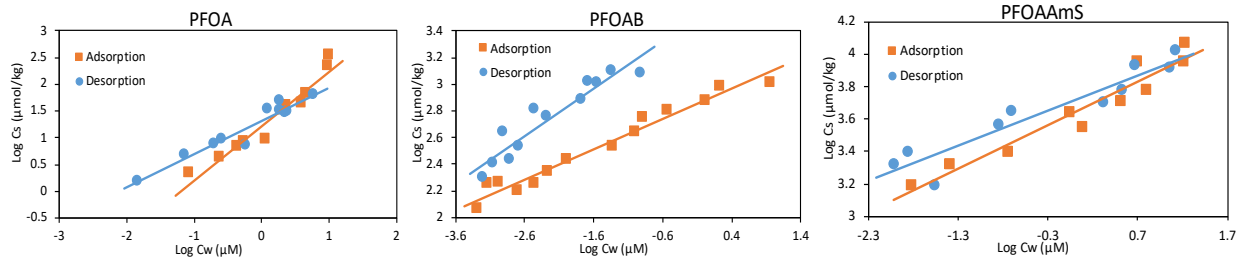
b. SW soil



c. NF soil



d. CE soil



e. BS soil

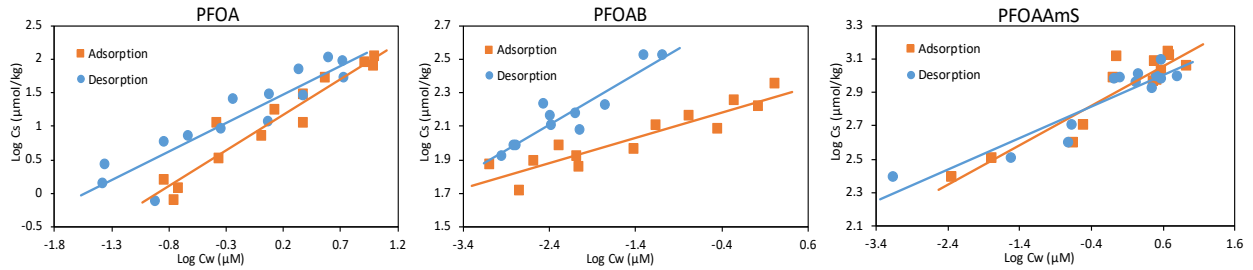


Figure 2.2. Adsorption and desorption isotherms of PFOA, PFOAB and PFOAAmS on five soils.

Table 2.4. Fitting parameters of Freundlich model for the sorption of PFOA, PFOAB and PFOAAmS onto five soils.

Soil	PFASs	Adsorption			Desorption		
		K_F	1/n	R^2	K_F	1/n	R^2
UND	PFOA	4.69	0.98	0.90	4.33	0.66	0.92
	PFOAB	693.3	0.32	0.90	756.1	0.34	0.91
	PFOAAmS	7,468	0.11	0.85	7,596	0.24	0.86
SW	PFOA	12.02	1.07	0.90	20.90	0.88	0.96
	PFOAB	414.7	0.43	0.83	27,479	0.75	0.82
	PFOAAmS	60,311	0.41	0.88	52,167	0.24	0.86
NF	PFOA	4.14	1.00	0.84	9.41	0.70	0.91
	PFOAB	973.2	0.28	0.90	2,390	0.28	0.91
	PFOAAmS	1,627	0.21	0.85	1,485	0.20	0.86
BS	PFOA	9.03	1.05	0.92	19.88	0.85	0.85
	PFOAB	175.2	0.15	0.85	686.1	0.30	0.86
	PFOAAmS	822.6	0.24	0.86	781.4	0.19	0.85
CE	PFOA	16.67	1.01	0.94	20.43	0.62	0.93
	PFOAB	746.8	0.23	0.97	3,486	0.36	0.90
	PFOAAmS	4,396	0.27	0.93	5,232	0.22	0.90

As shown in Table 2.4, the Freundlich model fitted the sorption data well with the coefficients of determination (R^2) ranging from 0.82 to 0.97. The adsorption ability of each soil on different PFASs could be roughly compared by the K_F value, and K_F values in all five soils showed a range that PFOA < PFOAB < PFOAAmS, which means that PFOAAmS has the highest affinity towards the soil. However, it might lead to biased results (Higgins and Luthy, 2006), if only K_F values were used to compare distribution coefficients between different PFASs and soils. Thus, based on the specific concentration, distribution coefficients were primarily considered for the comparison of sorption abilities among five soils, which was calculated by:

$$K_d = C_s/C_w = K_F \times C_w^{\frac{1}{n}-1} \quad (2.9)$$

where K_d is the distribution coefficient between the solid phase and liquid phase for the specific initial concentration, $L\ kg^{-1}$; all other parameters have been defined already on page 20. In this study, a low-level concentration and a high-level concentration of chemicals were selected to calculate K_d values for PFOA and PFOAB. For PFOAAmS, only 20 μM was chosen because the concentration range of PFOAAmS in five soils is different (e.g., 20 μM was the highest concentration on NF soil, while 20 μM was the lowest concentration on UND soil). From Table 2.5, it showed that the K_d value changed with the initial concentration of PFAS. When $1/n$ is greater than one, the K_d value increases with the aqueous equilibrium concentration; when $1/n$ is less than one (in most cases), the K_d value decreases with increasing aqueous equilibrium concentration.

Table 2.5. Distribution coefficients (K_d) between solid phase and liquid phase

Soil	Concentration of PFOA (μM)		Concentration of PFOAB (μM)		Concentration of PFOAAmS (μM)
	0.4	10	4	15	20
UND	6.48	3.85	48,753	1,226	32,254
SW	17.88	15.38	13,495	244	18,507
CE	3.60	7.85	20,895	233	1,022
NF	7.46	10.50	10,118	156	1,611
BS	15.28	22.01	40,969	705	4,944

2.3.3. Effect of soil properties on PFAS adsorption

Previous studies (Higgins and Luthy, 2006; Li et al., 2019; Kwadijk et al., 2013; Jeon et al., 2011) have shown that soil properties, including the fraction of soil organic matter (or soil

organic carbon), cation exchange capacity (CEC), and some minerals (e.g., iron and aluminum), have significant effects on the PFAS adsorption. Correlations among soil properties (Table 2.1) and selected distribution coefficients (K_d , Table 2.5) were studied to determine which parameter plays an important role in soil adsorption.

Figure 2.3 showed that for PFOA, when the fraction of soil organic matter or soil organic carbon increased, the K_d value increased with the coefficients of determination (R^2) from 0.78 to 0.92, if the result of UND soil was excluded, which was similar as other researchers' discoveries (Higgins and Luthy, 2006; Li et al., 2019; Kwadijk et al., 2013; Jeon et al., 2011). However, if UND soil was considered, the general trend between K_d and f_{om} (or f_{oc}) would become negative. This situation could be caused by natural organic acid (e.g., humic acid and fulvic acid), an important component of the soil organic matter, which usually have net negatively charged functional groups. PFOA in the buffer solution tends to lose a proton to be anionic. Thus, the soil organic matter and PFOA could not be easily attracted due to the electrostatic repulsion between both negative charges. Because the values of f_{om} or f_{oc} had slight or adverse effects on PFOA adsorption, other parameters (e.g., aluminum concentration, iron concentration, pore volume, and BET surface area) were supposed to be contemplated (results shown in Figure 2.4, 2.5, 2.6 & 2.7), tested by the linear regression. Positive correlations were found among the distribution coefficient value (K_d) with aluminum content (Pearson r from 0.74 to 0.87), soil pore volume (Pearson $r \sim 0.69$), and BET surface area of soil (Pearson $r \sim 0.76$). It did not show a significant correlation between K_d values and iron concentrations based on Figure 2.5.

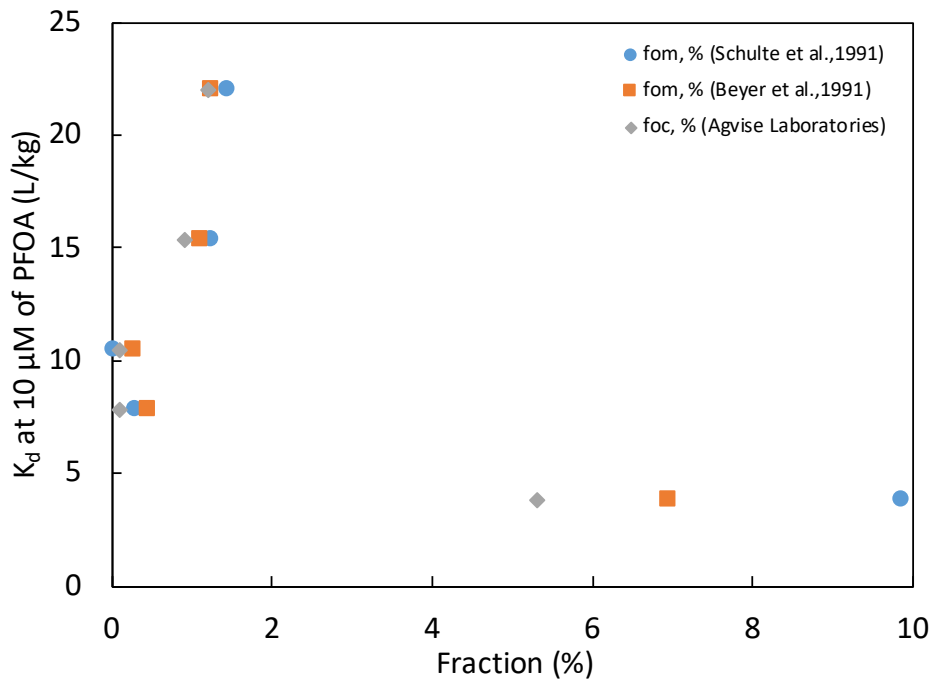
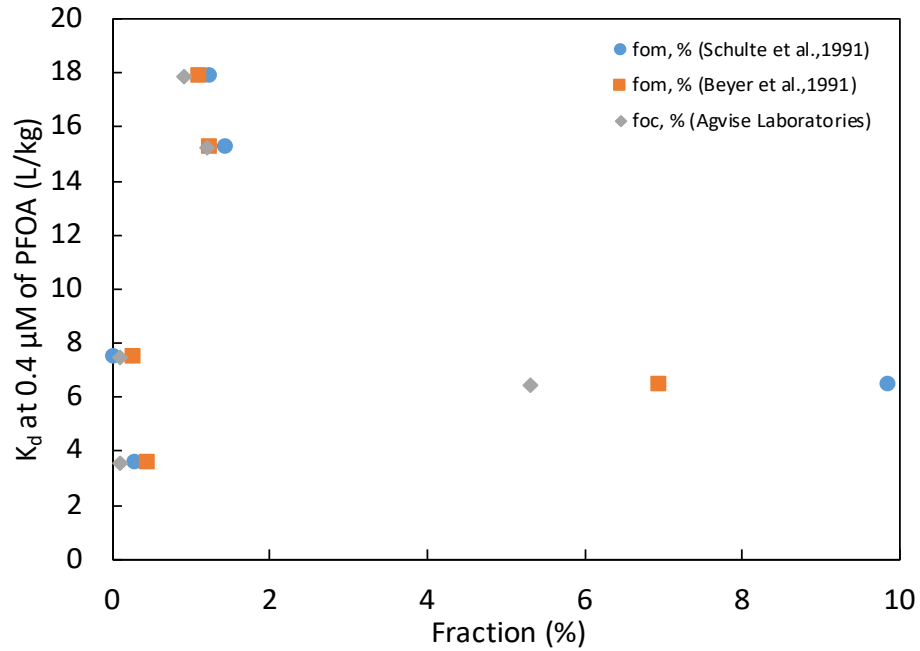


Figure 2.3. Dependence of distribution coefficient (K_d) of PFOA (0.4 μM and 10 μM) on the fraction of soil organic matter (f_{om}) and soil organic carbon (f_{oc}).

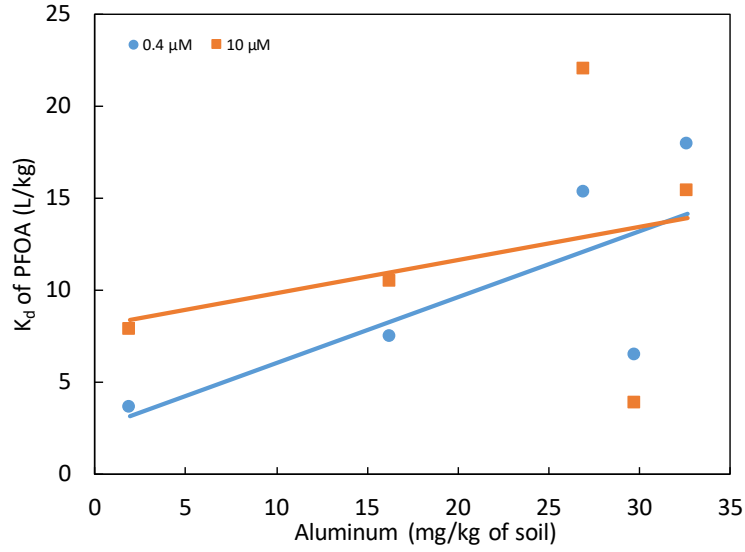


Figure 2.4. Dependence of distribution coefficient (K_d) of PFOA (0.4 μ M and 10 μ M) on the aluminum concentrations in soil.

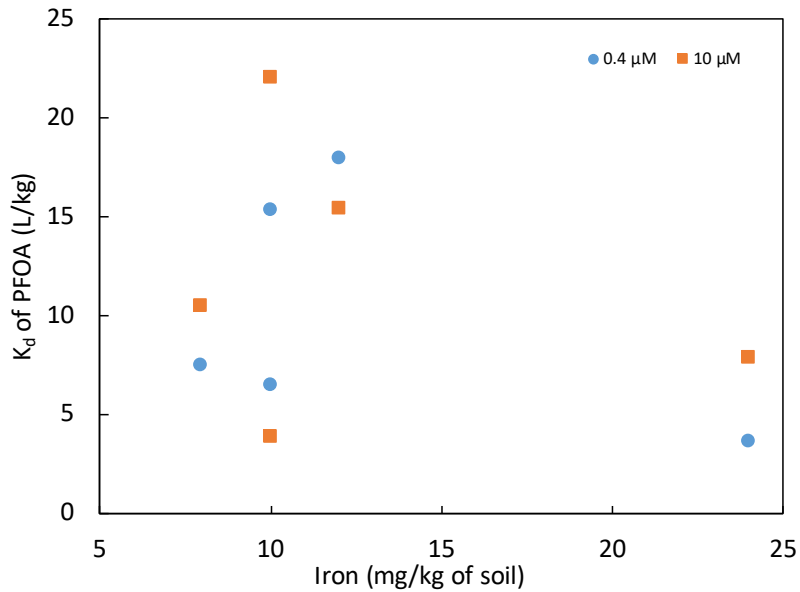


Figure 2.5. Dependence of distribution coefficient (K_d) of PFOA (0.4 μ M and 10 μ M) on the iron concentrations in soil.

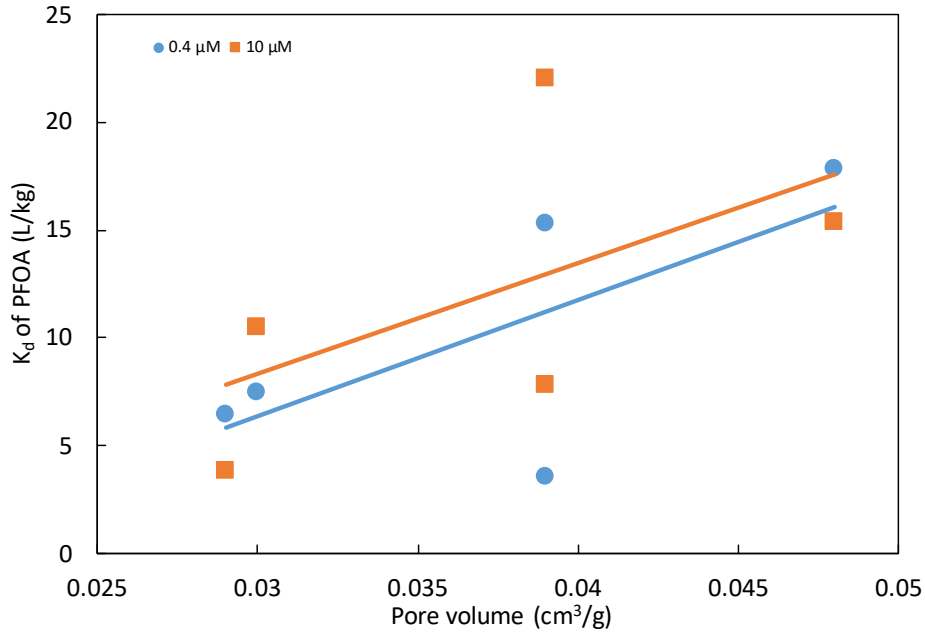


Figure 2.6. Dependence of distribution coefficient (K_d) of PFOA ($0.4 \mu\text{M}$ and $10 \mu\text{M}$) on the soil pore volumes.

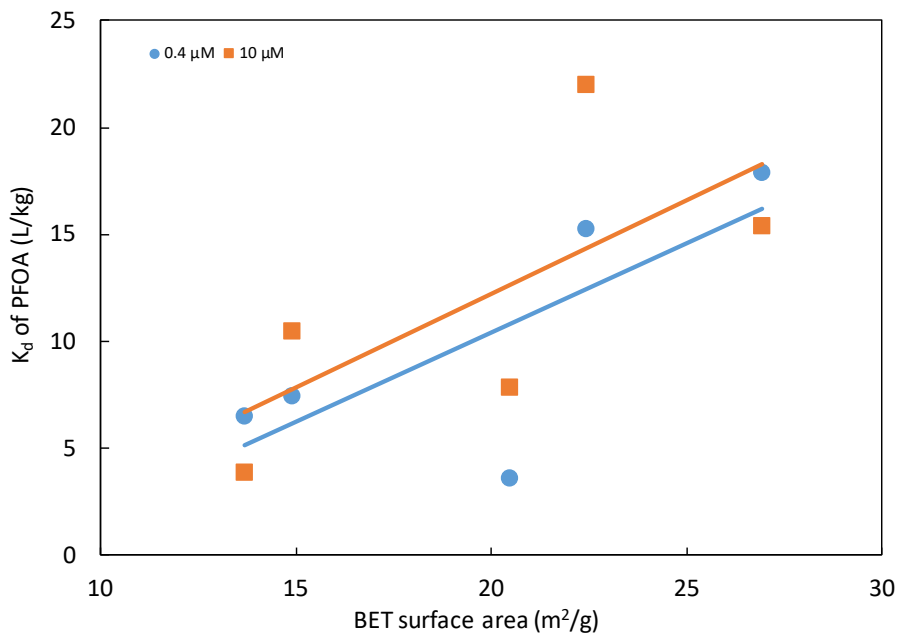


Figure 2.7. Dependence of distribution coefficient (K_d) of PFOA ($0.4 \mu\text{M}$ and $10 \mu\text{M}$) on the N_2 BET surface area of soils.

Based on all results above, the BET surface area and aluminum content were the main factors to affect the PFOA adsorption. Soils with higher BET surface area or higher aluminum concentration possess stronger sorption abilities for PFOA. An idea for PFOA removal in drinking water treatment is to use the adsorbent with the high BET surface area (e.g., activated carbon). In addition, due to the adsorption of aluminum, alum was supposed to remove PFOA during the enhanced coagulation in drinking water treatment, which was confirmed by Xiao et al. (2013).

In this study, we observed a high positive correlation ($r = 0.89\text{--}0.99$) between the sorption of PFOA_{AmS} (cationic) and f_{oc} of soils at relatively low concentrations (Figure 2.8). At high concentrations, a moderate to strong correlation ($r = 0.48\text{--}0.72$) between $K_{d,PFOA_{AmS}}$ and the CEC of soils was also observed (Figure 2.8). The results suggest that partition in SOM and cation exchange are important sorption mechanisms for this cationic PFAS. On the other hand, no significant correlation was found between the sorption of PFOAB (zwitterionic) and f_{oc} or CEC (Figure 2.9). In addition, the result (Figure A-2, A-3, and A-4) displayed that the BET surface area and the pore volume of soil did not have an apparent effect on the adsorption of PFOAB and PFOA_{AmS}.

The present results showed that the correlations between the mineral concentrations and the adsorption behaviors for three PFASs (based on K_d values) were not significant. The FT-IR method was employed to study further if the adsorption behavior was affected by the minerals (e.g., Fe and Al) by analyzing whether new coordination bonds could be generated between the metal ions and the coordination atoms (e.g., F and O) during the adsorption process. However, no new peak was discovered in the FT-IR results of SW soil (raw and post-adsorption soil for PFOA_{AmS}, shown in Figure A-5 and A-6, respectively). In summary, the effects of minerals on

PFAS adsorption were insignificant in the present experiment.

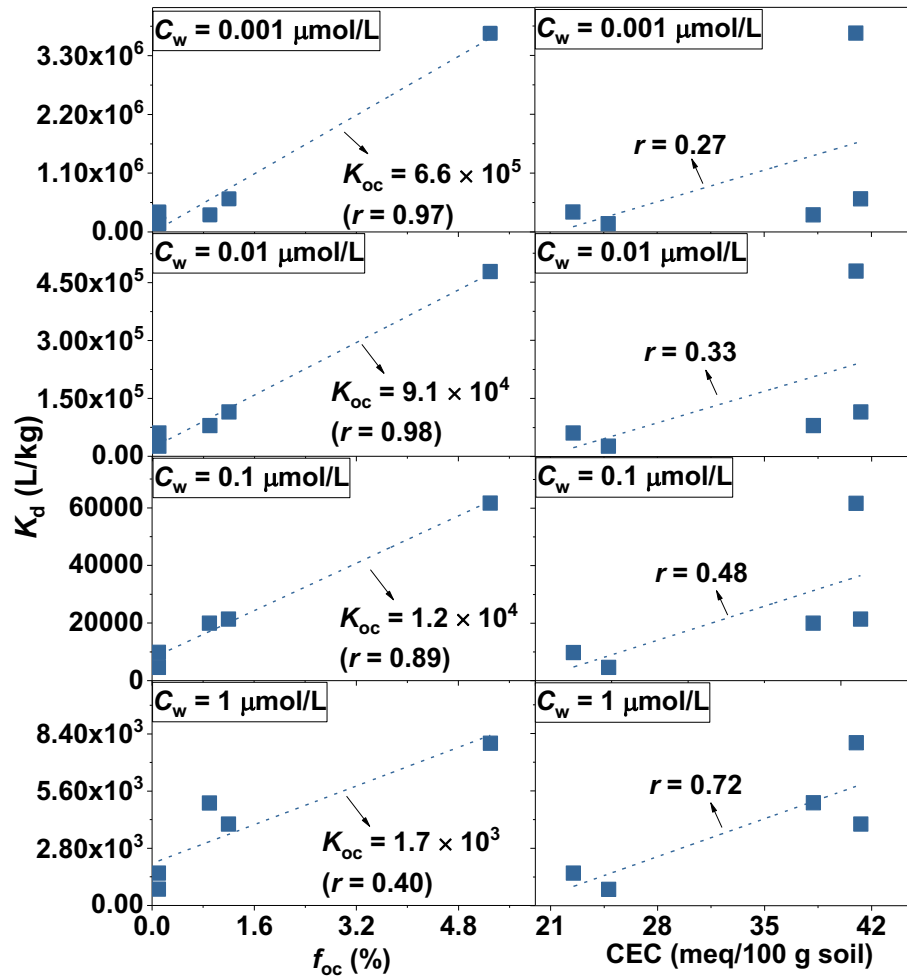


Figure 2.8. Correlation between sorption of PFOAAMS and f_{oc} (left) or CEC (right) of soils. The K_d was calculated using the Freundlich model at four concentrations (0.001, 0.01, 0.1, and 1 $\mu\text{mol/L}$).

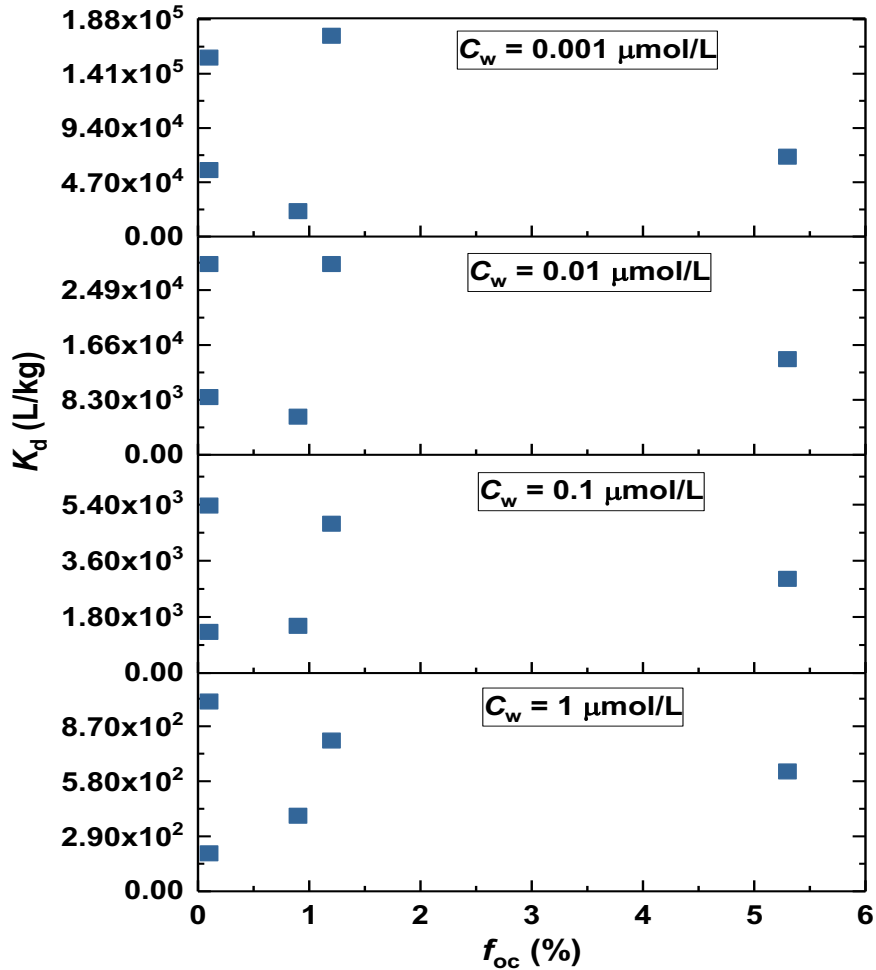


Figure 2.9. Correlation between sorption of PFOAB and foc of soils. The K_d was calculated using the Freundlich model at four concentrations (0.001, 0.01, 0.1, and 1 $\mu\text{mol/L}$).

2.3.5. Desorption hysteresis

The desorption hysteresis was found in Figure 2.2, where gaps between adsorption and desorption isotherms were apparently shown in PFOAB on SW, NF, BS and CE soil, and PFOA on all five soils at low concentration. Desorption on soil could help the chemicals (e.g., PFOA and PFOA_{MS}) desorb from the solid phase and return to the liquid phase where bacteria could degrade chemicals. However, if desorption hysteresis happened, chemicals might stay in the solid phase and maintain for a long time without degradation by bacteria, which might become

so-called “aged chemicals.” In this case, the removal of the PFAS with desorption hysteresis in soil or sediment would be hard during the environmental remediation. However, the aged chemical, due to the desorption hysteresis, would not always stay in the soil or sediment, and they could have another pathway to enter into human beings’ bodies through the food chains and food webs. The bioaccumulation study of those PFASs in the earthworm showed how PFASs passed through the soil system to the organism, which will be discussed in Chapter 3.

The Hysteresis Index (HI) was used to determine the quantitation of desorption hysteresis for PFOA, PFOAB, and PFOAAmS, and to study the significance of desorption hysteresis. The Hysteresis Index equation (Huang et al., 1998; Huang and Weber, 1997) was expressed as:

$$HI = \frac{q_e^d - q_e^s}{q_e^s} \Big| T, C_e \quad (2.10)$$

where q_e^s and q_e^d ($\mu\text{moles kg}^{-1}$) are predicted equilibrium concentrations of PFASs in solid phase for the adsorption and desorption experiments, respectively. They were calculated by Equation (2.6) & (2.7) at four different initial concentrations ($C_i = 0.01, 0.1, 1, \text{ and } 10 \mu\text{M}$); T stipulates conditions of constant temperature ($22.5 \text{ }^\circ\text{C} \pm 0.5 \text{ }^\circ\text{C}$); C_e was the residual equilibrium concentration in liquid phase. According to the calculation results of q_e^s and q_e^d (Table A-2 and Table A-3), hysteresis indices were shown in Table 2.6 for PFOA, PFOAB, and PFOAAmS on five soils, respectively. Based on Equation (2.10), if the value of q_e^d was lower than the value of q_e^s , the value of HI will be a negative number, which means the desorption hysteresis was not shown. For PFOAAmS, negative HI values were obtained from UND, SW, NF and BS groups. In addition, although each HI value of PFOAAmS on CE soil was larger than zero, it was so close to zero, especially at the high concentration ($10 \mu\text{M}$). Thus, PFOAAmS was thought with no desorption hysteresis. For PFOA, the desorption hysteresis was not significant ($HI < 0$) on all

five soils at the high concentration (10 μM), while at the low concentration, the desorption hysteresis was shown on all five soils. Since the consistency of HI values of PFOA was not displayed, it was unable to conclude that the desorption hysteresis was obviously exit for PFOA on five soils. For PFOAB, except UND soil, the desorption hysteresis was apparently shown in the other four soils based on both the HI value in Table 2.6 and Figure 2.2.

In summary, no significant desorption hysteresis was found for all three PFASs on UND soil with the highest level of SOM among the studied soils. For PFOA, the desorption hysteresis was not substantial due to the low HI value at high concentrations. Hysteresis was not significant for PFOAAmS on all five soils.

Table 2.6. Desorption hysteresis indices (HI)

PFAS		UND	SW	NF	BS	CE
PFOA (μM)	0.01	3.0301	3.1710	8.0488	4.5300	6.3847
	0.1	0.9289	1.6930	3.5351	2.4892	2.0084
	1	-0.0768	0.7388	1.2729	1.2016	0.2256
	10	-0.5581	0.1226	0.1392	0.3891	-0.5007
PFOAB (μM)	0.01	-0.0054	14.1798	1.4637	0.9627	1.5652
	0.1	0.0415	30.7152	1.4598	1.7724	2.4604
	1	0.0906	65.2624	1.4558	2.9161	3.6679
	10	0.1420	137.4417	1.4519	4.5316	5.2968
PFOAAmS (μM)	0.01	-0.4410	0.8923	-0.0443	0.1959	0.4983
	0.1	-0.2460	0.2794	-0.0660	0.0658	0.3354
	1	0.0171	-0.1350	-0.0873	-0.0501	0.1902
	10	0.3721	-0.4152	-0.1081	-0.1534	0.0607

The value of the desorption hysteresis versus soil properties was studied to explore the

important factors affecting the degree of hysteresis. Researchers (Huang and Weber, 1997) reported that the higher the soil organic matter was, the more apparent the desorption hysteresis would be. However, in this study (Figure 2.10), the fraction of soil organic matter did not correlate well with the desorption hysteresis. Also, there was no strong correlation (Figure A-7) between the desorption hysteresis and other soil properties (f_{oc} , CEC, iron, and aluminum).

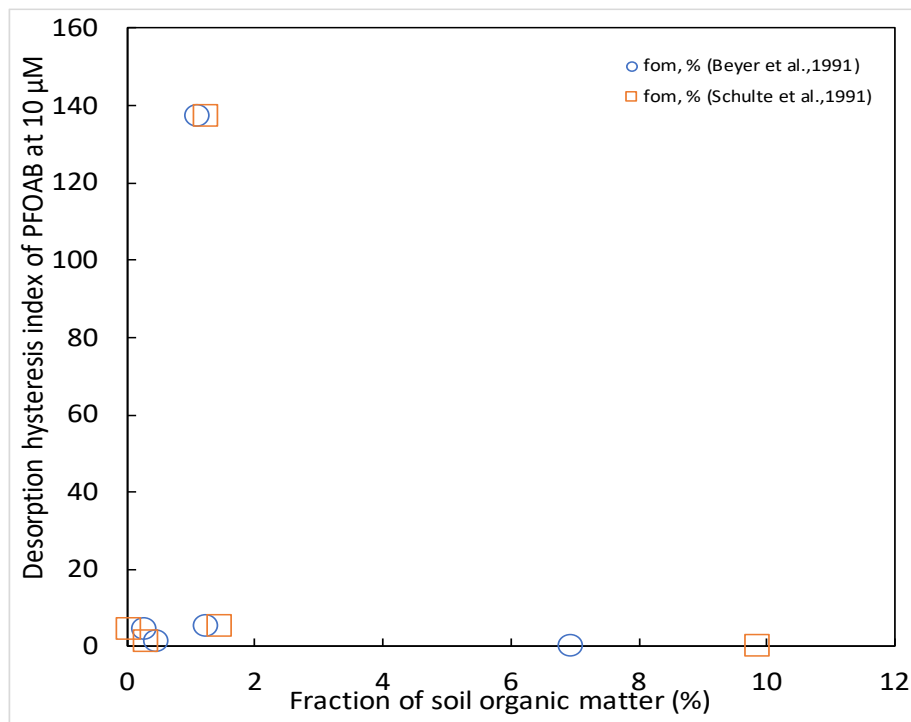


Figure 2.10. The desorption hysteresis index of PFOAB at 10 µM versus the fraction of soil organic matter.

In addition, studying the pore volume of three soils and their pore size distributions (Table 2.7, Figure 2.12 and Figure 2.13) can help to comprehend the desorption hysteresis at the micro- or the meso-level. In Figure 2.12, the pore volume of the SW soil and the NF soil

decreased after desorption, while this value of the UND soil increased. From Table 2.7, although the pore volume of the UND soil only increased $0.001 \text{ cm}^3 \text{ g}^{-1}$ after desorption, it displayed that chemicals escaped from the pore of the UND soil particle, or that at least, there were no more chemicals adsorbed during the desorption, which thoroughly explained why the UND soil did not show a significant desorption hysteresis for PFOAB. Figure 2.13 was an effective supplement for the principle of desorption hysteresis. From Figure 2.13, the half pore width of the SW soil and the NF soil exhibited a larger value after adsorption than desorption, which could support the desorption hysteresis on the SW and the NF soil that chemicals still moved to the soil from the liquid phase and occupied more pore volumes.

Table 2.7. N₂ BET surface area and pore volume of soils (raw, adsorption of PFOAB at 20 μM , and desorption of PFOAB at 20 μM)

Soil	BET surface area ($\text{m}^2 \text{ g}^{-1}$)			Pore volume ($\text{cm}^3 \text{ g}^{-1}$)		
	Raw soil	Post-adsorption soil	Post-desorption soil	Raw soil	Post-adsorption soil	Post-desorption soil
UND	13.70	7.87	6.60	0.029	0.020	0.021
SW	26.94	15.44	9.51	0.048	0.038	0.032
NF	20.49	12.22	9.99	0.039	0.033	0.027
BS	14.92	N/A	N/A	0.030	N/A	N/A
CE	22.42	N/A	N/A	0.039	N/A	N/A

N/A: Not available.

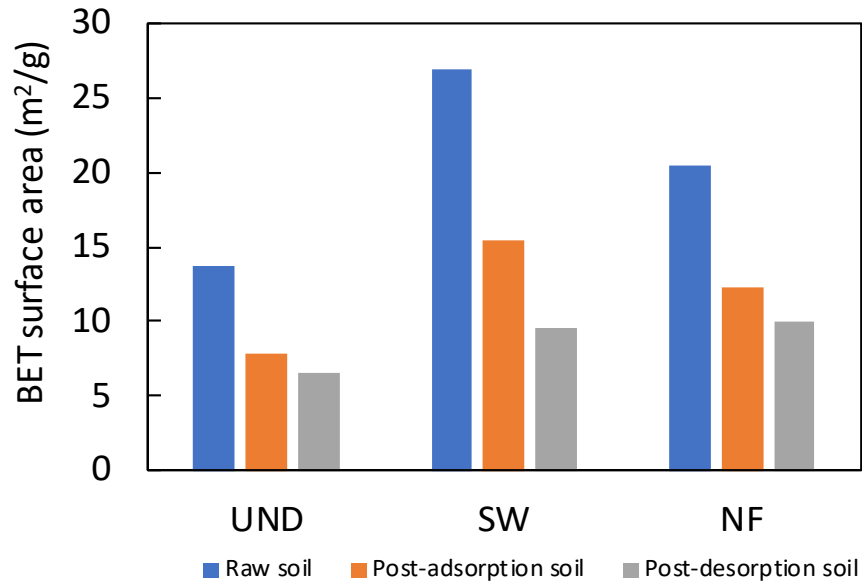


Figure 2.11. N₂ BET surface area of soils (raw, adsorption of PFOAB at 20 μM, and desorption of PFOAB at 20 μM).

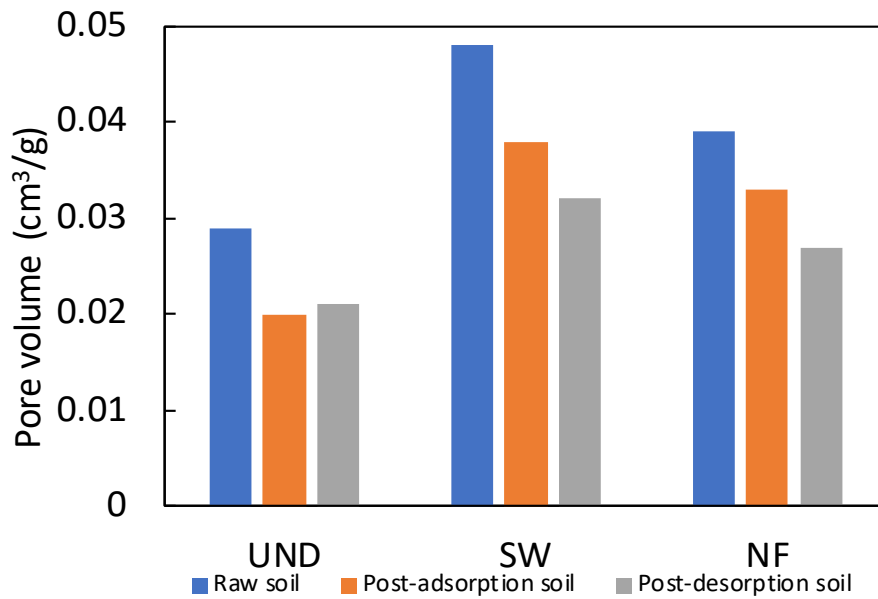


Figure 2.12. Pore volume of soils (raw, adsorption of PFOAB at 20 μM, and desorption of PFOAB at 20 μM).

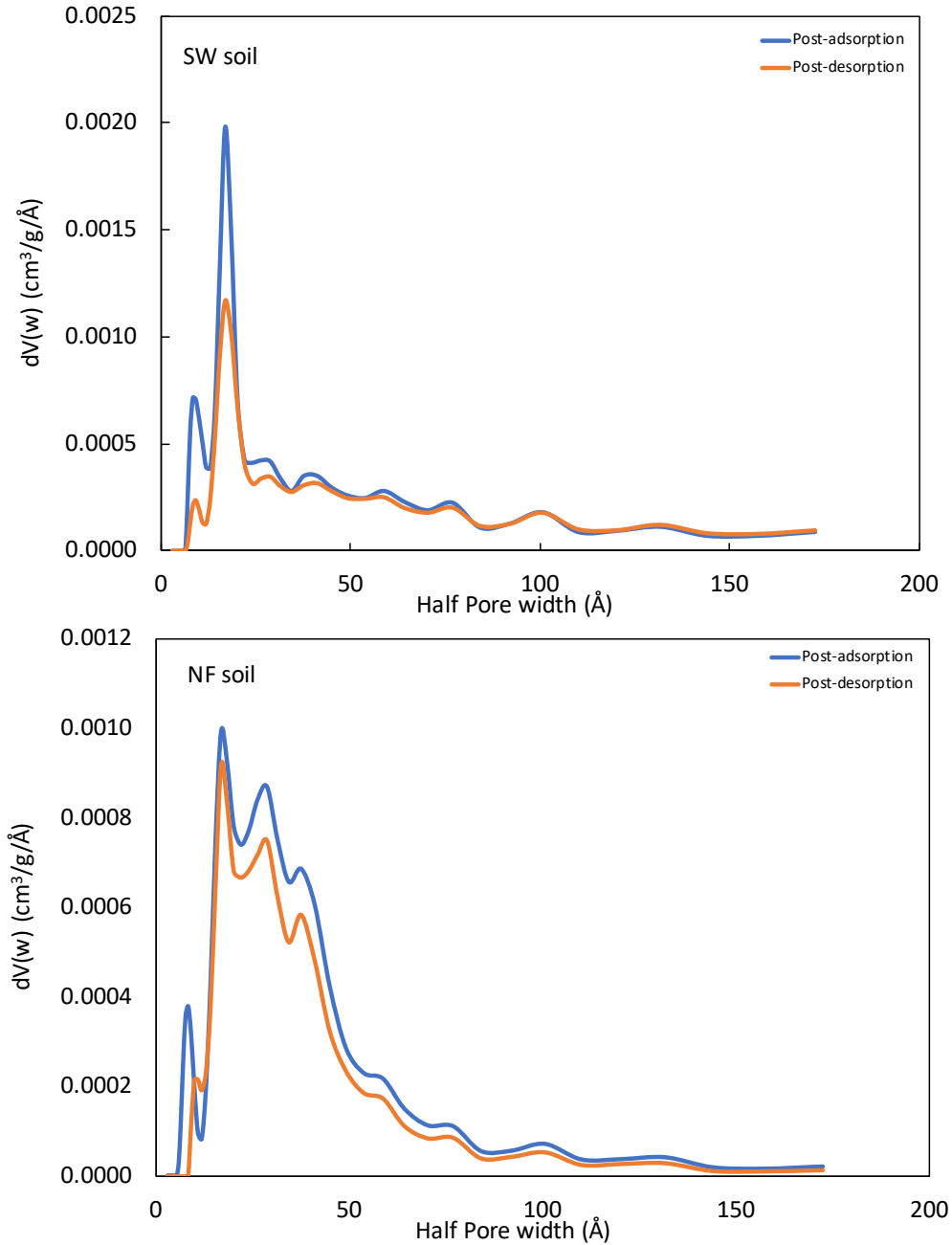


Figure 2.13. Pore size distributions of soils (adsorption and desorption of PFOAB at 20 μM).

2.3.6. Zeta potential (ζ) analysis

Figures 2.20 and 2.21 showed that when the initial concentrations of PFASs increased, the relevant ζ -potential increased as well on three soils (SW, UND, NF). Since both PFOAB and

PFOAAmS have a positive charge each, the higher concentrations of PFASs were, the more positive charges would be attracted on soil colloids in the liquid phase so that ζ -potential values became less negative. Previous studies (Gao and Chorover, 2012; Vane and Zang, 1997; Li et al., 2016; Bae et al., 2013; Kirby and Hasselbrink, 2004) presented that there were three main factors to affect the ζ -potential, ionic strength, pH and soil properties (including soil organic matter and minerals). In this research, buffer solution ($\text{pH} = 8.16 \pm 0.02$; $[\text{Na}^+] \approx 4 \text{ mM}$) was used to maintain stable pH and ionic strength. However, in the result of PFOAB on SW soil, pH had the largest standard deviation of 0.3 (considered as a type I error), which caused that there was a weak linear correlation between ζ -potential values and the initial concentrations.

In addition, from both Figures 2.14 and 2.15, the zeta potential of almost each UND batch sample displayed a higher value than other two soils, which could support the result of adsorption isotherms that the UND soil possessed the highest distribution coefficient (K_d) of both PFOAB and PFOAAmS. The reason could be because the UND soil contains more negative charges to help the soil particle adsorb more chemicals with positive charges. Moreover, PFOAAmS and PFOAB were cationic and zwitterionic, respectively. Due to the effect of the negative charge in PFOAB, the zeta potential of soil particles after adsorption of PFOAB was changed to a less degree than that in the case of PFOAAmS (Table 2.8).

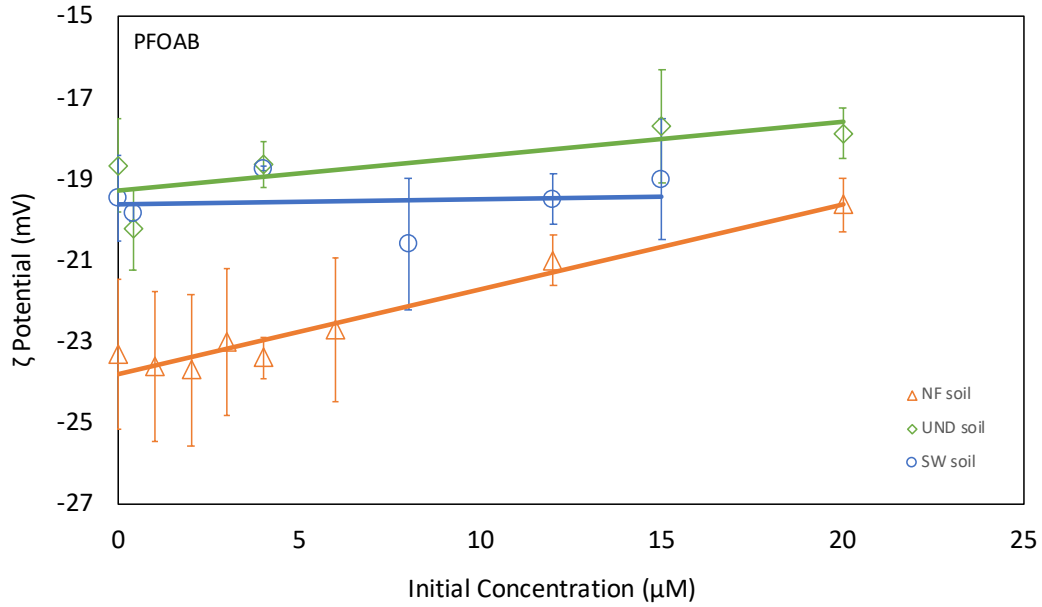


Figure 2.14. The zeta potential versus the different initial concentration of PFOAB in selected batch experiments for the UND, SW and NF soil.

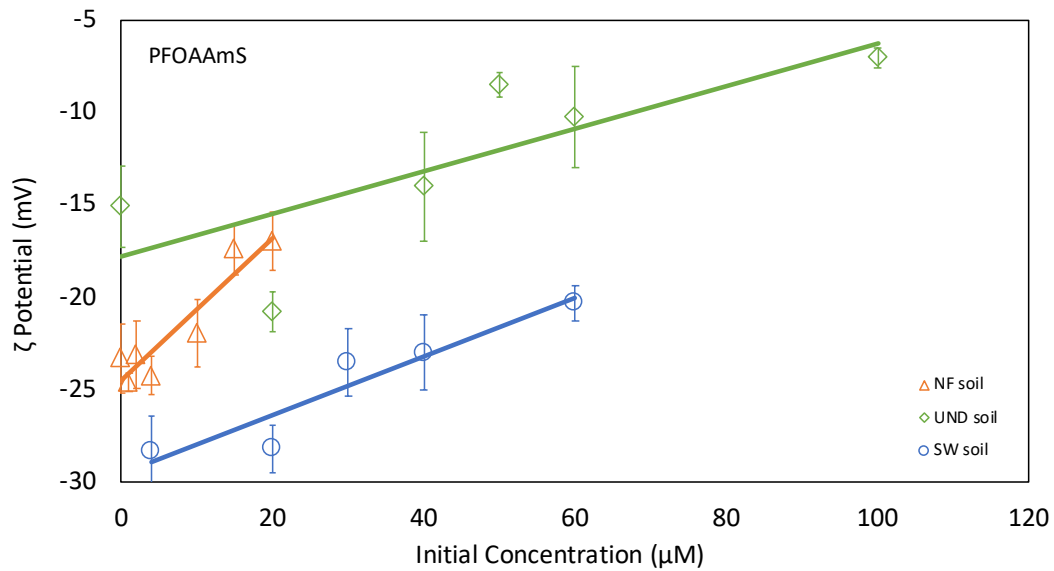


Figure 2.15. The zeta potential versus the different initial concentration of PFOAAmS in selected batch experiments for the UND, SW and NF soil.

Table 2.8. Zeta potential and pH in selected batch experiments of PFOAB and PFOAAmS adsorption

Soil	PFOAB				PFOAAmS			
	pH	ζ-potential (mV)	R ² _a	R ² _b	pH	ζ-potential (mV)	R ² _a	R ² _b
UND	7.97±0.04	-20.2 to -17.7	0.60	0.98	8.34±0.13	-20.8 to -7.0	0.61	0.89
SW	8.14±0.30	-20.6 to -19.0	< 0.1	0.32	8.55±0.17	-28.4 to -20.3	0.89	0.71
NF	8.24±0.11	-23.7 to -19.6	0.95	0.82	8.42±0.10	-24.6 to -17.0	0.88	0.76

- a. R² of initial concentration versus ζ-potential.
b. R² of logarithmic initial concentration versus ζ-potential.

2.3.7. The effect of the monovalent cation (Na⁺)

Previous researchers (Xiao et al., 2011) found that when the cationic sodium concentration increased, the PFOA adsorption on kaolinite particles was enhanced. PFOA tended to lose a proton to be anionic, and the soil surface was also negatively charged. Due to the electrostatic repulsion, PFOA was not effortless to be adsorbed on the soil. According to the double layer theory, sodium ions (Na⁺) as cationic counterions were intensely attracted on the negative surface of the soil, which provided a higher Stern potential on the Stern layer (Yukselen and Kaya, 2003). If the Na⁺ concentration was increased in the system, the soil surface would become less negatively charged. Thus, the PFOA surface electrostatic repulsion was reduced, and the PFOA adsorption was increased.

The effect of the sodium ions (Na⁺) on PFOAB and PFOAAmS adsorption was presented in Figure 2.16. As shown, the distribution coefficient of PFOAAmS correlated linearly. From Table 2.9, as the concentration of sodium ion increased, the K_d value of PFOAAmS decreased. For PFOAB, although K_d values also decreased when extra sodium ion was added, they did not present significant difference among three concentrations of sodium ion. According to the explanation of cationic effect on PFOA adsorption, the similar theory could be applied to

illuminate the situations of PFOAB and PFOAAmS. When the concentration of sodium ion augmented, positive charges gathered on the Stern layer. The electrostatic repulsion between the positive charge of PFOAB or PFOAAmS and the extra sodium ions on the Stern layer considerably reduce the attraction of chemicals on soil colloids. Therefore, PFOAAmS is notably not inclined to be adsorbed on the soil particle. For PFOAB, since it has both a positive and a negative charge, when the cation concentration increased, the distribution coefficient lessens at first due to the positive charge. Then, when the concentration of the sodium ion continues raising, the negative charge plays a more important role on the Stern layer, and the distribution coefficient slightly increased and finally maintained at a lower level compared with the adsorption in the buffer (Table 2.9).

In summary, when the PFAS adsorption happens in the soil-water system with high-level cationic activities, the adsorption will be improved if the PFAS is anionic or tends to lose a proton in the water, will be declined if the PFAS is cationic, or will be decreased first, and then increased, and finally sustain at a constant level if the PFAS is zwitterionic.

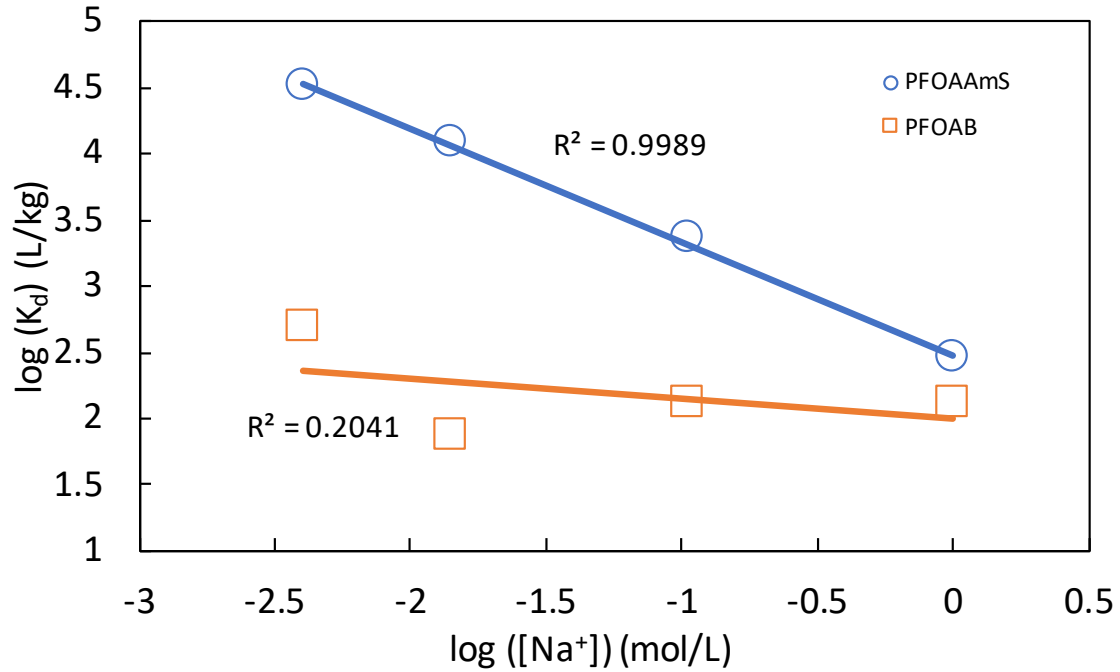


Figure 2.16. Effects of cationic concentration (Na⁺) on the adsorption of PFOAB and PFOAAmS by UND soil based on the distribution coefficient (K_d).

Table 2.9. The distribution coefficient (K_d) of PFOAB and PFOAAmS adsorption on UND at the different concentration of sodium ion

Sodium ion Concentration (mol L ⁻¹)	K _d at 20 μM of PFOAAmS (L kg ⁻¹)	K _d at 10 μM of PFOAB (L kg ⁻¹)
1.004	286	129
0.104	2,288	130
0.014	12,025	73
0.004	32,254	489

Chapter 3: Bioaccumulation and biotransformation of cationic and zwitterionic poly-PFASs by earthworms (*Lumbricus terrestris*) in soil

3.1. Introduction

Earthworms could be considered as the representative organisms to study the bioaccumulation behavior in the soil since they live in close contact with the soil (Jager et al., 2005). In addition, if the soil was contaminated, the effect will be shown in earthworms in a short time because they could consume large amounts of soil and due to their thin and permeable cuticles as well. Moreover, since earthworms are easy to obtain and are not hard to feed in the laboratory, they were chosen as the appropriate model organisms to study how the pollutants distributed between the terrestrial system and them. OCED/OCDE, accepted internationally as standard methods for chemical testing, has developed a standard bioaccumulation experiment (OECD 317, 2010) by using the earthworm as the typical terrestrial organism. Most researchers followed the OECD 317 to conduct their bioaccumulation tests for the targeted chemicals.

Although there were not plentiful literature of bioaccumulation behavior of PFASs in earthworm, the bioaccumulation of PFASs in many other animals has been deeply studied. Woodcroft et al. (2010) claimed that the principle of PFAS bioaccumulation was the protein bioaccumulation. Usually, the hydrophobic organic chemicals are more likely to be accumulated in the lipid, but due to the surfactant feature and the strong electronegativity of fluorine, the

small hydrophilic parts play a significant role in the bioaccumulation process. Conder et al. (2008) reported that the bioaccumulation behaviors were not significant when the fluorinated carbons were less than eight. Liu et al. (2011) stated that the PFAS bioaccumulation could not be explained by the conventional “buck phase” bioaccumulation and that the PFAS bioaccumulation was close to the adsorption behavior. In the previous PFAS bioaccumulation studies in earthworms, researchers (Zhao et al., 2013; Rich et al., 2015) found that with the increase of the fluorinated carbon chains, the bioaccumulation raised. In addition, many researchers (Zhao et al., 2013; Karnjanapiboonwong et al., 2018; Liu et al., 2011) have found the negative correlation between the initial PFAS concentration in the media and the values of bioaccumulation factors (BAF). Zhao et al. (2016) and Higgins et al. (2007) found that except for the bioaccumulation, the biotransformation behaviors were also presented during the uptake of N-ethyl perfluorooctane sulfonamide ethanol (N-EtFOSE) in earthworms and aquatic oligochaete *Lumbriculus variegatus*, respectively due to the detection of degradation products of N-EtFOSE in the organisms.

However, very little information is available with respect to the bioaccumulation potential of cationic and zwitterionic poly-PFASs. In this study, the cationic and the zwitterionic poly-PFASs were applied to investigate the bioaccumulation and biotransformation behaviors in earthworm.

3.2. Experimental section

3.2.1. Chemicals

In this study, two perfluorinated substances, PFOA and PFOS were purchased from Fluka

Chemie GmbH (Buchs, Switzerland). In addition, two precursors of PFOA, PFOAB and PFOAAmS, and two precursors of PFOS, PFOSB and PFOSAmS, were purchased from Beijing FLUOBON Surfactant Institute (Beijing, China). All PFAS standards were prepared in a 50/50 (v/v) solution of HPLC grade methanol (Thermo Fisher scientific, Geel, Belgium) and distilled water (UND Department of Chemical Engineering, Grand Forks, ND). Stock solutions were preserved in 125 mL HDPE wide-mouth-bottles (Thermo Fisher Scientific, Waltham, MA) and stored at 4 °C in the fridge. PFASs were not found in both the distilled water and methanol, detected by Waters UPLC coupled with QToF-MS (Waters Corporation, Milford, MA).

3.2.2. Soil and earthworm preparation

Loamy surface soils (5-15 cm) were collected from UND campus (47°55'11.8"N, 97°04'17.4"W), with no PFAS detected. Soil properties and soil pH were shown in Table 2.1 and Table 2.2, respectively (labeled as UND soil). The soil moisture of the fresh UND soil was about 25%.

The adult earthworm (*Lumbricus terrestris*), also commonly called as Nightcrawler, was purchased from DMF Bait Co. (Waterford, MI). In the beginning, the earthworm was incubated in the fresh UND soil in the 2-L glass beaker (Thermo Fisher Scientific, Waltham, MA) with no PFAS contamination at room temperature ($22.5\text{ °C} \pm 0.5\text{ °C}$) for about 48 hours to allow themselves to adapt to the new environment. The healthy and active earthworm was chosen from the beaker and allowed to purge its gut on the moist 9-cm filter paper (Curtin Matheson Scientific Inc., Houston, TX) in the covered glass plate (Thermo Fisher Scientific, Waltham,

MA) for about 16 hours before adding into the soil for the bioaccumulation experiment or into the liquid-solid phase for the bioconcentration test.

3.2.3. Bioaccumulation experimental setup

The bioaccumulation experiment was followed by the OECD guideline (OECD 317, 2010). There were two general steps in the bioaccumulation experiment: the uptake test and the elimination test. For the uptake test, the earthworm was introduced into the soil spiked with PFASs, while for the elimination test, the contaminated earthworm was depurated in the fresh UND soil. Both the uptake and elimination test were conducted in the 250-mL beaker (Thermo Fisher Scientific, Waltham, MA), containing about 150 g of fresh UND soil.

For the experimental group, the fresh UND soil was spiked with each of the six PFASs: PFOA, PFOAB, PFOAAmS, PFOS, PFOSB, and PFOSAmS. In some experiments, PFOA and PFOS were spiked together. A known volume of distilled water was added to the soil to obtain soil moisture of ~40%. The contaminated soil was then stirred vigorously by a plastic rod to make the chemicals evenly. Besides, a control group was set with only distilled water added, and no PFAS spiked in the fresh UND soil. The prepared earthworm was subsequently introduced to both the experimental beaker and the control beaker. The Glad Cling Plastic wrap (Rogers, AR) was used to cover the beakers to prevent the escape of earthworms. Small holes were generated on the plastic wrap to sustain enough oxygen to the earthworm. Every three days, the weight loss of the whole beaker was measured and counted as the loss of the soil moisture. The relative volume of distilled water was added, if necessary, to maintain stable soil moisture.

In this study, four main experiments were developed to fully understand the bioaccumulation and biotransformation behaviors of PFASs between the earthworm — soil

system. In the first experiment, PFOAB, PFOSB, PFOAAmS, and PFOSAmS were added into the soil respectively to obtain the initial concentration of $100,000 \mu\text{g kg}^{-1}$, individually. Earthworms were sampled on days 7, 12, 15, 21 and 28. At each sampling day, earthworms were supposed to purge their guts for about 16 hours on moist filter papers in covered plates. After purging, the earthworm was cleaned by distilled water, dried by the delicate task wiper (Kimberly Clark, Roswell, GA), stored in the clean glass plate and frozen at -18°C before extraction. Prior to the elimination test, the contaminated earthworm was prepared on the day 21 to purge its gut firstly ahead of being introduced into the fresh UND soil without PFAS contamination. Sampling method in the elimination test was the same as the uptake test. In the first elimination test, earthworms were sampled on days 1, 7, 8 and 18.

Other three bioaccumulation experiments were performed by following the same processes excluding the changed initial concentration of PFAS in the soil and the different sampling days. For the second experiment, the initial concentration of PFOAB, PFOSB, and PFOAAmS was set as $20,000 \mu\text{g kg}^{-1}$ each, except that the initial concentration of PFOSAmS in the soil was still $100,000 \mu\text{g kg}^{-1}$. Earthworms were sampled on days of 3, 5, 7, 10, 14, 18, 21 and 28 for the uptake test, and on days of 1, 3, 7, 10 and 18 for the elimination test. The initial concentration of combined PFOA and PFOS in the soil was set as $2,000 \mu\text{g kg}^{-1}$ each with the sampling time of days 3, 14 and 21 for the uptake test and day 21 for the elimination test. In the third experiment, the initial concentration of four precursor compounds was set as $20,000 \mu\text{g kg}^{-1}$, correspondingly. Earthworms were sampled on day 14 and day 21 for the uptake test, and only on the day 21 for the elimination test. In the fourth bioaccumulation experiment, only the uptake test was conducted with an initial concentration of $50 \mu\text{g kg}^{-1}$ respectively for PFOA and PFOS in the soil, with the sampling time of days 3, 7, 10, 14 and 21.

In selected experiments, earthworms were cut in half to examine any difference in PFASs in different parts of the worm. In this experiment, the initial concentration of four poly-PFAS in the soil was set as 20,000 $\mu\text{g kg}^{-1}$ each, and the initial concentration of combined PFOA and PFOS was respectively set as 50 $\mu\text{g kg}^{-1}$. With the same process as the previous uptake and elimination test, the earthworm was sampled on day 21 for both the uptake and the elimination test and was preserved at -18 °C. The frozen earthworm was cut to two parts (the “head” and the “tail”) according to the clitellum (Figure 3.1). The “head” part was from the prostomium to the beginning of clitellum, while the “tail” part started from the beginning of clitellum to the anus. As shown in Figure 3.2, all the principal organs of ingestion, digestion, reproduction, blood circulation, locomotion, and coordination are located in the “head” part, whereas the intestine is in the tail section. Both the “head” and the “tail” part had skin and vessels. This experiment was to present whether there was a difference between the of PFAS concentration in the “head” part and the “tail” part, and it could also help us understand which part would play a major role of the bioaccumulation and the biotransformation.

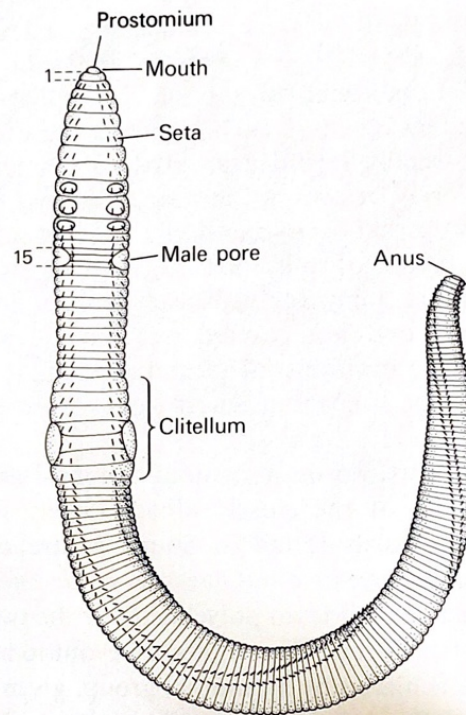


Figure 3.1. Earthworm morphology. (Lee, 1985)

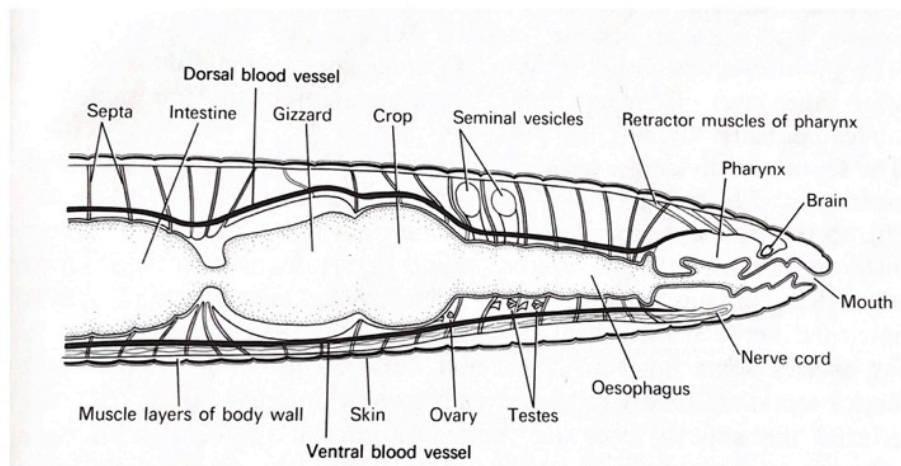


Figure 3.2. A typical “head” part of a lumbricid earthworm. (Lee, 1985)

3.2.4. Bioconcentration experimental setup

The 250-mL glass beaker was used in the bioconcentration test containing about 50 g of solid components (e.g., the glass bead with the diameter of 2.0 mm or the coarse sand with the diameter of 0.5 – 1.0 mm), and about 50 mL of the distilled water. PFOA/PFOS, PFOAB, PFOAAmS, PFOSB and, PFOSAmS were added to the beaker independently to obtain the initial concentration of $0.2 \mu\text{M L}^{-1}$. The beaker with no PFASs added was set as the control group. The prepared earthworm was introduced to the beaker with the plastic wrap covered in case the escape of the earthworm. Small holes were generated on the plastic wrap to sustain enough oxygen to the earthworm. The weight of the beaker was measured periodically, and distilled water was added to the beaker to keep the weight constant. Earthworms were sampled on after 3, 7, 14 and 21 days of exposure, and then cleaned by the distilled water, dried by wipers, and stored at -18°C in pre-cleaned glass plates before extraction.

3.2.5. Extraction and analysis of PFASs

Frozen earthworms were moved into the mortar (Thermo Fisher Scientific, Waltham, MA), and were ground to the powder with the liquid nitrogen added. The earthworm powder was weighed and then transferred into the 50-mL plastic centrifuge tubes. PFASs in earthworms were extracted by 10 mL of HPLC grade methanol in first and second bioaccumulation experiments, and with 15 mL of HPLC grade methanol and 0.5 M HPLC grade HCl was employed for the earthworm extraction. To extract PFASs from the soil, 10 g of soil sample was added into the 50-mL plastic centrifuge tube with 20 mL of HPLC grade methanol for the first and the second bioaccumulation experiments and with 15 mL of HPLC grade methanol and 0.5 M HPLC grade HCl added for all other experiments. All the sample tubes were placed in the ultrasonic bath

(Cole-Parmer, Vernon Hills, IL) for an hour at room temperature ($22.5\text{ }^{\circ}\text{C} \pm 0.5\text{ }^{\circ}\text{C}$), and were subsequently centrifuged by Clay Adams Dynac centrifuge (Parsippany, NJ) at 5000 rpm for 5 minutes. The supernatant was filtrated by a 0.2- μm nylon filter (Thermo Scientific, Rockwood, TN) to a 2-mL HPLC vial (Agilent, Santa Clara, CA), and stored in the fridge at $4\text{ }^{\circ}\text{C}$ before analysis. In addition, the soil sample was collected and heated at $105\text{ }^{\circ}\text{C}$ for 24 hours in the oven (Cascade TEK, Cornelius, OR) to calculate the weight loss to obtain the soil moisture for the quantitative analysis of the PFAS concentration in soil.

Samples were analyzed by a Waters Acquity ultrahigh-pressure liquid chromatography (UPLC) system coupled with a Waters Synapt G2-S HD QToF-MS (Waters Corporation, Milford, MA). The analytical condition was the same as the sorption study. The ionization modes and mass to charge ratios used in this experiment were shown in Table 3.6.

3.2.6. QA/QC

No fluorinated material was used in this experiment, and no PFAS was found in the distilled water and the HPLC grade Methanol. All the tubes and HPLC vials were pre-cleaned by the distilled water and the HPLC grade Methanol to assure that there was no PFAS contamination before all experiments. Calibration standards of PFASs were used to obtain the calibration curve to calculate the PFAS concentration.

The PFAS extraction efficiency test was conducted for both earthworm and UND soil. The GC syringe (Thermo Fisher Scientific, Waltham, MA) was applied to inject a known mass of PFASs into the earthworm's body. The injected earthworm was extracted by 10 mL of HPLC grade methanol or 15 mL HPLC grade methanol with 0.5 M HPLC grade HCl. The dry soil

sample (about 7.5 g) with PFASs spiked and 2.5 mL of distilled water was extracted by 20 mL of HPLC grade methanol or 15 mL HPLC grade methanol with 0.5 M HPLC grade HCl. Samples were put into the ultrasonic bath for one hour. Controls were prepared by spiking with a known mass of PFASs in either pure methanol or methanol (0.5 M HCl). The sample was analyzed by the UPLC QToF-MS/MS. The extraction efficiency was calculated based on the mass balance using the following equation:

$$E = C_0/C_{Control} \times 100\% \quad (3.1)$$

where C_0 is the concentration of PFAS in the sample, μM ; $C_{Control}$ is the concentration of PFAS in control, μM ; E is the extraction efficiency, %.

3.2.7. Data analysis

Two important parameters were explained carefully for the analysis of the bioaccumulation results. One is the uptake and elimination kinetics, and the other is the bioaccumulation factors. The kinetics of uptake data was fitted with a first-order model (OECD 317, 2010; Zhao et al., 2013) using the OriginPro 9.0 (Northampton, MA), expressed as:

$$C_a = \frac{k_u}{k_e} \times C_s \times (1 - e^{-k_e \cdot t}) \quad 0 < t < t_u \quad (3.2)$$

where C_a is the PFAS concentration in the earthworm (wet weight) at time t , $\mu\text{g g}^{-1}$ or ng g^{-1} ; k_u is the uptake rate of the PFAS concentration in the earthworm, d^{-1} ; k_e is the elimination rate of the PFAS concentration in the earthworm, d^{-1} ; C_s is the PFAS concentration in the dry soil $\mu\text{g g}^{-1}$ or ng g^{-1} ; t_u is the time at the end of uptake experiment, d. For some degradable PFAS (e.g., PFOAB in this study), another first-order with two-compartment model (Rich et al., 2014; Zhao

et al., 2016) was applied in the kinetic study:

$$C_a = \frac{k_u}{k_e - k_0} \times C_s \times (e^{-k_0 \cdot t} - e^{-k_e \cdot t}) \quad 0 < t < t_u \quad (3.3)$$

where k_0 is the degradation constant of the PFAS, d^{-1} ; other parameters are the same as shown in Equation 3.2.

The bioaccumulation factor (BAF) at steady state was calculated based on the PFAS concentration in the earthworm and the soil on day 21 (OECD 317, 2010):

$$BAF = C_a / C_s \quad (3.4)$$

where C_a is the PFAS concentration in the earthworm (wet weight) on day 21, $\mu g g^{-1}$ or $ng g^{-1}$; C_s is the PFAS concentration in the dry soil, $\mu g g^{-1}$ or $ng g^{-1}$. The value of the bioaccumulation factor value (BAF_k) could also be calculated by the result of kinetics (OECD 317, 2010):

$$BAF_k = k_u / k_e \quad (3.5)$$

where k_u is the uptake rate of the PFAS concentration in the earthworm, d^{-1} ; k_e is the elimination rate of the PFAS concentration in the earthworm, d^{-1} . The bioconcentration factor (BCF) at steady state could also be obtained in the earthworm — water experiment based on the PFAS concentration in the earthworm and the soil at the end of uptake (Belfroid et al., 1994; OECD 305, 2016; Ding et al., 2016):

$$BCF = C_a / C_w \quad (3.6)$$

where C_a is the PFAS concentration in the earthworm (wet weight) at the end of uptake, $ng g^{-1}$; C_w is the PFAS concentration in the water, $ng mL^{-1}$ or $ng g^{-1}$.

For the elimination test, the result was analyzed by the first order decay model considering the residual PFAS in earthworm (OECD 305, 2016):

$$C_a = C_r + C_A \times e^{-k'_e \cdot t} \quad (3.7)$$

where C_a is the PFAS concentration in the earthworm (wet weight) at time t , $\mu\text{g g}^{-1}$ or ng g^{-1} ; C_r is the concentration of the residual PFAS in earthworm when the elimination process reaches the equilibrium, $\mu\text{g g}^{-1}$ or ng g^{-1} ; C_A is the kinetic concentration of PFAS within the earthworm, $\mu\text{g g}^{-1}$ or ng g^{-1} ; k'_e is the depuration rate constants, d^{-1} . The elimination half-life was calculated by (Zhao et al.,2016; Zhao et al.,2013):

$$t_{\frac{1}{2},k_e} = \frac{\ln 2}{k_e} \quad (3.8)$$

$$t_{\frac{1}{2},k'_e} = \frac{\ln 2}{k'_e} \quad (3.9)$$

where k_e and k'_e are elimination rate constants in the uptake phase and elimination phase, respectively, d^{-1} .

3.3. Results and discussion

3.3.1. QA/QC

The results of the extraction efficiency of six PFASs in the soil and the earthworm were shown in Figure 3.3 and Figure 3.4, respectively. Figure 3.3 displayed that the extraction efficiencies of all six PFASs from soil were larger than 60% except for PFOAAmS extracted by methanol without 0.5 HCl. Previous researchers (Barzen-Hanson et al., 2017) reported that using

0.5 M HCl in methanol as the extractant could achieve a good (90% – 100%) recovery of PFAS in the soil. Following their study, the acidic methanol was employed to extract PFASs in both the soil and the earthworm after the second bioaccumulation experiment. Figure 3.3 showed that the methanol with 0.5 M HCl significantly improved the extraction of cationic and zwitterionic PFASs compared with the pure methanol. For PFOA and PFOS, the two extractants displayed a close extraction efficiency of ~100%. However, when the acidic methanol was utilized in the extraction of earthworm, it did not show a strong advantage compared with the methanol without acid. On the contrary, the acidic methanol had a reverse effect on the extraction of PFOAB, PFOSAmS, and PFOAAmS in the earthworm. The extraction efficiency of PFASs from earthworm was relatively low (Figure 3.4).

Other researchers (Zhao et al., 2013; Wen et al., 2015) found that using 10 mM NaOH methanol as extractant could obtain recovery rate of about 76% – 105% and 78% – 101%, for ten perfluoroalkyl chemicals and PFOA/PFOS, respectively, in the earthworm. Karnjanapiboonwong et al. (2018) found that applying the QuEChERS (Quick, Easy, Cheap, Effective, Rugged and Safe) technique could provide a recovery rate of $87 \pm 3.0\%$ for PFBS, $76 \pm 4.9\%$ for PFHxS, $75 \pm 6.1\%$ for PFNA, and $61 \pm 4.4\%$ for PFHpA in earthworm. The recovery rates of PFOA and PFOS in earthworm in this study were similar to the results from previous researchers. No recovery rate of comparable poly-PFASs was reported before. The extraction efficiency rate was applied for the quantitative analysis of the PFAS concentration in the earthworm.

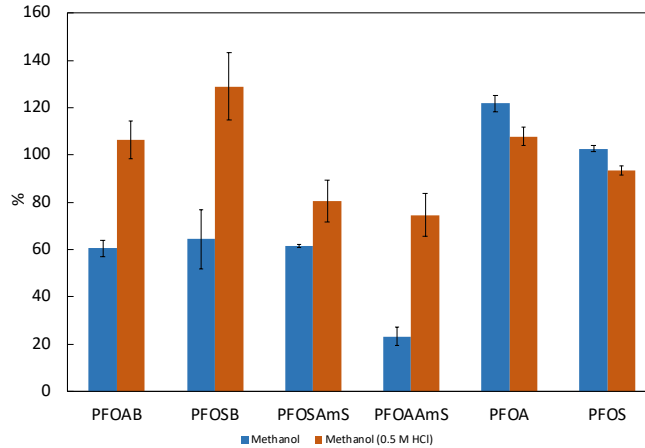


Figure 3.3. Extraction efficiency of PFAS in soil by using two extractants: pure methanol and methanol with 0.5 M HCl.

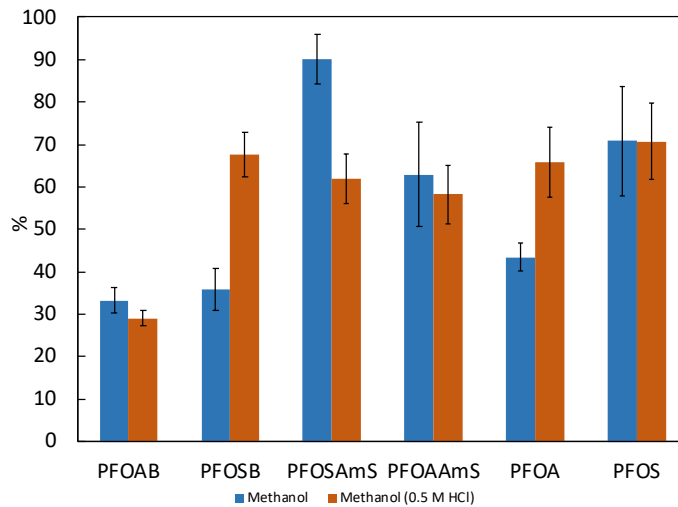


Figure 3.4. Extraction efficiency of PFAS in earthworm by using two extractants: pure methanol and methanol with 0.5 M HCl.

3.3.2. Earthworm mortality and health

The total survival rate of earthworms was 91.1% in all uptake experiments, while all earthworms in control groups and depuration groups in the fresh clean soil survived. All survived earthworms were healthy and active, and eggs of earthworms were even found in some samples.

Table 3.1 shows the earthworm mortality rate at the different initial PFAS concentration in the soil. Pearson correlation analysis was used to analyze the relationship between the earthworm mortality and different initial PFAS concentrations in soil by SPSS (Armonk, NY), which showed that the relationship was not significant ($p = 0.092 > 0.05$). However, Yuan et. al (2017) reported that the LC50 for PFOA and PFOS for earthworm in soil on day 14 was 811.42 mg kg⁻¹ and 540.97 mg kg⁻¹, respectively. If the data 540 mg kg⁻¹ of PFAS with 50% of earthworm mortality was added in the analysis for the Pearson correlation analysis, the result showed a significant relationship ($p = 0.003 < 0.01$) between the earthworm mortality and the initial PFAS concentration in the soil.

Table 3.1. Earthworm mortality

PFAS concentration mg/kg	Survivals (n)	Mortality (n)	Total earthworms (n)	Mortality rate %
100	54	10	64	15.62
20	105	11	116	9.48
2	27	0	27	0
0.05	30	0	30	0

When the dose of PFASs in soil was high (e.g., 20 mg/kg), some earthworms became inactive and died in 36 hours. The dead earthworms were usually showed symptoms like tumors (shown in Figure 3.5). Moreover, we found that one dead earthworm without removing in time could quickly lead to other earthworms' death in the same beaker due to the so-called "protein poisoning" (Garg, 2015).

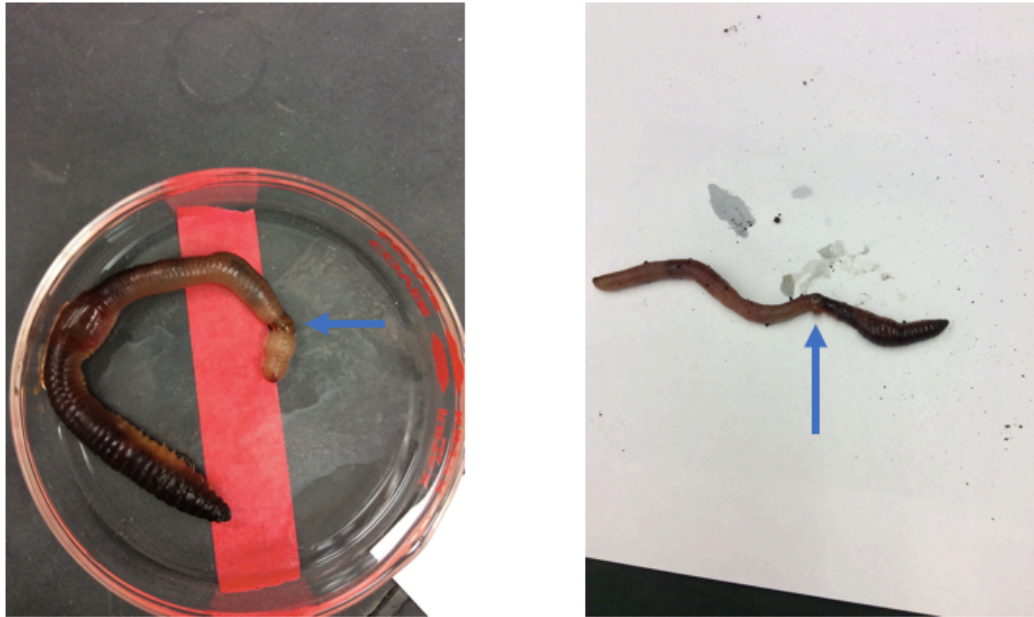


Figure 3.5. Tumors in dead earthworms.

In the bioconcentration test, earthworms could live up to 21 days, but some earthworms died on the third or fourth day of exposure. A previous study has confirmed that earthworms could live in water for a long time, if two important factors, enough oxygen and frequently changed water, were satisfied (Roots, 1955). In this study, since the concentrations of PFASs were all set at a low level, $0.2 \mu\text{M}$ (roughly equal to 0.1 mg kg^{-1}) in the liquid phase, the primary reasons for the earthworm mortality were not likely to be the toxicity of PFASs. The reason for earthworm's death in 3 or 4 days was because of the lack of oxygen. When fresh air was given every two days, earthworms could survive to 21 days, except the earthworms in PFOAB/PFOSB group. The reason for earthworm mortality in this group was mainly due to the stale water. Earthworm excreted ammonia and urea in water, which were toxic (Lee, 1985). Wolf (1940) reported that the total urine that earthworm produced in one day was about 60% of its body weight. If earthworms live in the water without frequently changed, they would be sick soon and

die eventually due to the high concentrations of ammonia and urea.

3.3.3. Uptake and elimination kinetics of PFASs in earthworms

Uptake and elimination results of the first and the second bioaccumulation experiment were shown in Figures 3.6, 3.7 and 3.8. All PFASs could be detected in earthworm on day 3 according to the result of the second experiment. As the protein content of earthworm (*Lumbricus terrestris*) was ~60% in its dry weight (Lee, 1985), and PFAS was protein bioaccumulation (Woodcroft et al., 2010), the bioaccumulation of PFASs proceeded fast in the earthworm. The highest level of PFAS concentration in earthworm approximately appeared sometime during day 10 to day 15. After 15 days of exposure, the PFAS concentration was more stable, and some even decreased a little bit.

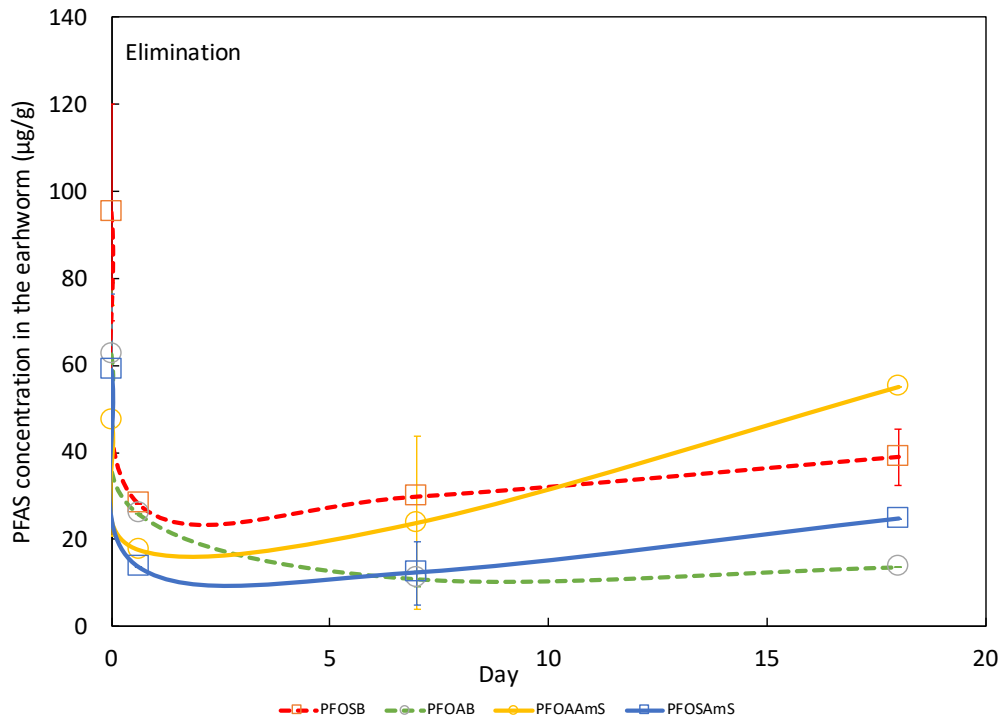
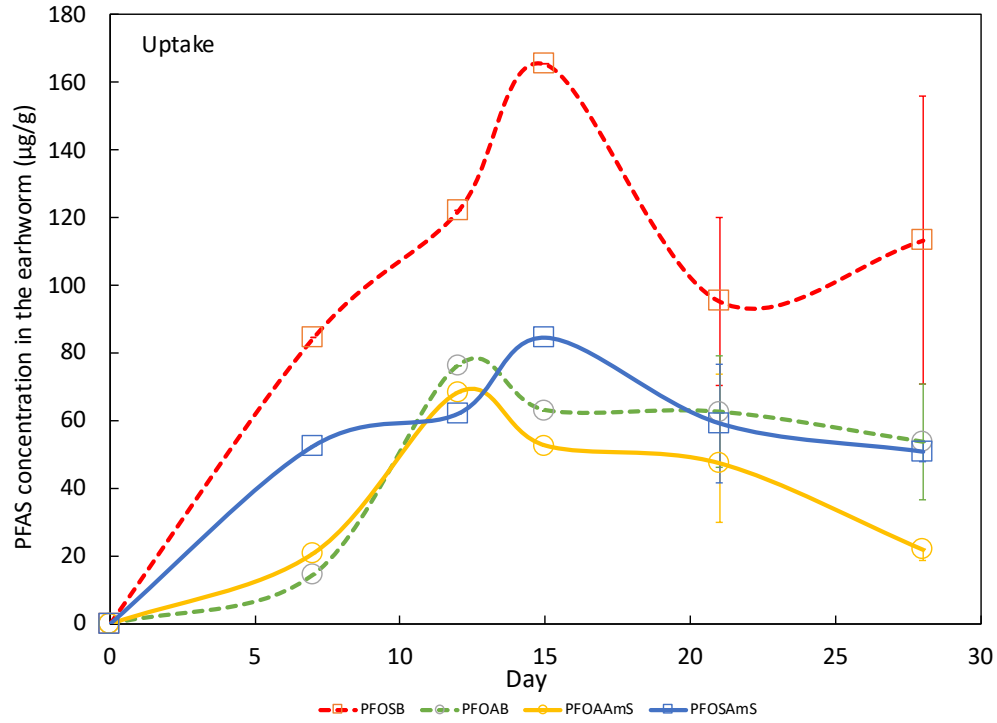


Figure 3.6. Uptake and elimination of four poly-PFASs in earthworm in the first bioaccumulation experiment.

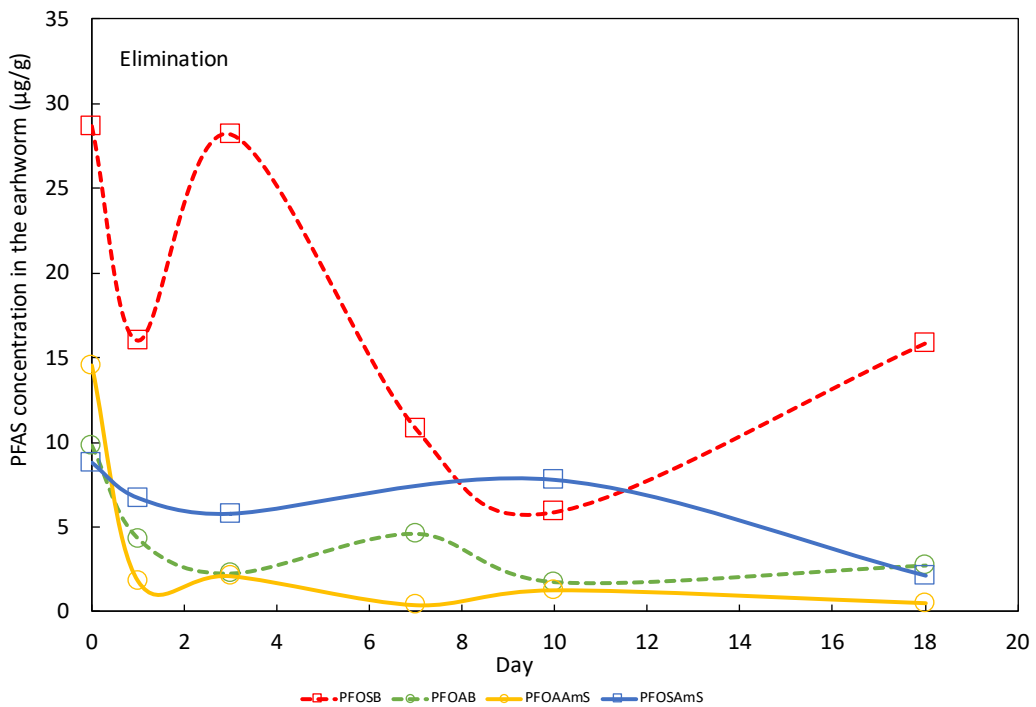
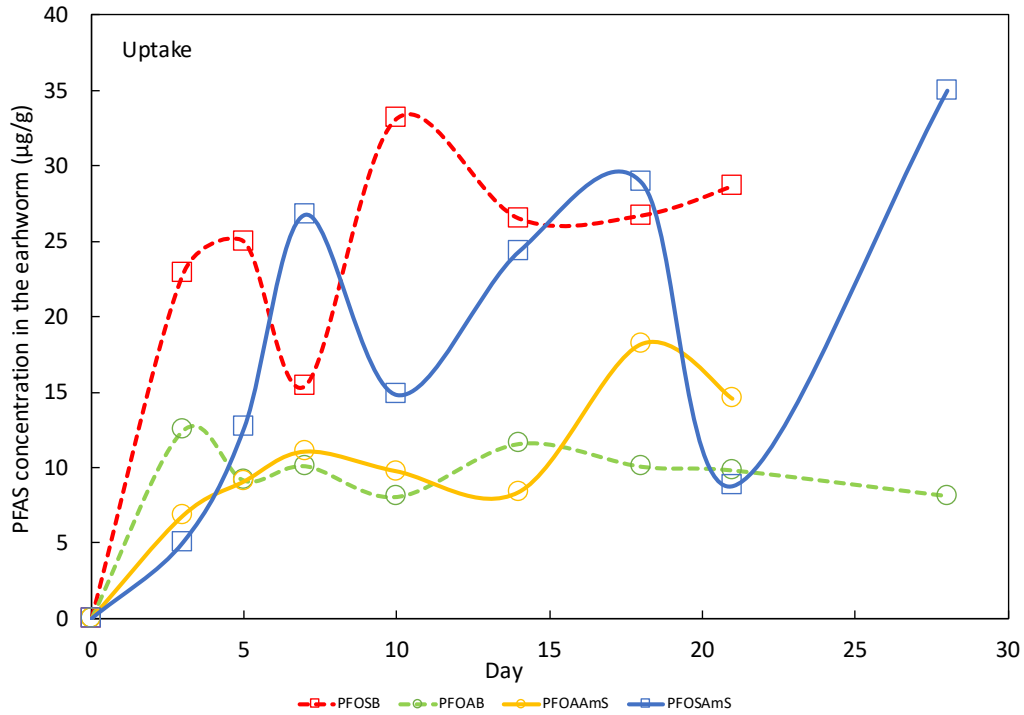


Figure 3.7. Uptake and elimination of four poly-PFASs in earthworm in the second bioaccumulation experiment.

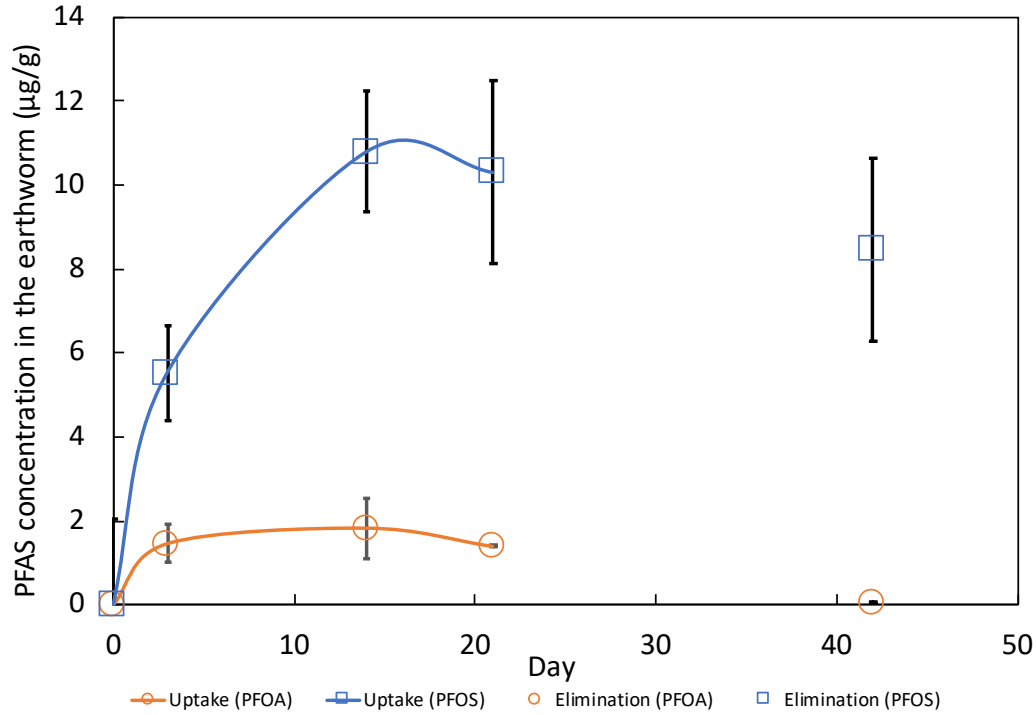


Figure 3.8. Uptake and elimination of PFOA and PFOS in earthworm in the second bioaccumulation experiment.

The uptake kinetic data were fitted by the Equation (3.2) for all PFASs, and Equation (3.3) for PFOAB only (degradation of other PFASs in UND soil was not significant, unpublished data) with the soil degradation rate of 0.0359 d^{-1} (k_0 , unpublished data). The result was summarized in Table 3.2, and the fitting curves were shown in Figure B-1, B-2, and B-3. From Table 3.2, the uptake rate (k_u) of PFOAB was the largest one (0.275 d^{-1} and 0.554 d^{-1} , respectively) among the four poly-PFASs (the k_u value of PFOAB obtained from Equation 3.3) in both the first and the second experiment. Also, Figure 3.9 displayed that the order of uptake rates was $\text{PFOSB} > \text{PFOSAmS} > \text{PFOAB} > \text{PFOSB}$ in the first experiment, and that the order was $\text{PFOS} > \text{PFOSB} > \text{PFOA} > \text{PFOAB} > \text{PFOAmS} > \text{PFOSAmS}$ in the second experiment including PFOA and PFOS. Anionic PFASs, PFOA and PFOS, were adsorbed fast by earthworm

with the highest uptake rates. Zwitterionic PFASs, PFOAB and PFOSB, also showed higher uptake rates. Since both anionic and zwitterionic PFASs contain negative charges, the negative charge was considered to have a positive effect on earthworm uptake rate of PFASs.

Table 3.2. Computed values of uptake kinetic rate (k_u), elimination kinetic rate (k_e) in the uptake phase, elimination half-life ($t_{1/2}$) and kinetic bioaccumulation factor ($BAF_{kinetic}$) in the first and the second experiment for six PFASs

Compound	First experiment					Second experiment				
	R^2	k_u (d^{-1})	k_e (d^{-1})	$BAF_{kinetic}$	$t_{1/2}$ (d)	R^2	k_u (d^{-1})	k_e (d^{-1})	$BAF_{kinetic}$	$t_{1/2}$ (d)
PFOA	N/A	N/A	N/A	N/A	N/A	0.50	0.410	0.788	0.520	0.88
PFOAAmS	0.41	0.065	0.163	0.402	4.26	0.72	0.141	0.159	0.889	4.36
PFOAB ¹	0.56	0.148	0.140	1.061	4.96	0.88	0.718	0.651	1.102	1.06
PFOAB ²	0.60	0.138	0.065	2.136	10.70	0.89	0.289	0.149	1.946	4.67
PFOS	N/A	N/A	N/A	N/A	N/A	0.87	1.269	0.249	5.105	2.79
PFOSAmS	0.64	0.160	0.395	0.404	1.75	0.82	0.037	0.083	0.440	8.31
PFOSB	0.50	0.275	0.288	0.956	2.41	0.75	0.554	0.469	1.181	1.48

1: Fitted by Equation (3.2).

2: Fitted by Equation (3.3) for degradable PFASs.

N/A: PFOA and PFOS were not used in the first bioaccumulation experiment.

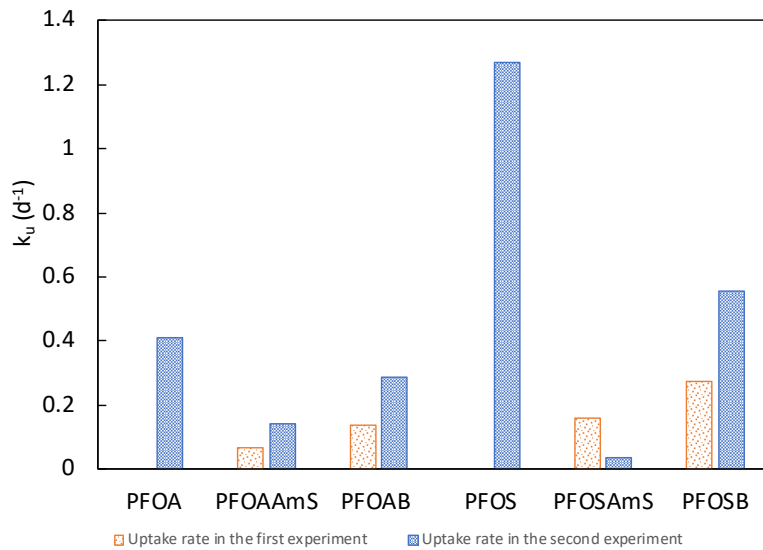
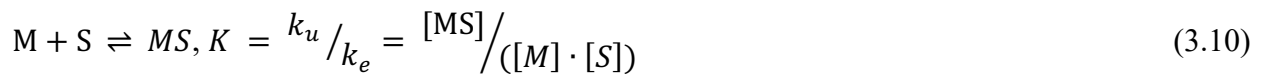


Figure 3.9. Uptake rates of six PFASs in the first and the second experiments.

Another important finding in Table 3.2 and Figure 3.9 was that compared with the first experiment, the uptake rate of poly-PFAS (except PFOSAmS) was larger in the second experiment, although the exposure concentration in the second experiment was 5 times lower than in the first experiment. The similar situation was also found in another bioaccumulation study of PFASs (Jeon et al., 2010). Previous researchers (Liu et al., 2011; Conder et al., 2008) have attempted to interpret the correlation between bioaccumulation and concentration. Conder et al. (2008) reported that PFASs, as surface-active chemicals, tend to enrich at surfaces and that the PFASs partitioning is more likely to accord with the absorption process, instead of bulk phase accumulation, which was the common model of the conventional bioaccumulation. Furthermore, Liu et al. (2011) developed a new theory based on the “binding sites” to explain the PFAS bioaccumulation in green mussels (*Perna viridis*). The mechanism was expressed as:



where M is the amount of PFAS; S is the free binding site; MS is the bonded PFAS; k_u is the uptake rate, also the forward reaction rate; k_e is the elimination rate, also the reverse reaction rate; K is the equilibrium constant. Not only the exposure concentration was considered, but the effect of the free binding site was also added in the conventional kinetic model. According to this theory, an increase in the PFAS concentration in the media could cause a decrease in the uptake rate. The same tendency was also found in $BAF_{kinetics}$ value of PFOAAmS and PFOSB (Figure B-7) that the $BAF_{kinetics}$ value was larger in the second experiment than in the first experiment.

Elimination kinetic data were fitted by Equation (3.7). The result was shown in Table 3.3, and the fitting curve was displayed in Figure B-4, B-5, and B-6. Except for PFOSAmS in the second experiment, all depuration constants were larger than 1 d^{-1} , which meant that elimination

proceeded so quickly that the concentration of PFAS could reduce by half within one day. However, PFASs could not be completely removed from the earthworm's body after 18 or 21 days living in the PFAS-free soil. Table 3.3 showed the estimated residual PFAS concentration in the earthworm. To understand PFAS elimination, the same theory used to explain the bioaccumulation was employed that the elimination was also the adsorption-like process. Thus, the PFAS molecule could be rapidly distributed to the soil particle and form a new equilibrium between the organism phase and the soil phase. Under the new equilibrium, there was some PFASs remaining in the earthworm. Since the elimination test was conducted in the 250-mL beaker with about 150 g of soil, if the contaminated earthworm lived in nature with access to unlimited uncontaminated soil, the PFAS concentration in earthworm might reduce much more or even close to zero.

Table 3.3. Computed value of depuration kinetic rate (k'_e) in the elimination phase for four poly-PFASs

Compound	First experiment				Second experiment				Additional experiment*			
	R ²	C _r (μg g ⁻¹)	k' _e (d ⁻¹)	t _{1/2} (d)	R ²	C _r (μg g ⁻¹)	k' _e (d ⁻¹)	t _{1/2} (d)	R ²	C _r (μg g ⁻¹)	k' _e (d ⁻¹)	t _{1/2} (d)
PFOAAmS	0.999	12.386	3.066	0.226	0.979	1.072	2.894	0.239	N/A	N/A	N/A	N/A
PFOAB	0.990	11.611	2.042	0.340	0.819	2.864	1.611	0.430	0.933	0.089	1.973	0.351
PFOSAmS	0.904	12.292	5.856	0.118	0.935	2.019	0.208	3.340	0.887	4.379	2.087	0.332
PFOSB	0.975	31.890	218	0.003	0.655	10.863	1.239	0.559	N/A	N/A	N/A	N/A

N/A: Not applicable.

*: Additional elimination test was based on the third experiment. The contaminated earthworm was depurated in the clean soil, and sampled at every several hours.

3.3.4. Bioaccumulation of poly-PFASs in earthworms

BAF is an important criterion to assess the bioaccumulation potential of the chemical in the organism (Conder et al., 2008), and the BAF value was obtained from empirical

bioaccumulation data, calculated by Equation (3.2). BAF values of four poly-PFASs were shown in Table 3.4. In all three bioaccumulation experiments, BAF values of PFOAB and PFOSB were higher than BAF values of PFOAAmS and PFOSAmS, excluding BAF values of PFOSB in the third experiment. It could be explained by referring to the adsorption study in Chapter 2. Because the soil adsorption ability of cationic poly-PFASs was stronger than zwitterionic poly-PFASs, when the earthworm ingested the soil, cationic poly-PFASs were more likely to stay on the soil particle than to redistribute on the organism.

Table 3.4. BAF values of four poly-PFASs in the first, second and third experiments

Compound	First experiment	Second experiment	Third experiment
PFOAB	1.04 ± 0.28	2.23	1.04 ± 0.22
PFOSB	0.80 ± 0.21	1.26	0.40 ± 0.02
PFOSAmS	0.40 ± 0.12	0.34	0.78 ± 0.56
PFOAAmS	0.36 ± 0.20	0.87	0.37 ± 0.17

Also, to study the concentration effect on BAF values, the average BAF value was calculated under the same concentration of each poly-PFAS. Figure 3 displayed that the higher the initial concentration was, the lower the BAF value was if BAF values of PFOSB in the third experiment were not considered. The binding theory (Liu et al., 2011) could be well-fitted to provide an elucidation here. According to the mechanism, Equation (3.11), (adapted from Liu et al., 2011) of adsorption-like process, the fractional surface coverage of adsorbent, θ , could be calculated by:

$$\theta = \frac{[MS]}{[MS] + [S]} = \frac{K \cdot [M][S]}{K \cdot [M][S] + [S]} = \frac{K \cdot [M]}{K \cdot [M] + 1} \quad (3.11)$$

where K was the equilibrium constant, and $[M]$ is the amount of PFAS in the media. In the bioaccumulation experiment, the final concentration of the PFAS in the earthworm (C_a) could be expressed as:

$$C_a = n \cdot \theta \quad (3.12)$$

where constant n is the total binding sites per gram of organism. The value of $[M]$ here could be substituted by the PFAS concentration in the soil (C_s). Thus, equation (3.4) could also be calculated as:

$$BAF = \frac{n \cdot \theta}{C_s} = \frac{n \cdot \frac{K \cdot C_s}{K \cdot C_s + 1}}{C_s} = \frac{n \cdot K}{K \cdot C_s + 1} \quad (3.13)$$

According to Equation 3.13, with the increase of the initial PFAS concentration, the BAF value would decrease, which could explain the observed result as shown in Figure 3.10.

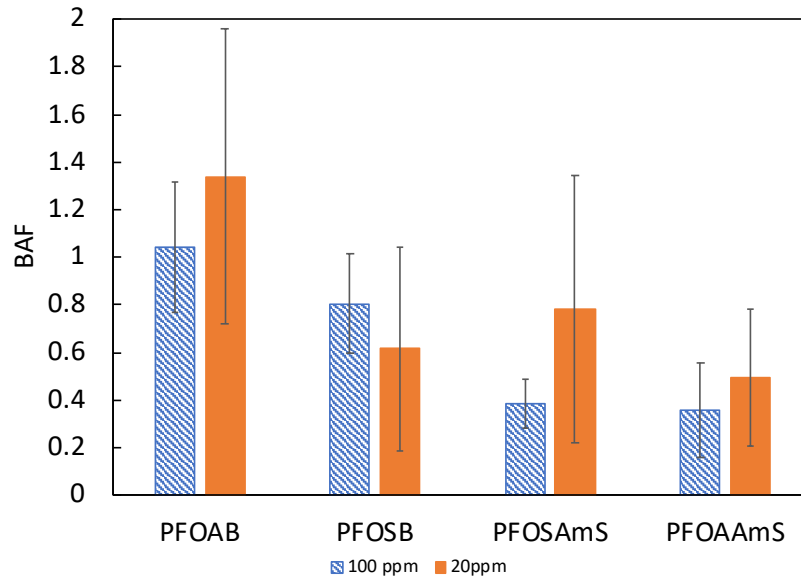


Figure 3.10. Observed bioaccumulation factors (BAF) of four poly-PFASs.

Furthermore, if the observed BAF value was compared with the kinetic BAF value (Figure 3.11 and 3.12), the difference between two BAF values are not significant, which could help to endorse the fitting model and the accuracy of the experiment. Due to the Equation (3.2), (3.4), and (3.5), the observed BAF value and the kinetic BAF value could also be expressed as:

$$BAF = \frac{C_a}{C_s} = \frac{k_u}{k_e} \times (1 - e^{-k_e \cdot t}) = BAF_k \times (1 - e^{-k_e \cdot t}) \quad 0 < t < t_u \quad (3.14)$$

If the time “t” was equal to day 21, the value of “ $e^{-k_e \cdot t}$ ” would become very small, and could be ignored mathematically. Thus, under these circumstances, BAF calculated based on the concentrations in worm and soil at the end of exposure was in the same range as the kinetic BAF. The difference between two BAF values of PFOAB in the first experiment was more distinct than other PFASs.

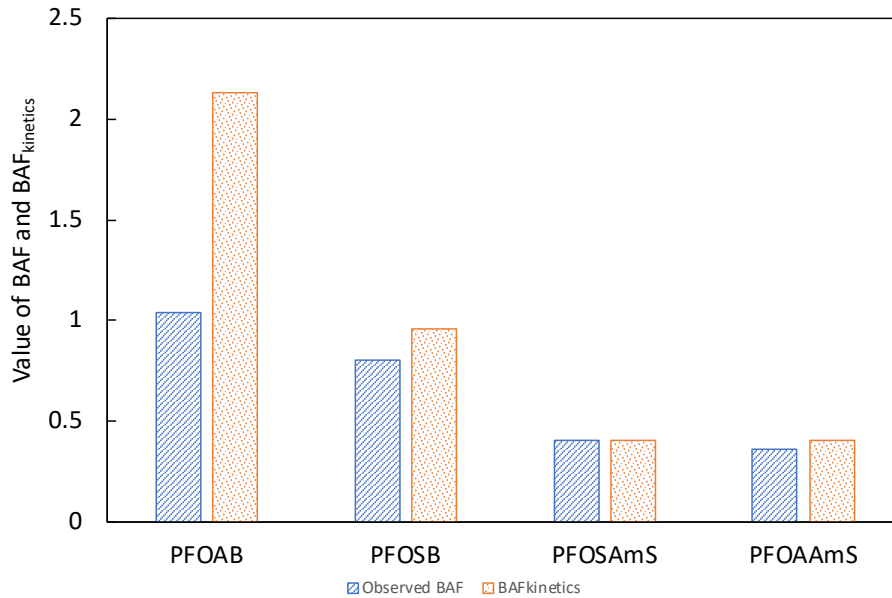


Figure 3.11. Comparison between observed and kinetic BAF values in the first experiment.

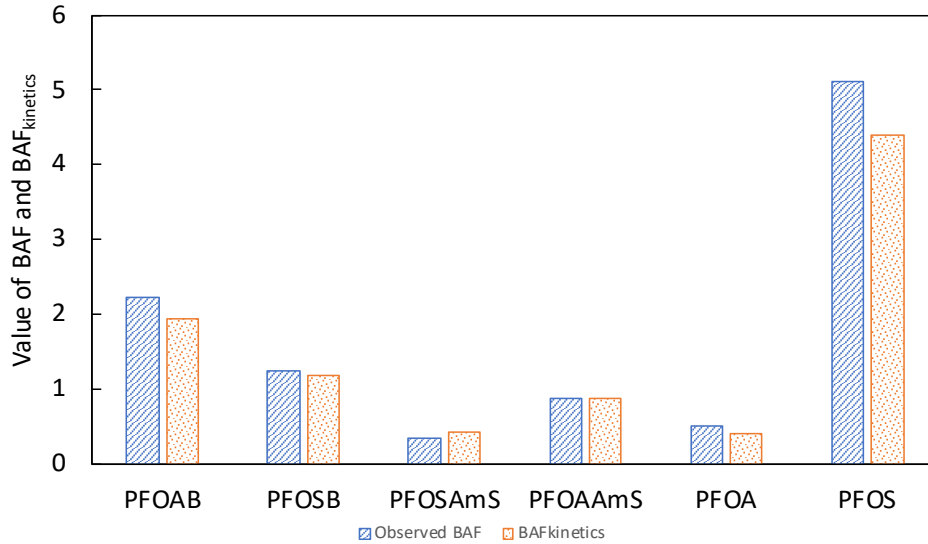


Figure 3.12. Comparison between observed and kinetic BAF values in the second experiment.

In addition, previous researchers (Woodcroft et al., 2010; Cheng and Ng, 2018) reported the protein affinity of PFASs by studying the binding mechanisms between the selected PFASs and the liver fatty acid-binding protein (L-FABP). *Lumbricus terrestris* have ~60% of protein of their dry weights (Lee, 1985), and Sánchez-Hernández and Wheelock (2009) found that the content of protein in the anterior part of *Lumbricus terrestris* is higher than the tail part (behind the clitellum, Figure 3.1). If PFASs were protein bioaccumulation in the earthworm, the PFAS concentration in the anterior part would be higher than in the tail part. Paired t-tests were conducted by SPSS (Armonk, NY), and the result showed that the concentration of four poly-PFASs in the anterior part of earthworm was significantly higher ($p = 0.037 < 0.05$) than in the tail part (Table B-2). If all six PFASs were considered with the confidence level set as 90%, the concentration of six PFASs in the anterior part was also higher ($p = 0.069 < 0.1$) than in the tail part (Table B-1).

3.3.5. Bioconcentration of PFASs in earthworms

In addition to the ingestion pathway, earthworm may also accumulate PFASs from soil pore water. The uptake process of earthworm in the water showed a similar trend (Figure 3.13) as the bioaccumulation study. The bioconcentration factor (BCF) of each PFAS was calculated by Equation (3.6). However, since only the concentration of PFOA could be quantified in the liquid phase, the BCF value of PFOA on day 14 was 10.7 ± 1.2 , which was much higher than the bioaccumulation factor of PFOA. As the initial concentration of each PFAS in water was the same, the bioconcentration ability could be estimated by the PFAS concentration in earthworm on the same day. All earthworms died on day 16 in PFOAB and PFOSB group, and thus, the fourteenth day was selected for the discussion. As shown in Table 3.4, the concentrations of PFOA and PFOS in earthworm were much higher than the concentrations of their precursor compounds. In addition, the concentrations of both zwitterionic poly-PFASs (PFOAB and PFOSB) were lower than the concentrations of cationic poly-PFASs (PFOAAmS and PFOSAmS) in earthworm on day 14.

By comparing the bioconcentration and the bioaccumulation experiments, a conceivable conclusion could be stated that the main approach of the bioaccumulation of PFASs was through the food and the ingestion and that the minor way of PFAS intake was through the pore water. If the primary pathway of PFAS bioaccumulation in earthworm was through the pore water, the BAF values of both zwitterionic poly-PFASs (PFOAB and PFOSB) should be lower than the BAF values of cationic poly-PFASs (PFOAAmS and PFOSAmS). In contrast, the BAF values of PFOAB and PFOSB were higher than their BCF values (Table 3.4). Additionally, based on the adsorption study in Chapter 2, poly-PFASs were easily adsorbed on the soil. The residual concentration of the poly-PFAS in the pore water was at a lower level.

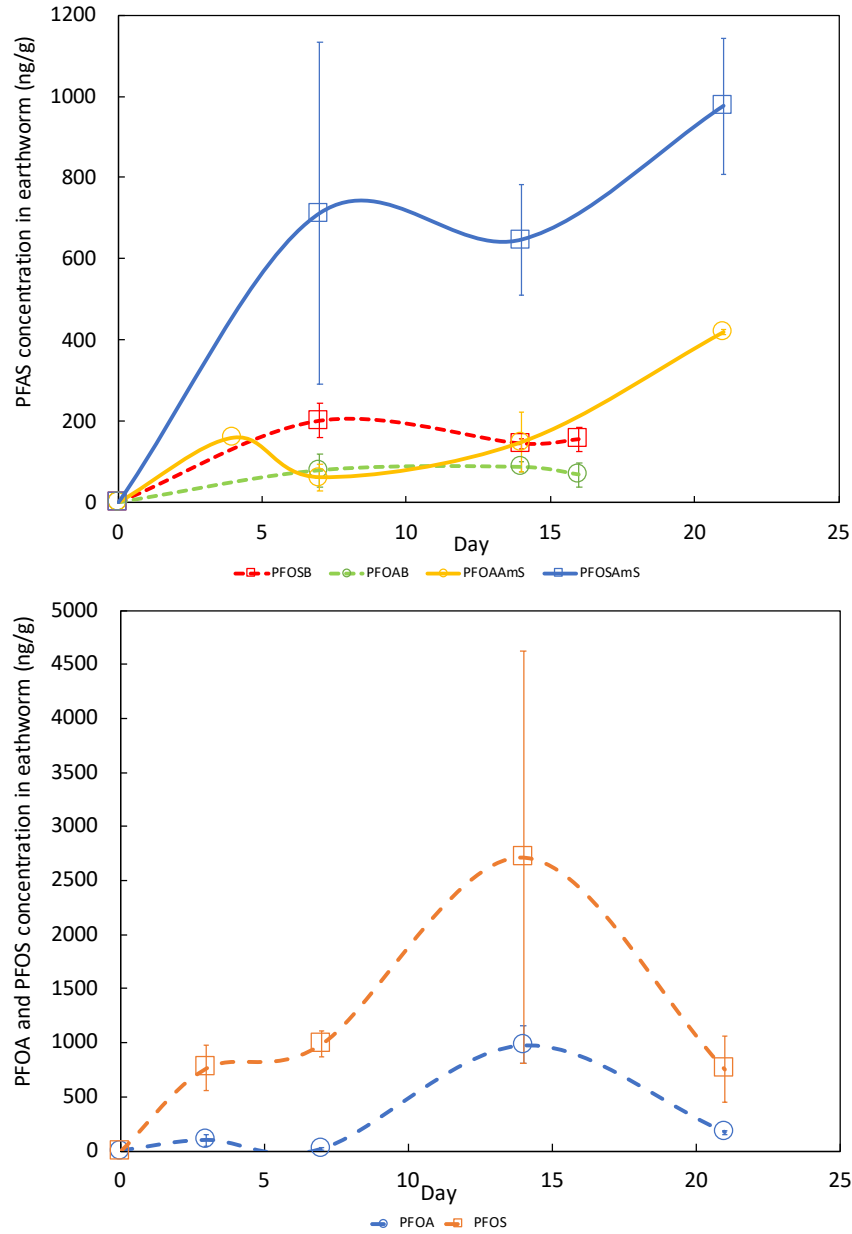


Figure 3.13. Bioconcentration of six PFASs in water experiments.

Table 3.5. Concentration of six PFASs in earthworm on Day 14

Compound	PFOAB	PFOSB	PFOSAmS	PFOAAmS	PFOA	PFOS
Concentration (ng g ⁻¹)	88 ± 13	146 ± 37	646 ± 137	149 ± 73	981 ± 172	2716 ± 1906

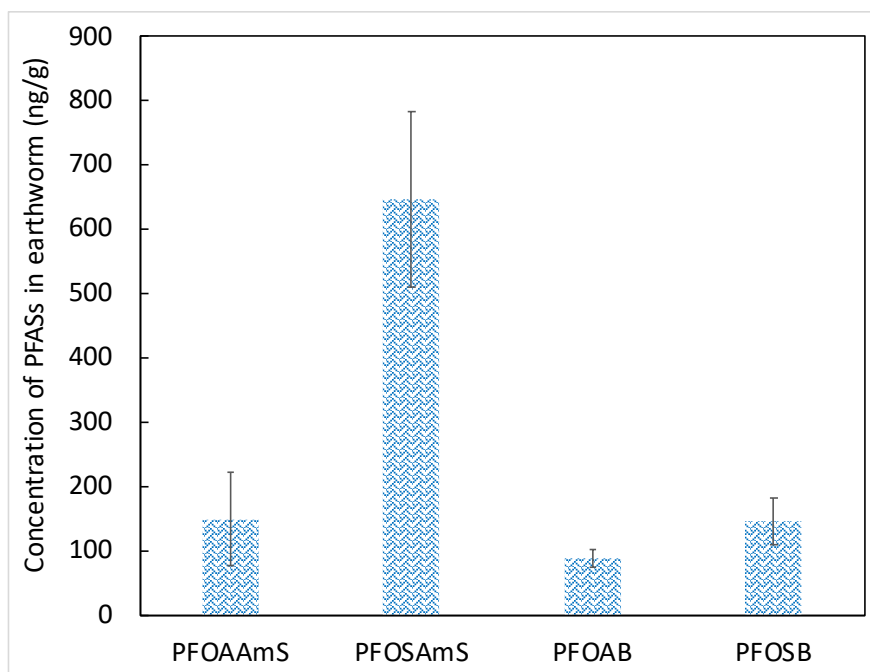


Figure 3.14. Concentration of four poly-PFASs in earthworm on Day 14.

3.3.6. Generation of PFOA and PFOS from the precursor compounds in earthworms

In the first experiment, PFOA and PFOS were found in the earthworm's body in both the uptake and elimination test (Figure 3.15), although PFOA and PFOS were not spiked in the soil. However, it was detected that the stock solution of each precursor compound contained a low concentration of PFOA or PFOS. The mole percentage of PFOA in PFOAB and PFOAAmS is 4.74% and 0.09%, respectively, and the mole percentage of PFOS in PFOSB and PFOSAmS is 1.12% and 0.50%, respectively. Thus, in the first experiment, the initial concentration of PFOA in the soil was approximately $5,000 \mu\text{g kg}^{-1}$ and $100 \mu\text{g kg}^{-1}$ in PFOAB and PFOAAmS group, respectively, and the initial concentration of PFOS in the soil was approximately $1,000 \mu\text{g kg}^{-1}$ and $500 \mu\text{g kg}^{-1}$ in PFOSB and PFOSAmS group, respectively. The comparable situation was observed in the second experiment as well. In the second experiment, the initial concentration of PFOA was approximately $1,000 \mu\text{g kg}^{-1}$ and $20 \mu\text{g kg}^{-1}$ in PFOAB and PFOAAmS group,

respectively, and the initial concentration of PFOS in the soil was approximately $200 \mu\text{g kg}^{-1}$ and $100 \mu\text{g kg}^{-1}$ in PFOsB and PFOsAmS group, respectively.

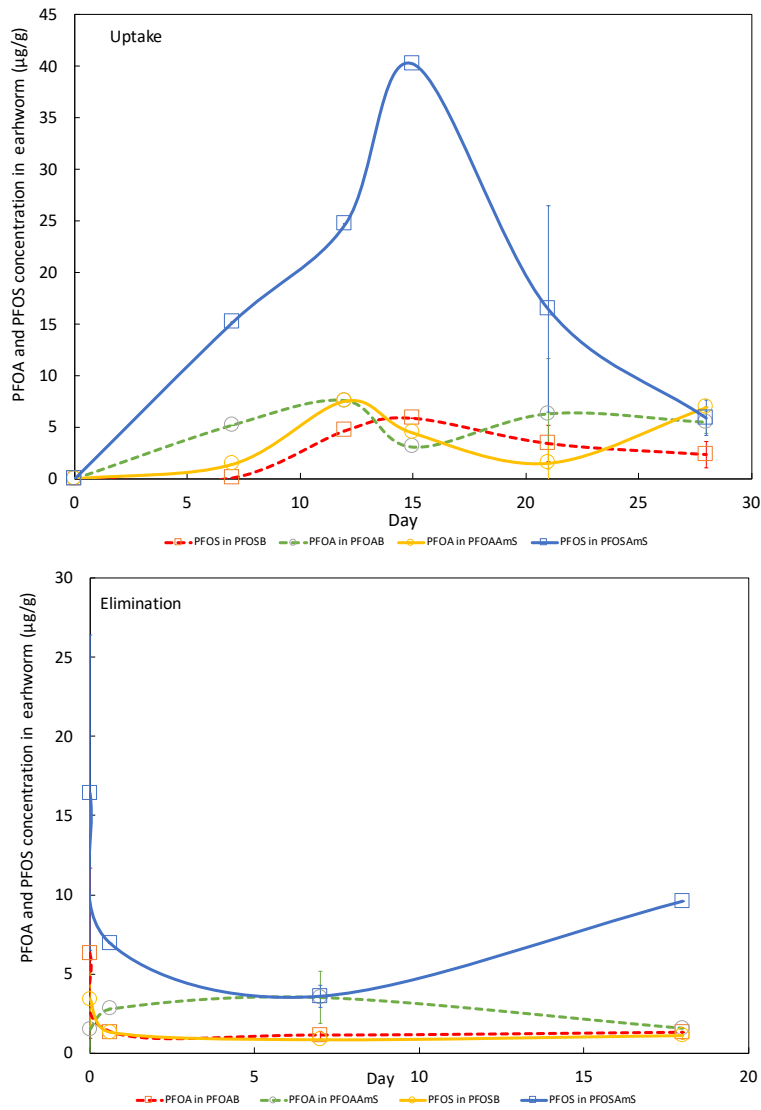


Figure 3.15. PFOA and PFOS were generated from four poly-PFASs in the first bioaccumulation experiment.

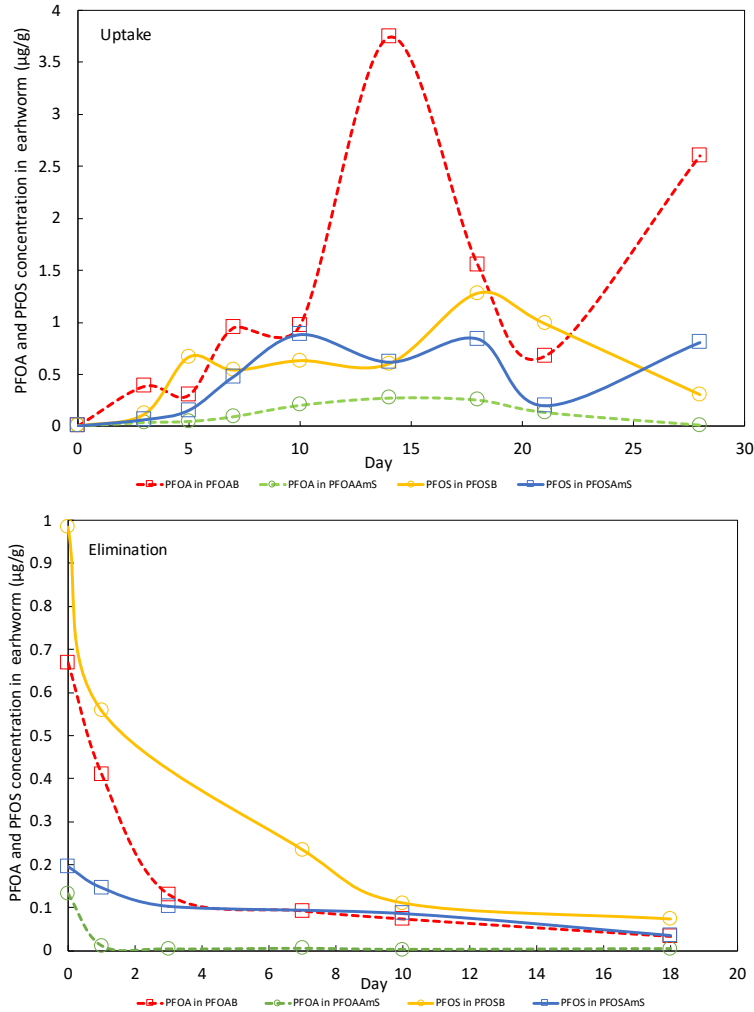


Figure 3.16. PFOA and PFOS were generated from four poly-PFASs in the second bioaccumulation experiment.

Previous studies (Zhao et al., 2016; Mejia-Avenidaño et al., 2016; Wang et al., 2009; Higgins et al., 2007) reported that the biotransformation of PFOA or PFOS precursor compounds could occur in both soil and earthworm. Zhao et al. (2016) and Higgins et al. (2007) both reported that a PFOS precursor compound, N-ethyl perfluorooctane sulfonamide ethanol (N-EtFOSE), could be degraded in organisms, such as earthworms and *L. variegatus*, and soil or sediment. Wang et al. (2009) found a PFOA precursor compound, 8-2 Fluorotelomer alcohol (8-

2 FTOH), could be transformed to PFOA in the soil.

In this study, the reasons that PFOA and PFOS were shown in earthworm could be due to (1) the biotransformation behavior of the precursor compounds in earthworm's body, like through the earthworm's digestion system or circulatory system; (2) the bioaccumulation of PFOA or PFOS directly from the soil; (3) the bioaccumulation of PFOA or PFOS generated through the biodegradation in the soil; and (4) all (1), (2) and (3). Since biodegradation behaviors of poly-PFASs in soil and bioaccumulation behaviors of PFOA and PFOS have been well-studied, what should be focused on was to clearly comprehend whether zwitterionic and cationic poly-PFASs could be transformed in the earthworms' bodies or the organism. We further studied this by (1) comparing the bioaccumulation factors of PFOA and PFOS in groups of precursor compounds and groups of PFOA and PFOS; (2) analyzing the biotransformation pathway; and (3) conducting the bioconcentration experiment in water without any potential soil bacteria.

Firstly, we performed multiple PFOA/PFOS bioaccumulation tests at concentrations similar to the initial concentrations in precursor compounds. If BAF values obtained from PFOA/PFOS uptake tests on day 21 were smaller than BAF values in precursor compound groups, it could support the hypothesis that PFOA and PFOS were generated in earthworm from the precursor compound groups. Based on the estimated concentration of PFOA or PFOS in the precursor compounds, several comparisons among BAF values on day 21 were shown in Figure 3.17 and 3.18. It could be observed that the average BAF values of PFOA and PFOS from their precursor compound groups were higher than BAF values from their own groups. Thus, the results suggested that PFOA or PFOS was generated from their precursor compounds to raise its concentration level in earthworm to make higher BAF values.

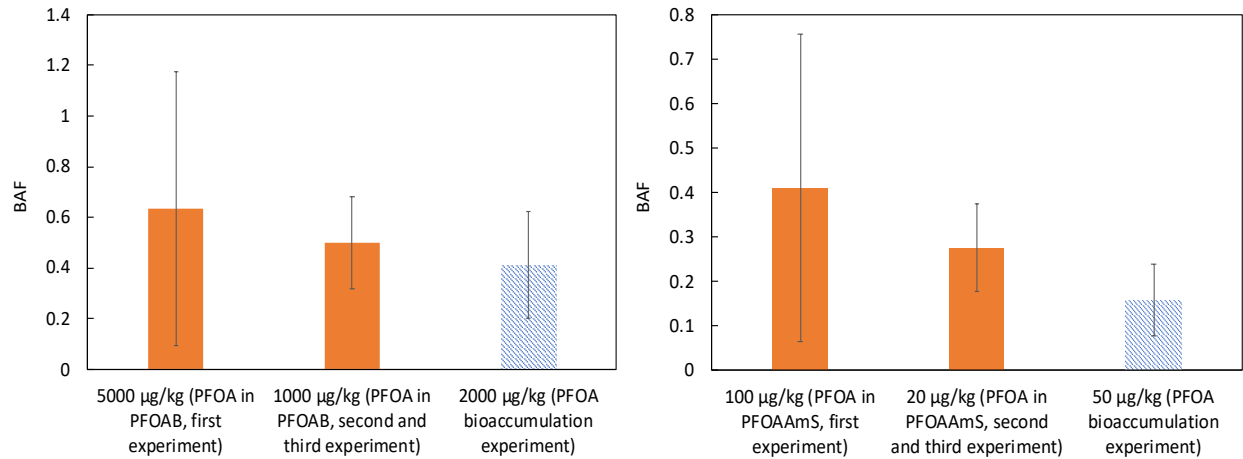


Figure 3.17. BAF values of PFOA from bioaccumulation experiments of PFOA and its precursor compounds.

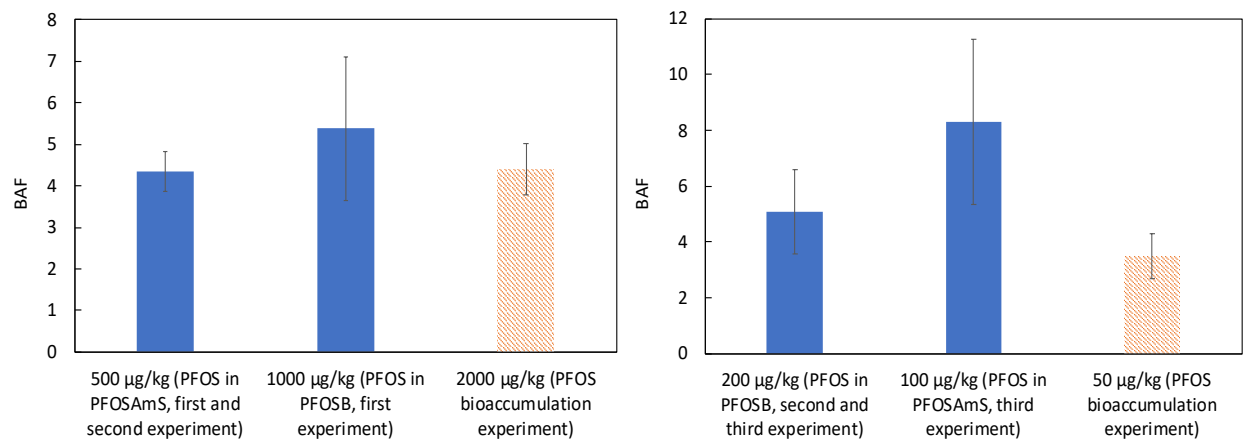
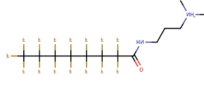


Figure 3.18. BAF values of PFOS from bioaccumulation experiments of PFOS and its precursor compounds.

However, we still lacked sufficient evidence to claim that PFOA and PFOS were generated directly from their precursor compounds in the earthworm since it was not statistically significant ($p > 0.1$) by comparing the means of BAF values of PFOA or PFOS in different groups with “t-test.” In addition, the concentrations of PFOA or PFOS in the soil in poly-PFAS bioaccumulation experiments were not the exact same as the concentration in PFOA or PFOS

bioaccumulation experiment. Thus, it is important to investigate the biotransformation pathway by analyzing intermediate chemicals. Mejia-Avenidaño et al. (2016) reported several potential biodegradation pathways of PFOAAmS and PFOSAmS in the soil. The precursor compounds gradually lost some functional groups in the soil, and were finally converted to PFOA or PFOS, instead of a one-step process. The intermediate PFASs could be analyzed and confirmed by the

MS/MS. Figure 3.19 represented one intermediate PFAS ( , labeled as b) was discovered in MS/MS in positive mode. In this study, four and three biotransformation products were found from PFOAB/PFOSB and PFOAAmS/PFOSAmS groups, respectively. The details of those intermediate PFASs were shown in Table 3.6. Mass accuracy error was applied to verify the potential intermediate PFASs, which was calculated by:

$$\text{Mass accuracy error (ppm)} = \frac{\text{Observed mass} - \text{Theoretical mass}}{\text{Theoretical mass}} \times 10^6 \quad (3.15)$$

If the mass error was over 10 ppm, or sometimes 20 ppm, the selected chemical could not be confirmed.

Mejia-Avenidaño et al. (2016) discovered eleven potential intermediate PFASs (six under ESI+ and five under ESI-) from PFOAAmS and PFOSAmS each during the biodegradation in soil. Xiao et al. (2018) reported that ten confirmed and tentative intermediate PFASs (three under ESI+ and seven under ESI-) were formed from PFOAB, PFOSB, PFOAAmS, and PFOSAmS by ozone or chlorine oxidization. However, other related mass found by previous researchers could not be confirmed in this study due to the large mass error. Except that PFOA and PFOS were discovered under ESI negative mode and that they could be confidently confirmed by the standards, other intermediate PFASs were all tentatively confirmed under ESI positive mode

with unknown chemical structures.

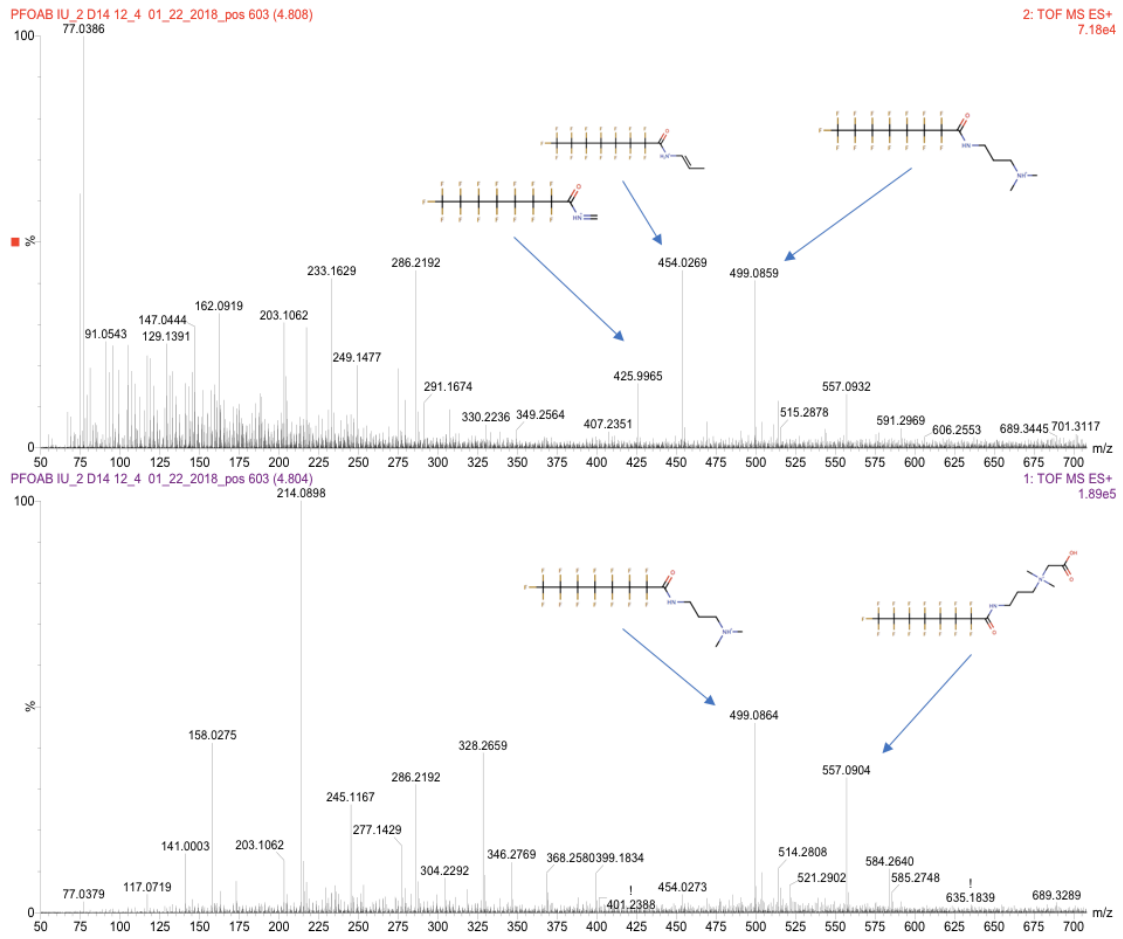


Figure 3.19. Mass spectrum of an intermediate PFAS (labeled as b) in PFOAB group in earthworm.

Table 3.6. Mass information of PFOA, PFOS, PFOA precursor compounds, PFOS precursor compounds, and the intermediate poly-PFASs in earthworm

Compound	Molecular formula	$[M + H]^+$ or $[M - H]^-$	Theoretical m/z value	Observed m/z value	Mass Error (ppm)	Retention time (min)
a. PFOAB	$F(CF_2)_7CONH(CH_2)_3N(CH_3)_2^+CO_2^-$	$C_{15}F_{15}N_2O_3H_{16}^+$	557.0916	557.0911	-0.898	4.81
b.	$F(CF_2)_7CONH(CH_2)_3N(CH_3)_2$	$C_{13}F_{15}N_2OH_{14}^+$	499.0861	499.0864	0.601	4.77
c.	$F(CF_2)_7CONH(CH_2)_3NHCH_3$	$C_{12}F_{15}N_2OH_{12}^+$	485.0710	485.0689	-4.329	4.68
d. PFOAAmS	$F(CF_2)_7CONH(CH_2)_3N(CH_3)_3^+$	$C_{14}F_{15}N_2OH_{16}^+$	513.1017	513.1010	-1.364	4.63
e. PFOA	$F(CF_2)_7COOH$	$C_8F_{15}O_2^-$	412.9664	412.9661	-0.726	4.69
f. PFOSB	$F(CF_2)_8SO_2NH(CH_2)_3N(CH_3)_2^+CO_2^-$	$C_{15}F_{17}SN_2O_4H_{16}^+$	643.0554	643.0551	-0.467	5.23
g. PFOSAmS	$F(CF_2)_8SO_2NH(CH_2)_3N(CH_3)_3^+$	$C_{14}F_{17}SN_2O_2H_{16}^+$	599.0656	599.0647	-1.502	5.12
h.	$F(CF_2)_8SO_2NH(CH_2)_3N(CH_3)_2$	$C_{13}F_{17}SN_2O_2H_{14}^+$	585.0499	585.0515	2.735	5.26
i.	$F(CF_2)_8SO_2NH(CH_2)_3NHCH_3$	$C_{12}F_{17}SN_2O_2H_{12}^+$	571.0343	571.0336	-1.226	5.18
j. PFOS	$F(CF_2)_8SO_3H$	$C_8F_{17}SO_3^-$	498.9302	498.9290	-2.405	4.99

The prospective bioconversion pathways of PFOA precursor compounds and PFOS precursor compounds were displayed in Figure 3.20 and 3.21, respectively. In some samples, PFOAB or PFOSB was easier to be transformed directly to chemical b or h instead of firstly being transformed to PFOAAmS or PFOSAmS.

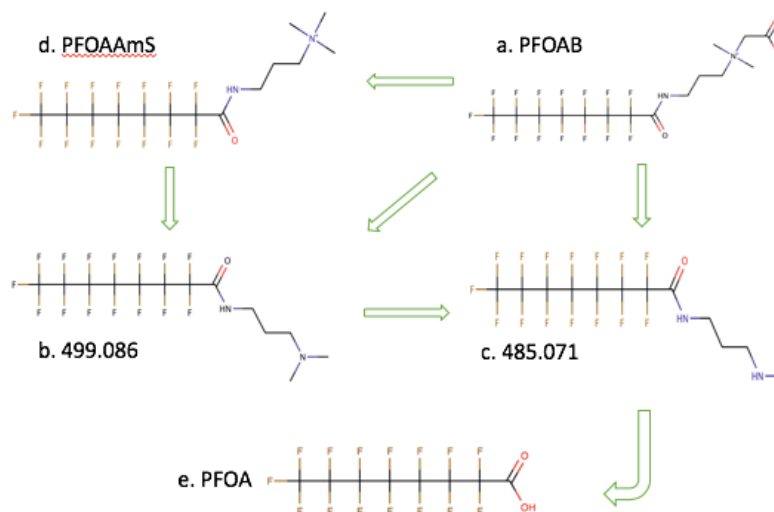


Figure 3.20. Predicted biotransformation pathway of PFOAB and PFOAAmS.

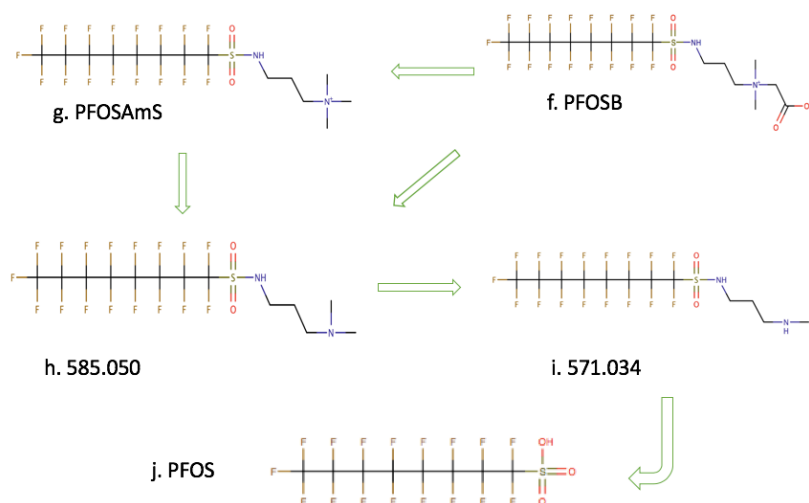


Figure 3.21. Predicted biotransformation pathway of PFOSB and PFOSAmS.

The ratio between the peak heights of the intermediate PFAS and its precursor compounds was employed to conduct the semi-quantitative analysis during the uptake process in the third experiment. From Figure 3.22, intermediate b. and c. had similar trends as the uptake of PFOAB in earthworm that the amount of PFAS increased and reached the maximum on day 14, and then decreased. PFOAAmS and PFOA from PFOAB group in earthworm raised all the time during the uptake with a decreasing and an increasing growth rate, respectively. From Figure 3.22 and 3.23, intermediate b. and c. from PFOAAmS group grew sustainably in 21 days. Although the ratios of PFOA from PFOAB and PFOAAmS groups in earthworm were lower than the ratios in soil, the higher ratios of intermediate PFASs were supposed to support the generation of PFOA. Figure 3.24 and 3.25 displayed the dynamics of intermediate PFASs from PFOSAmS and PFOSB group, respectively. The ratios of all intermediate PFASs from PFOSB and PFOSAmS groups in earthworm were higher than the ratios in soil. Thus, the generation of PFOS from PFOSB and PFOSAmS could be confidently confirmed. Also, the intermediate

PFASs were discovered in earthworm bioconcentration test in water. Since there were no soil bacteria in the water, it could help confirm that PFOA and PFOS were generated from their precursor compounds by the earthworm.

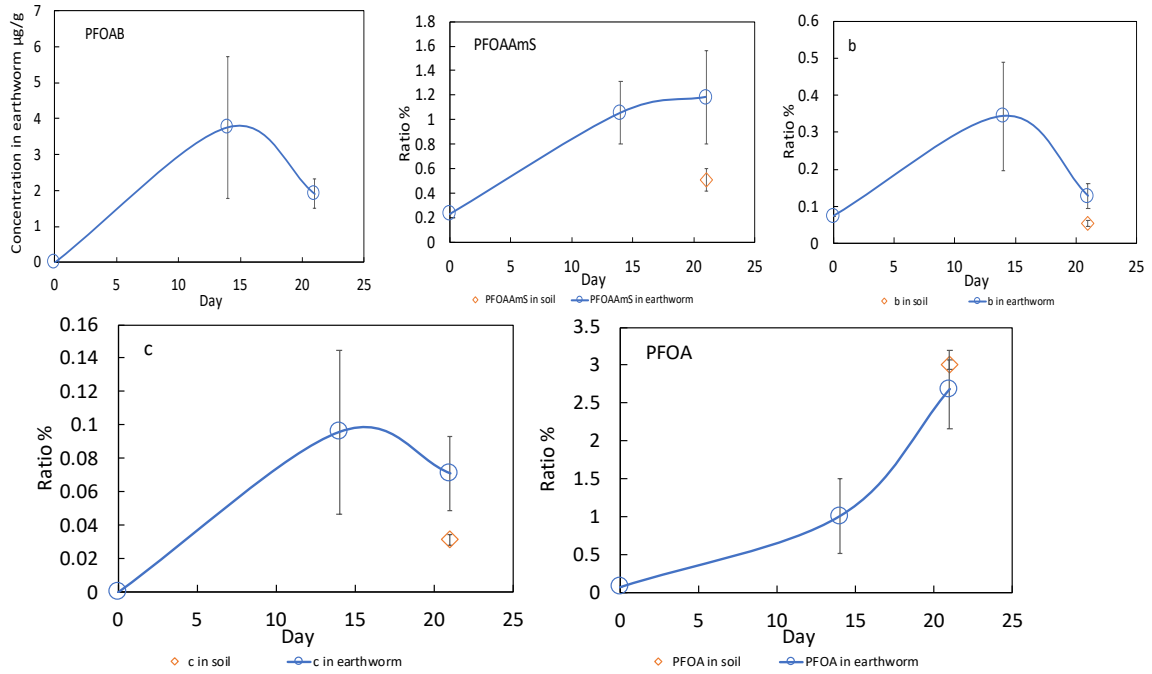


Figure 3.22. Intermediate PFASs in PFOAB group in earthworm and soil.

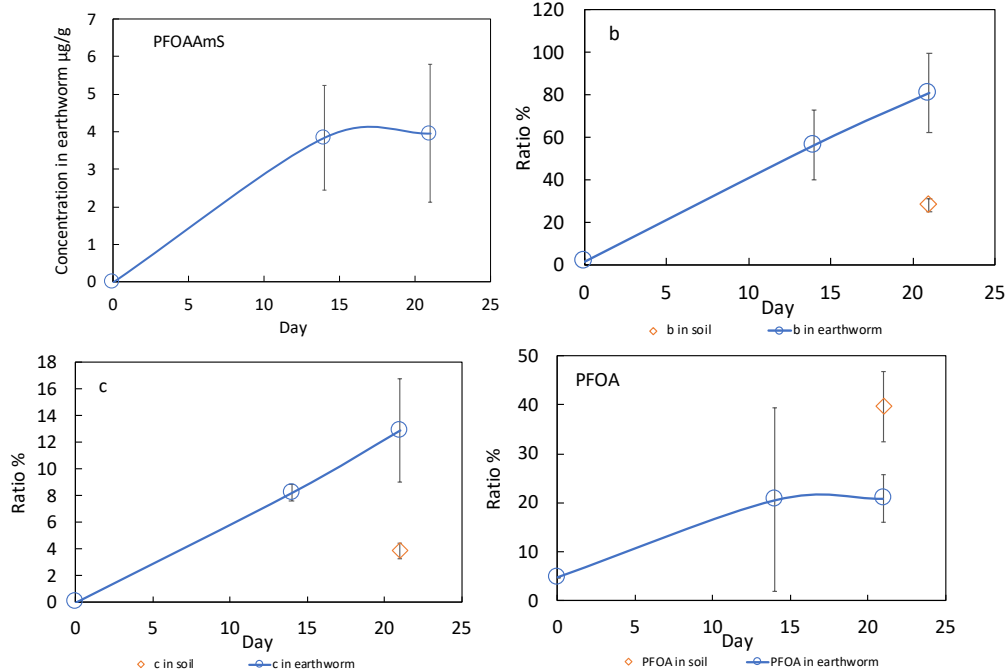


Figure 3.23. Intermediate PFASs in PFOAAmS group in earthworm and soil.

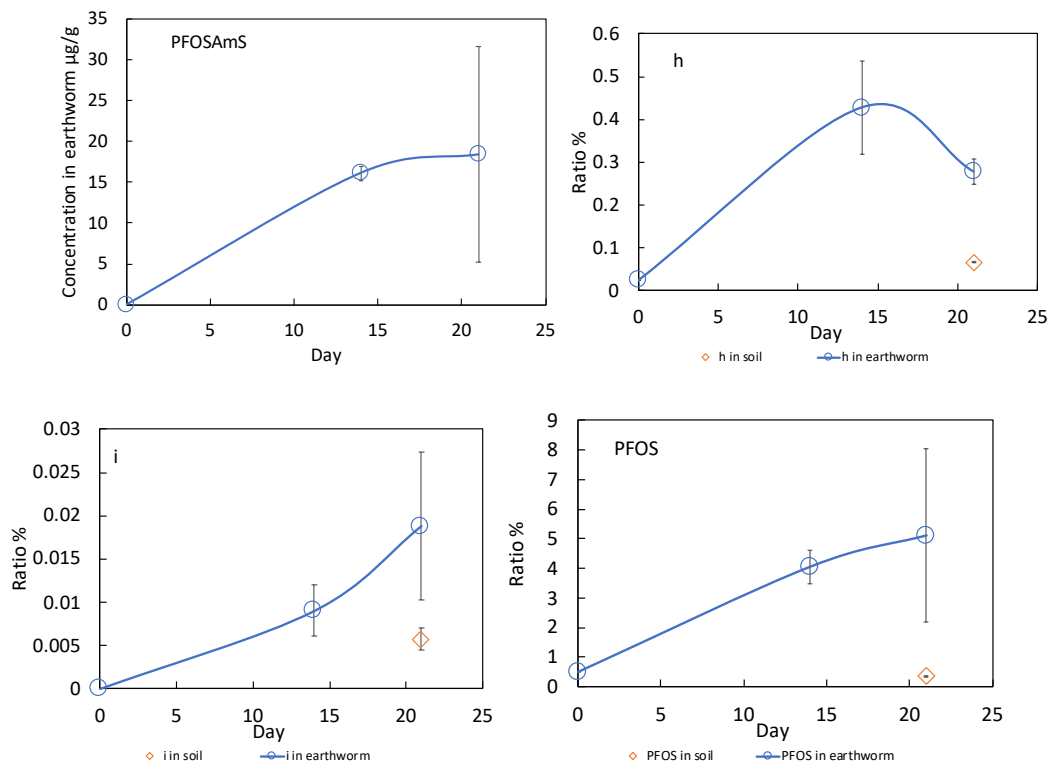


Figure 3.24. Intermediate PFASs in PFOSAmS group in earthworm and soil.

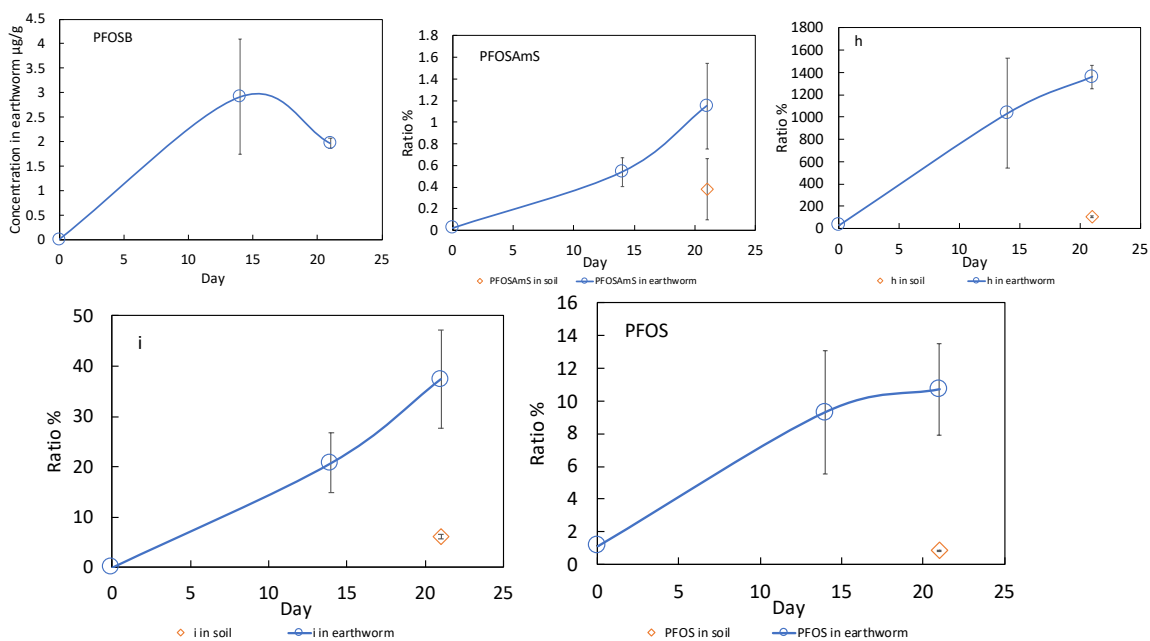


Figure 3.25. Intermediate PFASs in PFOSB group in earthworm and soil.

Previous researchers have developed several mechanisms of degradation of poly-PFASs in organisms. Benskin et al. (2009) found that a model PFOS-precursor (N-ethylperfluorooctane sulfonamide, NEtFOSA) was degraded by Cytochrome P450 isozymes and membrane-bound enzymes (human liver microsomes). Fasano et al. (2006) reported that the PFOA precursor, 8-2 FTOH could be degraded by enzymes of the mercapturic acid pathway. In addition, several important enzymes, such as cholinesterase and carboxylesterase in earthworm were confirmed by Rault et al. (2007) and Sánchez-Hernández and Wheelock (2009), respectively, for the degradation activity of organic chemicals. By comparing the ratio of intermediate PFASs in the precursor compounds in the “head” part and the “tail” part of earthworm, the enzyme activities on biotransformation could be supported that the ratio in the “head” part with more protein (or enzyme) was higher. However, in the present study, we did not measure the specific enzymes that would help degrade PFASs.

Chapter 4: Conclusions and Recommendations to Future Work

It is important to understand the environmental behaviors of emerging contaminants by investigating how they are distributed in the water-soil system and the organism-soil system. In this research, we developed the mechanisms of sorption and desorption of cationic and zwitterionic poly-PFASs on five soils and studied the bioaccumulation and biotransformation of these chemicals in the earthworm.

The adsorption abilities of two precursor compounds of PFOA, PFOAAmS, and PFOAB, were much higher than PFOA on all five soils. The main factor was due to the positive charge in the cationic and the zwitterionic poly-PFAS, respectively, which could be estimated by zeta potentials, and the related calculation results of adsorption Gibbs free energy. In addition, the soil organic matter or the soil organic carbon had a significant effect on the soil adsorption of PFOAAmS. Other soil properties, such as the BET surface area and the cation exchange capacity could also affect the adsorption of PFOAAmS. Furthermore, with the increase of monovalent cation (e.g., Na^+) in the liquid phase, the adsorption of anionic PFAS (e.g., PFOA) on soil was enhanced, while the adsorption of cationic PFAS (e.g., PFOAAmS) on soil was decreased, which could be explained by the double layer theory. The desorption hysteresis was observed in PFOAB on CE, SW, NF and BS soils.

PFOA, PFOS and their precursor compounds, PFOAB, PFOAAmS, PFOSB, and

PFOSAmS were all readily bioaccumulated by earthworm. The BAF value of PFOS was observed the highest one in all the experiments. The order of BAF value was PFOAB > PFOSB > PFOSAmS > PFOAAmS in the first bioaccumulation experiment. The BAF value was also likely to be concentration dependent, and it decreased with the increasing concentration of PFAS. The “free binding” theory developed by Liu et al. (2011) who postulated the bioaccumulation of PFASs in green mussels (*Perna viridis*) as an “adsorption-like” process, was able to explain some of the experimental results. Moreover, the generation of PFOA and PFOS from their precursor compounds in earthworm body was confirmed by (1) comparing the BAF values of PFOA and PFOS among the precursors’ groups and the solo groups, (2) studying the degradation byproducts in earthworm’s body, and (3) bioconcentration experiment.

Some important physicochemical properties, as well as the bioaccumulation and biotransformation behaviors of several typical cationic and zwitterionic poly-PFASs have been investigated, and thus, the potential environmental fate and the transport pathways of the emerging PFASs in the aquatic and terrestrial ecosystems could be estimated according to this research. Future studies are needed to develop novel treatment systems and remediation technologies for PFAS removal from drinking water and wastewater. In addition, it is important to investigate the mechanism of PFAS biotransformation in organisms by studying the enzymes.

REFERENCES

- Giesy, J. P. and Kannan, K. Peer Reviewed: Perfluorochemical Surfactants in the Environment. *Environ. Sci. Technol.* **2002**, *36* (7), 146A–152A.
- Wang, Z.; DeWitt, J. C.; Higgins, C. P.; Cousins, I. T. A Never-Ending Story of Per- and Polyfluoroalkyl Substances (PFASs)? *Environ. Sci. Technol.* **2017**, *51*, 2508–2518.
- Prevedouros, K.; Cousins, I. T.; Buck, R. C.; Korzeniowski, S. H. Sources, Fate and Transport of Perfluorocarboxylates. *Environ. Sci. Technol.* **2006**, *40* (1), 32–44.
- Barzen-Hanson, K. A.; Roberts, S. C.; Choyke, S.; Oetjen, K.; McAlees, A.; Riddell, N.; McCrindle, R.; Ferguson, P. L.; Higgins, C. P.; Field, J. A. Discovery of 40 Classes of Per- and Polyfluoroalkyl Substances in Historical Aqueous Film-Forming Foams (AFFFs) and AFFF-Impacted Groundwater. *Environ. Sci. Technol.* **2017**, *51* (4), 2047–2057.
- Xiao, X.; Ulrich, B. A.; Chen, B.; Higgins, C. P. Sorption of Poly- and Perfluoroalkyl Substances (PFASs) Relevant to Aqueous Film-Forming Foam (AFFF)-Impacted Groundwater by Biochars and Activated Carbon. *Environ. Sci. Technol.* **2017**, *51* (11), 6342–6351.
- Kishi, T.; Arai, M. Study on the generation of perfluorooctane sulfonate from the aqueous film forming foam. *J. Hazard. Mater.* **2008**, *159*, 81–86.
- Thomas, P. The use of fluoropolymers for non-stick cooking utensils. *Surf. Coat. Int.* **1998**, *81* (12), 604–609.
- Sperati, C. A. Polytetrafluoroethylene: History of its Development and some Recent Advances. In *High Performance Polymers: Their Origin and Development*; Seymour, R. B., Kirshenbaum, G. S., Eds.; Elsevier Science Publishing Co., Inc.: New York, USA, 1986; pp 267–278.
- Harris, M. H.; Rifas-Shiman, S. L.; Calafat, A. M.; Ye, X.; Mora, A. M.; Webster, T. F.; Oken, E.; Sagiv, S. K. Predictors of Per- and Polyfluoroalkyl Substance (PFAS) Plasma Concentrations in 6–10 Year Old American Children. *Environ. Sci. Technol.* **2017**, *51* (9), 5193–5204.
- Holmström, K. E.; Järnberg U.; Bignert, A. Temporal trends of PFOS and PFOA in guillemot eggs from the Baltic Sea, 1968- 2003. *Environ. Sci. Technol.* **2005**, *39*, 80–84.
- Taniyasu, S.; Kannan, K.; Horii, Y.; Hanari, N.; Yamashita, N. A survey of perfluorooctane sulfonate and related perfluorinated organic compounds in water, fish, birds, and humans from Japan. *Environ. Sci. Technol.* **2003**, *37*, 2634–2639.
- Olsen, G. W.; Church, T.; Miller J. P.; Burris, J. M.; Hansen, K. J.; Lundberg, J. K. Perfluorooctanesulfonate and other fluorochemicals in the serum of American Red Cross adult blood donors. *Environ. Health Perspect.* **2003**, *111*, 1892–1901.

Van de Vijver, K. I.; Hoff, P. T.; Van Dongen, W.; Esmans, E. L.; Blust, R.; de Coen, W. Exposure patterns of perfluorooctane sulfonate in aquatic invertebrates from the Western Scheldt estuary and the Southern North Sea. *Environ. Toxicol. Chem.* **2003**, *22*, 2037–2041.

Butt, C. M.; Mabury, S. A.; Kwan, M.; Wang, X.; Muir, D. C. Spatial trends of perfluoroalkyl compounds in ringed seals (*Phoca hispida*) from the Canadian Arctic. *Environ. Toxicol. Chem.* **2008**, *27* (3), 542–53.

Guyton, K. Z.; Chiu, W. A.; Bateson, T. F.; Jinot, J.; Scott, C. S.; Brown, R. C.; Caldwell, J. C. A reexamination of the PPAR- α activation mode of action as a basis for assessing human cancer risks of environmental contaminants. *Environ. Health Perspect.* **2009**, *117*, 1664–1672.

U.S. EPA (Environmental Protection Agency). 2005. Draft Risk Assessment of the Potential Human Health Effects Associated with Exposure to Perfluorooctanoic Acids and Its Salts. Available: <http://www.epa.gov/oppt/pfoa/pubs/pfoarisk.pdf> [accessed 7 July 2010].

U.S. EPA (Environmental Protection Agency). 2006. Scientific Advisory Board's Response to EPA's Draft Risk Assessment [Letter]. Available: http://www.epa.gov/sab/pdf/sab_06_006.pdf [accessed 7 July 2010].

Lau, C.; Anitole, K.; Hodes, C.; Lai, D.; Pfahles-Hutchens, A.; Seed, J. Perfluoroalkyl acids: a review of monitoring and toxicological findings. *Toxicol. Sci.* **2007**, *99* (2), 366–94.

Lau, C.; Thibodeaux, J.; Hanson, R.; Rogers, J.; Grey, B.; Stanton, M.; Butenhoff, J.; Stevenson, L. Exposure to perfluorooctane sulfonate during pregnancy in rat and mouse. II: postnatal evaluation. *Toxicol. Sci.* **2003**, *74*, 382.

Martin, J. W.; Whittle, D. M.; Muir, D. C. G.; Mabury, S. A. Perfluoroalkyl contaminants in a food web from Lake Ontario. *Environ. Sci. Technol.* **2004**, *38*, 5379–5385.

Martin, J. W.; Mabury, S. A.; Solomon, K. R.; Muir, D. C. G. Bioconcentration and tissue distribution of perfluorinated acids in rainbow trout (*Oncorhynchus mykiss*). *Environ. Toxicol. Chem.* **2003**, *22*, 196–204.

Schultz, M. M.; Barofsky, D. F.; Field, J. A. Fluorinated alkyl surfactants. *Environ. Eng. Sci.* **2003**, *20*, 487–501.

Hekster, F. M.; Laane, R. W. P. M.; de Voogt, P. Environmental and toxicity effects of perfluoroalkylated substances. *Rev. Environ. Contam. Toxicol.* **2003**, *179*, 99–121.

Wang, T.; Wang, Y.; Liao, C.; Cai, Y.; Jiang, G. Perspectives on the inclusion of perfluorooctane sulfonate into the Stockholm convention on persistent organic pollutants. *Environ. Sci. Technol.* **2009**, *43*, 5171–5175.

U.S. EPA (Environmental Protection Agency). 2013. The third unregulated contaminant monitoring rule (UCMR 3): data summary. EPA, Washington DC.

Fang, C.; Zhang, X.; Dong, Z.; Wang, L.; Megharaj, M.; Naidu, R. Smartphone app-based/portable sensor for the detection of fluoro-surfactant PFOA. *Chemosphere* **2018**, *191*, 381–388.

Kato, K.; Wong, L. Y.; Jia, L. T.; Kuklennyik, Z.; Calafat, A. M. Trends in exposure to polyfluoroalkyl chemicals in the U.S. Population: 1999–2008. *Environ. Sci. Technol.* **2011**, *45* (19), 8037–8045.

Olsen, G. W.; Mair, d. C.; Lange, C. C.; Harrington, L. M.; Church, T. R.; Goldberg, C. L.; Herron, R. M.; Hanna, H.; Nobiletti, J. B.; Rios, J. A.; Reagen, W. K.; Ley, C. A. Per-and polyfluoroalkyl substances (PFAS) in American Red Cross adult blood donors, 2000–2015. *Environ. Res.* **2017**, *157*, 87–95.

Paul, A. G.; Jones, K. C.; Sweetman, A. J. A first global production, emission, and environmental inventory for perfluorooctane sulfonate. *Environ. Sci. Technol.* **2009**, *43*, 386–392.

Sunderland, E. M.; Hu, X. C.; Dassuncao, C.; Tokranov, A. K.; Wagner, C. C.; Allen, J. G. A review of the pathways of human exposure to poly- and perfluoroalkyl substances (PFASs) and present understanding of health effects. *J. Exposure Sci. Environ. Epidemiol.* **2019**, *29*, 131–147.

Papadopoulou, E.; Sabaredzovic, A.; Namork, E.; Nygaard, U. C.; Granum, B.; Haug, L. S. Exposure of Norwegian toddlers to perfluoroalkyl substances (PFAS): The association with breastfeeding and maternal PFAS concentrations. *Environ. Int.* **2016**, *94*, 687–694.

Gyllenhammar, I.; Benskin, J. P.; Sandblom, O.; Berger, U.; Ahrens, L.; Lignell, S.; Wiberg, K.; Glynn, A. Perfluoroalkyl acids (PFAAS) in serum from 2-4-month-old infants: influence of maternal serum concentration, gestational age, breast-feeding, and contaminated drinking water. *Environ. Sci. Technol.* **2018**, *52* (12), 7101–7110.

Lang, J. R.; Allred, B. M.; Peaslee, G. F.; Field, J. A.; Barlaz, M. A. Release of per- and polyfluoroalkyl substances (PFASs) from carpet and clothing in model anaerobic landfill reactors. *Environ Sci Technol.* **2016**, *50* (10), 5024–5032.

Benskin, J. P.; Li, B.; Ikononou, M. G.; Grace, J. R.; Li, L. Y. Per- and polyfluoroalkyl substances in landfill leachate: Patterns, time trends, and sources. *Environ. Sci. Technol.* **2012**, *46* (21), 11532–11540.

Allred, B. M.; Lang, J. R.; Barlaz, M. A.; Field, J. A. Physical and biological release of poly- and perfluoroalkyl substances (PFASs) from municipal solid waste in anaerobic model landfill reactors. *Environ Sci Technol.* **2015**, *49* (13), 7648–7656.

Lei, Y. D.; Wania, F.; Mathers, D.; Mabury, S. A. Determination of vapor pressures, octanol-air, water-air partition coefficients for polyfluorinated sulfonamide, sulfonamidoethanols, and telomere alcohols. *J. Chem. Eng. Data* **2004**, *49*, 1013–1022.

Vallero D. Fundamentals of air pollution (Fifth Edition). Academic Press, 2014, pp 963–970.
Conder, J. M.; Hoke, R. A.; De Wolf, W.; Russell, M. H.; Buck, R. C. Are PFCAs bioaccumulative? A critical review and comparison with regulatory criteria and persistent lipophilic compounds. *Environ. Sci. Technol.* **2008**, *42*, 995–1003.

Steenland, K.; Fletcher, T.; Savitz, D. A. Epidemiologic evidence on the health effects of perfluorooctanoic acid (PFOA). *Environ. Health Perspect.* **2010**, *118* (8), 1100–1108.

Jantzen, C. E.; Toor, F.; Annunziato, K. A.; Cooper, K. R. Effects of chronic perfluorooctanoic acid (PFOA) at low concentration on morphometrics, gene expression, and fecundity in zebrafish (*Danio rerio*). *Reprod. Toxicol.* **2017**, *69*, 34–42.

Li, X.; Wang, Z.; Klaunig, J. E. The effects of perfluorooctanoate on high fat diet induced non-alcoholic fatty liver disease in mice. *Toxicology* **2019**, *416*, 1–14.

Butenhoff, J.; Costa, G.; Elcombe, C.; Farrar, D.; Hansen, K.; Iwai, H.; Jung, R.; Kennedy, G.; Lieder, P.; Olsen, G.; Thomford, P. Toxicity of ammonium perfluorooctanoate in male cynomolgus monkeys after oral dosing for 6 months. *Toxicol. Sci.* **2002**, *69* 244–257.

Bhatarai, B.; Gramatica, P. Oral LD50 Toxicity Modeling and Prediction of Per- and Polyfluorinated Chemicals on Rat and Mouse. *Mol. Diversity* **2011**, *15*, 467–476.

Yuan, Z.; Zhang, J.; Zhao, L.; Li, J.; Liu, H. Effects of perfluorooctanoic acid and perfluorooctane sulfonate on acute toxicity, superoxide dismutase, and cellulase activity in the earthworm *Eisenia fetida*. *Environ. Sci. Pollut. Res.* **2017**, *24* (22), 1–7.

Anderson-Mahoney, P.; Kotlerman, J.; Takhar, H.; Gray, D.; Dahlgren, J. Self-reported health effects among community residents exposed to perfluorooctanoate. *New. Solut.* **2008**, *18*, 129–143.

Daly, E.R.; Chan, B.P.; Talbot, E.A.; Nassif, J.; Bean, C.; Cavallo, S.J.; Metcalf, E.; Simone, K.; Woolf, A.D. Per-and polyfluoroalkyl substance (PFAS) exposure assessment in a community exposed to contaminated drinking water, New Hampshire, 2015. *Int. J. Hyg. Environ. Health* **2018**, *221* (3), 569–577.

Winkens, K.; Vestergren, R.; Berger, U.; Cousins, I. T. Early life exposure to per- and polyfluoroalkyl substances (PFASs): A critical review. *Emerging Contaminants* **2017**, *3* (2), 55–68.

Butenhoff, J. L.; Kennedy, G. L.; Frame, S. R.; O'Connor, J. C.; York, R. G. The reproductive toxicology of ammonium perfluorooctanoate (APFO) in the rat. *Toxicology* **2004**, *196* (1-2), 95–116.

Yang, Q; Abedi-Valugerdi, M.; Xie, Y.; Zhao, X. Y.; Möller, G.; Nelson, B. D.; DePierre, J. W. Potent suppression of the adaptive immune response in mice upon dietary exposure to the potent peroxisome proliferator, perfluorooctanoic acid. *Int. Immunopharmacol.* **2002**, *2* (2-3), 389–397.

Zhao, S.; Zhu, L.; Liu, L.; Liu, Z.; Zhang, Y. Bioaccumulation of perfluoroalkyl carboxylates (PFCAs) and perfluoroalkane sulfonates (PFASs) by earthworms (*Eisenia fetida*) in soil. *Environ. Pollut.* **2013**, *179* (0), 45–52.

Liu, C.; Gin, K. Y. H.; Chang, V. W. C.; Goh, B. P. L.; Reinhard, M. Novel Perspectives on the Bioaccumulation of PFCs – the Concentration Dependency. *Environ. Sci. Technol.* **2011**, *45* (22), 9758–9764.

Gebbink, W. A.; van Asseldonk, L.; van Leeuwen, S. P. J. Presence of emerging per- and polyfluoroalkyl substances (PFASs) in river and drinking water near a fluorochemical production plant in The Netherlands. *Environ. Sci. Technol.* **2017**, *51* (19), 11057–11065.

Farré, M.; Barceló, D. Analysis of emerging contaminants in food. *TrAC, Trends Anal. Chem.* **2013**, *43*, 240–253.

Backe, W. J.; Day, T. C.; Field, J. A. Zwitterionic, cationic, and anionic fluorinated chemicals in aqueous film forming foam formulations and groundwater from US military bases by nonaqueous large-volume injection HPLC-MS/MS. *Environ. Sci. Technol.* **2013**, *47* (10), 5226–5234.

Munoz, G.; Duy, S. V.; Labadie, P.; Botta, F.; Budzinski, H.; Lestremau, F.; Liu, J.; Sauve, S. Analysis of zwitterionic, cationic, and anionic poly- and perfluoroalkyl surfactants in sediments by liquid chromatography polarity-switching electrospray ionization coupled to high resolution mass spectrometry. *Talanta* **2016**, *152*, 447–456.

Xiao, X.; Ulrich, B. A.; Chen, B.; Higgins, C. P. Sorption of Poly- and Perfluoroalkyl Substances (PFASs) Relevant to Aqueous Film-Forming Foam (AFFF)-Impacted Groundwater by Biochars and Activated Carbon. *Environ. Sci. Technol.* **2017**, *51* (11), 6342–6351.

Ahrens, L.; Bundschuh, M. Fate and effects of poly- and perfluoroalkyl substances in the aquatic environment: A review. *Environ. Toxicol. Chem.* **2014**, *33* (9), 1921–1929.

Schaider, L. A.; Balan, S.; Blum, A.; Andrews, D. Q.; Strynar, M. J.; Dickinson, M. E. L.; David, M.; Lang, J. R.; Peaslee, G. F. Fluorinated compounds in U.S. fast food packaging. *Environ. Sci. Technol. Lett.* **2017**, *4* (3), 105–111.

Ahrens, L. Polyfluoroalkyl compounds in the aquatic environment: a review of their occurrence and fate. *J. Environ. Monit.* **2011**, *13*, 20–31.

Xiao, F.; Simcik, M. F.; Halbach, T. R.; Gulliver, J. S. Perfluorooctane sulfonate (PFOS) and perfluorooctanoate (PFOA) in soils and groundwater of a U.S. metropolitan area: Migration and implications for human exposure. *Water Res.* **2015**, *72*, 64–74.

Xiao, F.; Simcik, M. F.; Gulliver, J. S. Perfluoroalkyl Acids in Urban Stormwater Runoff: Influence of Land Use. *Water Res.* **2012a**, *46* (20), 6601–6608.

Xiao, F.; Halbach, T. R.; Simcik, M. F.; Gulliver, J. S. Input characterization of perfluoroalkyl substances in wastewater treatment plants: Source discrimination by exploratory data analysis. *Water Res.* **2012b**, *46* (9), 3101–3109.

Gebbink, W.A.; Bossi, R.; Rigét, F.F.; Rosing-Asvid, A.; Sonne, C.; Dietz, R. Observation of emerging per- and polyfluoroalkyl substances (PFASs) in Greenland marine mammals. *Chemosphere* **2016**, *144*, 2384–2391.

Dassuncao, C.; Hu, X. C.; Nielsen, F.; Weihe, P.; Grandjean, P.; Sunderland, E. M. Shifting global exposures to poly- and perfluoroalkyl substances (PFASs) evident in longitudinal birth cohorts from a seafood-consuming population. *Environ. Sci. Technol.* **2018**, *52* (6), 3738–3747.

Miller, A.; Elliott, J. E.; Elliott, K. H.; Lee, S.; Cyr, F. Temporal trends of perfluoroalkyl substances (PFAS) in eggs of coastal and offshore birds: increasing PFAS levels associated with offshore bird species breeding on the Pacific coast of Canada and wintering near Asia. *Environ. Toxicol. Chem.* **2015**, *34*, 1799–1808.

Xiao, F.; Golovko, S. A.; Golovko, M. Y. Identification of Novel Non-Ionic, Cationic, Zwitterionic, and Anionic Polyfluoroalkyl Substances Using UPLC–TOF–MSE High-Resolution Parent Ion Search. *Anal. Chim. Acta* **2017**, *988*, 41–49.

Brusseau, M. L. The influence of molecular structure on the adsorption of PFAS to fluid-fluid interfaces: Using QSPR to predict interfacial adsorption coefficients. *Water Res.* **2019**, *152*, 148–158.

Liu, Y.; Zhang, Y.; Li, J.; Wu, N.; Li, W.; Niu, Z. Distribution, partitioning behavior and positive matrix factorization-based source analysis of legacy and emerging polyfluorinated alkyl substances in the dissolved phase, surface sediment and suspended particulate matter around coastal areas of Bohai Bay, China. *Environ. Pollut.* **2019**, *246*, 34–44.

Xiao, F.; Hanson, R. A.; Golovko, S. A.; Golovko, M. Y.; Arnold, W. A. PFOA and PFOS are generated from zwitterionic and cationic precursor compounds during water disinfection with chlorine or ozone. *Environ. Sci. Technol. Lett.* **2018**, *5* (6), 382–388.

Mejia-Avenidaño, S.; Vo Duy, S.; Sauvé, S.; Liu, J. Generation of Perfluoroalkyl Acids from Aerobic Biotransformation of Quaternary Ammonium Polyfluoroalkyl Surfactants. *Environ. Sci. Technol.* **2016**, *50* (18), 9923–9932.

Xiao, F.; Zhang, X.; Penn, L.; Gulliver, J. S.; Simcik, M. F. Effects of monovalent cations on the competitive adsorption of perfluoroalkyl acids by kaolinite: Experimental studies and modeling. *Environ. Sci. Technol.* **2011**, *45*, 10028–10035.

Higgins, C. P.; Luthy, R. G. Sorption of perfluorinated surfactants on sediments. *Environ. Sci. Technol.* **2006**, *40*, 7251–7256.

Pereira, H. C.; Ullberg, M.; Kleja, D. B.; Gustafsson, J. P.; Ahrens, L. Sorption of perfluoroalkyl substances (PFASs) to an organic soil horizon—effect of cation composition and pH. *Chemosphere* **2018**, *207*, 183–191.

Lee, H.; Mabury, S. A. Sorption of Perfluoroalkyl Phosphonates and Perfluoroalkyl Phosphinates in Soils. *Environ. Sci. Technol.* **2017**, *51*, 3197–3205.

Li, F.; Fang, X.; Zhou, Z.; Liao, X.; Zou, J.; Yuan, B.; Sun, W. Adsorption of perfluorinated acids onto soils: Kinetics, isotherms, and influences of soil properties. *Sci. Total Environ.* **2019**, *649*, 504–514.

Schulte, E. E.; Kaufmann, C.; Peter, B. J. The influence of sample size and heating time on soil weight loss-on-ignition. *Commun. Soil Sci. Plant Anal.* **1991**, *22* (1-2), 159–168.

Beyer, L.; Blume, H. P.; Peters, M. Biological activity and organic matter transformations in typical soils of Schleswig-Holstein. *Geoderma.* **1991**, *49* (3-4), 273–284.

Qiu, L.; Zhang, X.; Cheng, J.; Yin, X. Effects of black locust (*Robinia pseudoacacia*) on soil properties in the loessial gully region of the Loess Plateau, China. *Plant Soil* **2010**, *332* (1-2), 207–217.

Warncke, D.; Brown, J. R. Potassium and Other Basic Cations. In: Recommended Chemical Soil Test Procedures for the North Central Region. 1998. North Central Regional Publication No. 221. NDSU Bull. No. 499. 31–33.

Tang, C. Y.; Fu, Q. S.; Gao, D. W.; Criddle, C. S.; Leckie, J. O. Effect of solution chemistry on the adsorption of perfluorooctane sulfonate onto mineral surfaces. *Water Res.* **2010**, *44*, 2654–2662.

Xiao, F.; Bedane, A. H.; Zhao, J. X.; Mann, M. D.; Pignatello, J. J. Thermal air oxidation changes surface and adsorptive properties of black carbon (char/biochar). *Sci. Total Environ.* **2018**, *618*, 276–283.

Saadati, N.; Abdullah, M. P.; Zakaria, Z.; Tavakoly Sany, S. B.; Rezayi, M.; Hassonizadeh, H. Limit of detection and limit of quantification development procedures for organochlorine pesticides analysis in water and sediment matrices. *Chem. Cent. J.* **2013**, *7* (1), 1–10.

Lu, G. W.; Gao, P. Emulsions and microemulsions for topical and transdermal drug delivery. In: Handbook of non-invasive drug delivery systems. William Andrew Publishing, 2010, 59–94.

Gumustas, M.; Sengel-Turk, C. T.; Gumustas, A.; Ozkan, S. A.; Uslu, B. Chapter 5—Effect of Polymer-Based Nanoparticles on the Assay of Antimicrobial Drug Delivery Systems. In: Multifunctional Systems for Combined Delivery, Biosensing and Diagnostics; Grumezescu, A.M., Ed.; Elsevier: Amsterdam, The Netherlands, 2017, 67–108.

Pan, H.; Marsh, J. N.; Christenson, E. T.; Soman, N. R.; Ivashyna, O.; Lanza, G. M.; Schlesinger, P. H.; Wickline, S. A. Postformulation peptide drug loading of nanostructures. *Methods Enzymol.* **2012**, *508*, 17–39.

Lath, S.; Knight, E. R.; Navarro, D. A.; Kookana, R. S.; McLaughlin, M. J. Sorption of PFOA onto different laboratory materials: Filter membranes and centrifuge tubes. *Chemosphere* **2019**, *222*, 671–678.

Chandramouli, B.; Benskin, J. P.; Hamilton, M. C.; Cosgrove, J. R. Sorption of per- and polyfluoroalkyl substances (PFASs) on filter media: implications for phase partitioning studies. *Environ. Toxicol. Chem.* **2015**, *34* (1), 30–36.

Kwadijk, C. J. A. F.; Velzeboer, I.; Koelmans, A. A. Sorption of Perfluorooctane Sulfonate to Carbon Nanotubes in Aquatic Sediments. *Chemosphere* **2013**, *90* (5), 1631–1636.

Jeon, J.; Kannan, K.; Lim, B. J.; An, K. G.; Kim, S. D. Effects of salinity and organic matter on the partitioning of perfluoroalkyl acid (PFAs) to clay particles. *J. Environ. Monit.* **2011**, *13* (6), 1803–1810.

Huang, W.; Yu, H.; Weber, W. J. J. Hysteresis in the Sorption and Desorption of Hydrophobic Organic Contaminants by Soils and Sediments. 1. A Comparative Analysis of Experimental Protocols. *J. Contam. Hydrol.* **1998**, *31*, 129–148.

Huang, W.; Weber, W. J., Jr. A Distributed Reactivity Model for Sorption by Soils and Sediments. 10. Relationships between Desorption, Hysteresis, and the Chemical Characteristics of Organic Domains. *Environ. Sci. Technol.* **1997**, *31* (9), 2562–2569.

Xiao, F.; Simcik, M. F.; Gulliver, J. S. Mechanisms for removal of perfluorooctane sulfonate (PFOS) and perfluorooctanoate (PFOA) from drinking water by conventional and enhanced coagulation. *Water Res.* **2013**, *47*, 49–56.

Xiao, F.; Zhang, X. R.; Penn, L.; Gulliver, J. S.; Simcik, M. F. Effects of Monovalent Cations on the Competitive Adsorption of Perfluoroalkyl Acids by Kaolinite: Experimental Studies and Modeling. *Environ. Sci. Technol.* **2011**, *45* (23), 10028–10035.

Yukselen, Y.; Kaya, A. Zeta potential of kaolinite in the presence of alkali, alkaline earth and hydrolyzable metal ions. *Water, Air, Soil Pollut.* **2003**, *145*, 155–168.

Jager, T.; Van Der Wal, L.; Fleuren, R. H. L. J.; Barendregt, A.; Hermens, J. L. M. Biaccumulation of organic chemicals in contaminated soils: Evaluation of bioassays with earthworms. *Environ. Sci. Technol.* **2005**, *39*, 293–298.

Woodcroft, M. W.; Ellis, D. A.; Rafferty, S. P.; Burns, D. C.; March, R. E.; Stock, N. L.; Trumpour, K. S.; Yee, J.; Munro, K. Experimental characterization of the mechanism of perfluorocarboxylic acids' liver protein bioaccumulation: The key role of the neutral species. *Environ. Toxicol. Chem.* **2010**, *29* (8), 1669–1677.

Rich, C. D.; Blaine, A. C.; Hundal, L.; Higgins, C. P. Bioaccumulation of perfluoroalkyl acids by earthworms (*Eisenia fetida*) exposed to contaminated soils. *Environ. Sci. Technol.* **2015**, *49* (2), 881–888.

Karnjanapiboonwong, A.; Deb, S. K.; Subbiah, S.; Wang, D.; Anderson, T. A. Perfluoroalkylsulfonic and carboxylic acids in earthworms (*Eisenia fetida*): accumulation and effects results from spiked soils at PFAS bracketing environmental relevance. *Chemosphere* **2018**, *199*, 168–173.

Zhao, S.; Ma, X.; Fang, S.; Zhu, L. Behaviors of N-ethyl perfluorooctane sulfonamide ethanol (N-EtFOSE) in a soil-earthworm system: Transformation and bioaccumulation. *Sci. Total Environ.* **2016**, *554–555*, 186–191.

Higgins, C. P.; McLeod, P. B.; MacManus-Spencer, L. A.; Luthy, R. G. Bioaccumulation of perfluorochemicals in sediments by the aquatic oligochaete *Lumbriculus variegatus*. *Environ. Sci. Technol.* **2007**, *41*, 4600–4606.

Garg, V. K. Vermicomposting: An overview. *Soil Biodiversity: Inventory, Functions and Management*. 2015, Bishen Singh Mahendra Pal Singh, p.173.

Cheng, W.; Ng, C. Predicting Relative Protein Affinity of Novel Per- and Polyfluoroalkyl Substances (PFASs) by An Efficient Molecular Dynamics Approach. *Environ. Sci. Technol.* **2018**, *52*, 7972–7980.

Fasano, W. J.; Carpenter, S. C.; Gannon, S. A.; Snow, T. A.; Stadler, J. C.; Kennedy, G. L.; Buck, R. C.; Korzeniowski, S. H.; Hinderliter, P. M.; Kemper, R. A. Absorption, distribution, metabolism and elimination of 8:2 fluorotelomer alcohol in the rat. *Toxicol. Sci.* **2006**, *91*, 341–355.

Sánchez-Hernández, J. C.; Wheelock, C. E. Tissue distribution, isozyme abundance and sensitivity to chlorpyrifos-oxon of carboxylesterases in the earthworm *Lumbricus terrestris*. *Environ. Pollut.* **2009**, *157*, 264–272.

Benskin, J. P.; Holt, A.; Martin, J. W. Isomer-specific biotransformation rates of a perfluorooctane sulfonate (PFOS)-precursor by cytochrome P450 isozymes and human liver microsomes. *Environ. Sci. Technol.* **2009**, *43*, 8566–8572.

Lee, K.E. *Earthworms: Their Ecology and Relationships with Soils and Land Use*. Academic Press, New York (1985).

OECD (2010), Test No. 317: Bioaccumulation in Terrestrial Oligochaetes, OECD Guidelines for the Testing of Chemicals, Section 3, OECD Publishing, Paris, <https://doi.org/10.1787/9789264090934-en>.

OECD (2012), Test No. 305: Bioaccumulation in Fish: Aqueous and Dietary Exposure, OECD Guidelines for the Testing of Chemicals, Section 3, OECD Publishing, Paris, <https://doi.org/10.1787/9789264185296-en>.

Belfroid, A.; Meiling, J.; Sijm, D.; Hermens, J.; Seinen, W.; Van Gestel, K. Uptake of hydrophobic halogenated aromatic hydrocarbons from food by earthworms (*Eisenia andrei*). *Arch. Environ. Contam. Toxicol.* **1994**, *27*, 260–265.

Ding, J.; Lu, G.; Liu, J.; Yang, H.; Li, Y. Uptake, depuration, and bioconcentration of two pharmaceuticals, roxithromycin and propranolol, in *Daphnia magna*. *Ecotoxicol. Environ. Saf.* **2016**, *126*, 85–93.

Wen, B.; Zhang, H.; Li, L.; Hu, X.; Liu, Y.; Shan, X.; Zhang S. Bioavailability of perfluorooctane sulfonate (PFOS) and perfluorooctanoic acid (PFOA) in biosolids-amended soils to earthworms (*Eisenia fetida*). *Chemosphere* **2015**, *118*, 361–366.

Roots, B. I. The water relations of earthworms. I. The activity of the nephridistome cilia of *Lumbricus terrestris* L. and *Allobophora chlorotica* (Sav.) in relation to the concentration of the bathing medium. *J. Exp. Biol.* **1955**, *32*, 765–774.

Wolf, A. V. Paths of water exchange in the earthworm. *Physiol. Zool.* **1940**, *13*, 294–308.

Jeon, J.; Kannan, K.; Lim, H. K.; Moon, H. B.; Ra, J. S.; Kim, S. D. Bioaccumulation of perfluorochemicals in pacific oyster under different salinity gradients. *Environ. Sci. Technol.* **2010**, *44*, 2695–2701.

Rault, M.; Mazzia, C.; Capowiez, Y. Tissue distribution and characterization of cholinesterase activity in six earthworm species. *Comp. Biochem. Physiol. B: Biochem. Mol. Biol.* **2007**, *147* (2), 340–346.

APPENDICES

Appendix A

Table A-1. Filter adsorption study of PFOA, PFOAB and PFOAAmS

PFASs	Theoretical Concentration of Control (μM)	Group 1* (μM)	Group 2* (μM)	Concentration decreasing rate between Group 1 and 2 (%)
PFOAAmS	2	0.95	0.45	52.5
	5	1.77	1.82	-2.6
	10	6.24	4.49	28.0
	15	10.20	8.53	16.4
PFOAB	0.8	0.30	0.92	-211.5
	2	1.14	1.58	-38.4
	8	6.38	6.84	-7.2
	15	11.10	13.00	-17.1
	20	13.91	17.01	-22.3
PFOA	0.4	0.68	0.72	-6.5
	1	1.60	1.50	6.6
	2	2.89	2.79	3.7
	4	5.46	5.40	1.1
	10	10.75	10.25	4.6

*The sample in Group 1 was taken directly to the HPLC vial without filtered.

*The sample in Group 2 was filtered by the nylon filter to the HPLC vial.

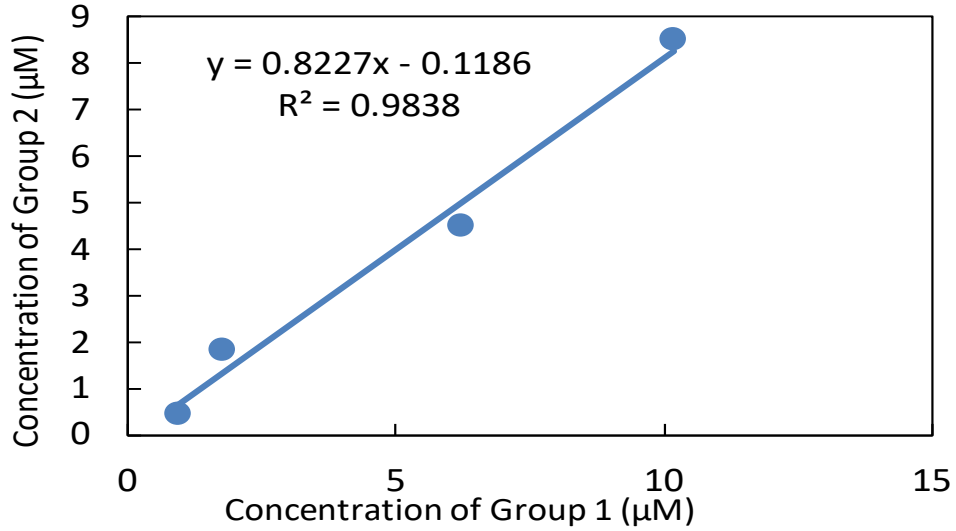


Figure A-1. Relationships for PFOAAmS concentrations between Group 1 and Group 2 (the equation in the figure was used to correct concentrations of PFOAAmS control group).

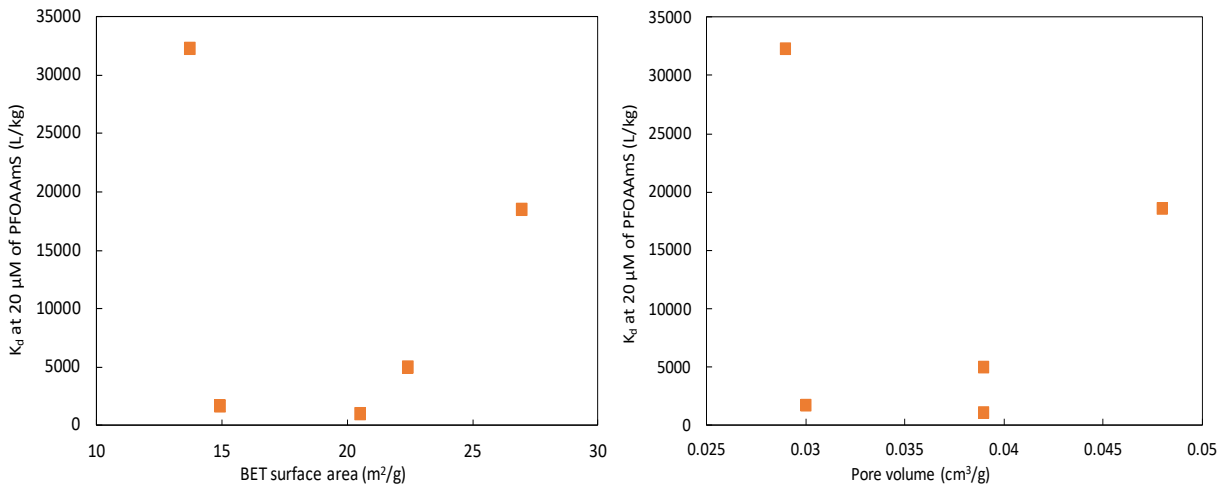


Figure A-2. Dependence of distribution coefficient (K_d) of PFOAAmS at 20 µM on the N₂ BET surface area and pore volume of soils.

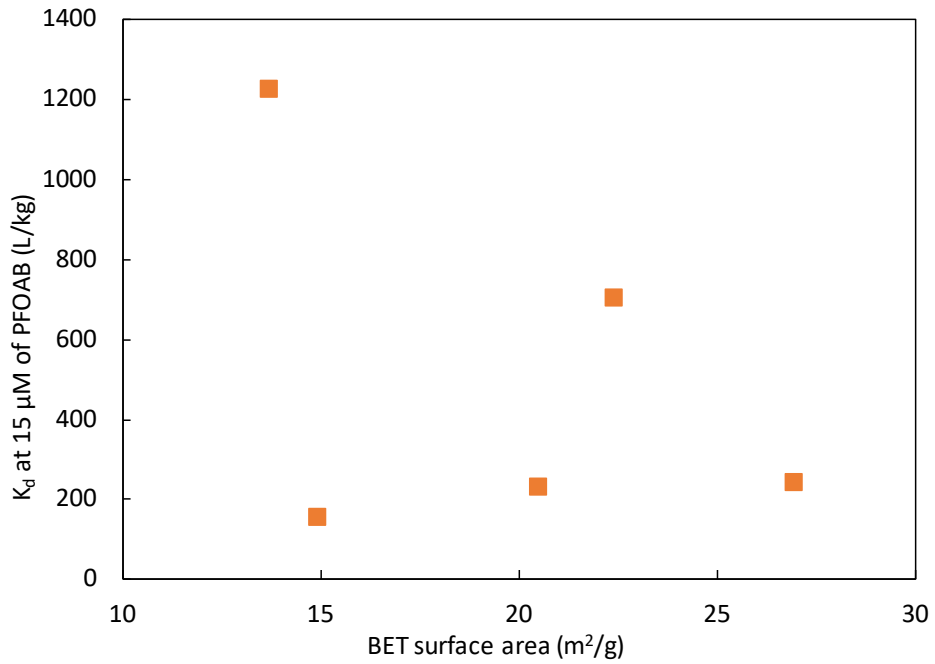
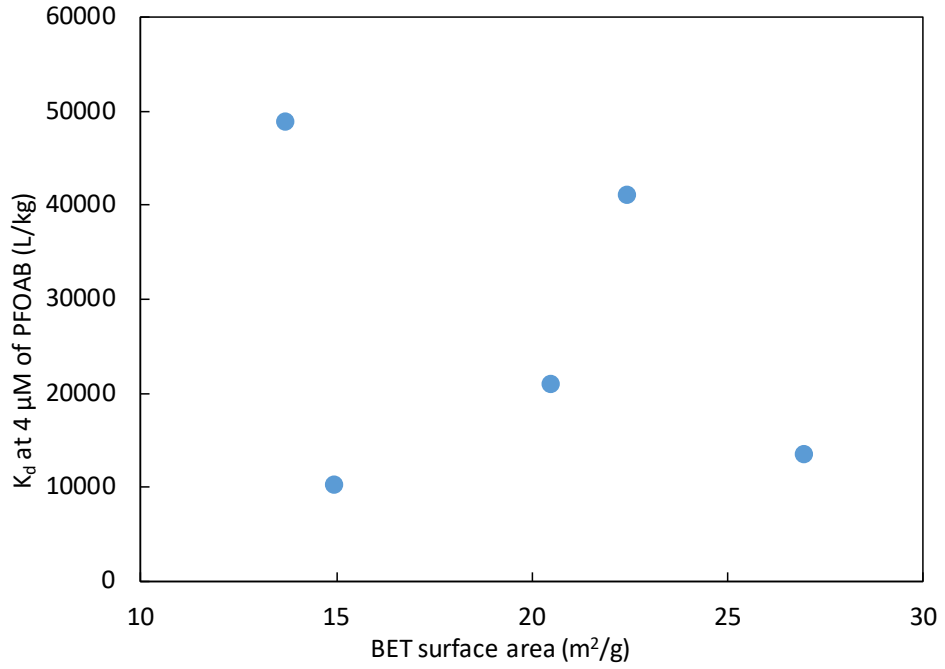


Figure A-3. Dependence of distribution coefficient (K_d) of PFOAB (4 μ M and 15 μ M) on the N_2 BET surface area of soils.

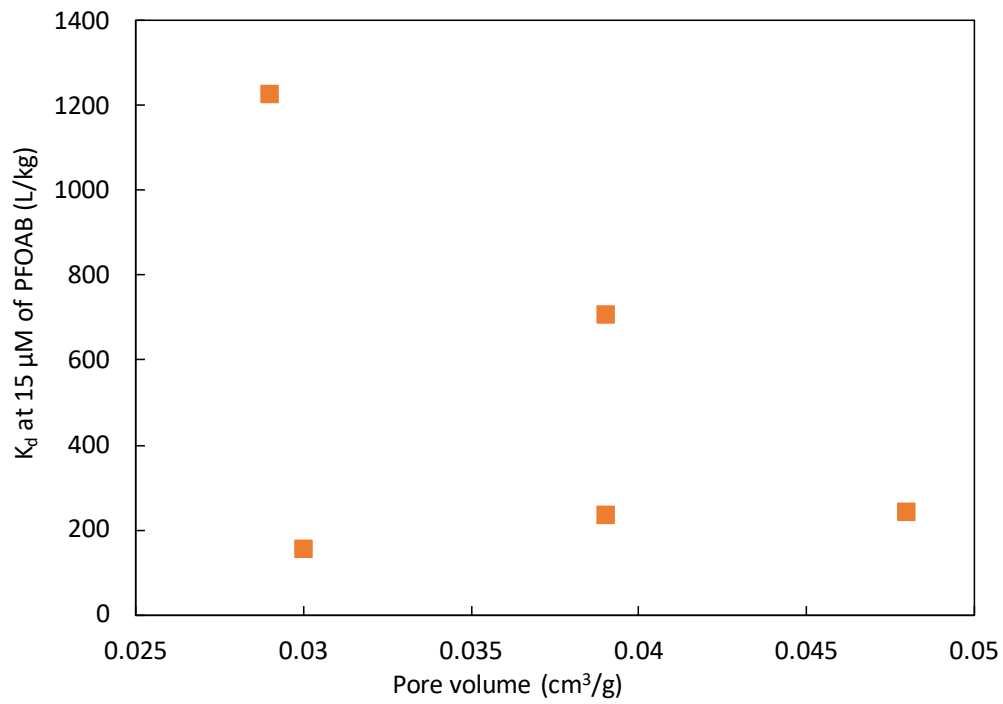
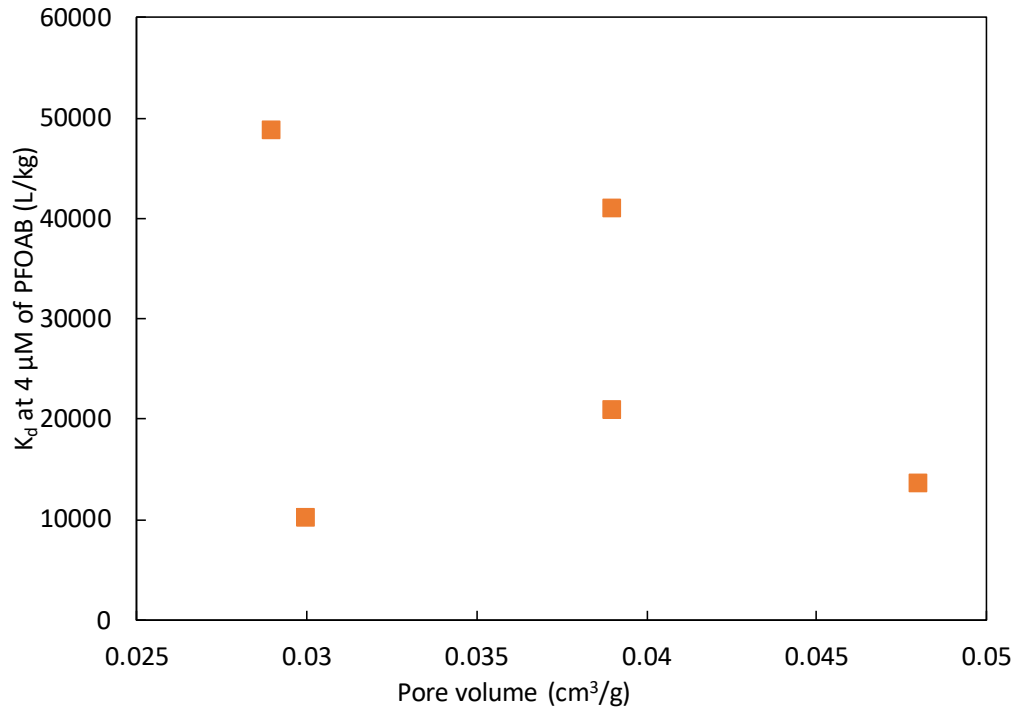


Figure A-4. Dependence of distribution coefficient (K_d) of PFOAB (4 μM and 15 μM) on the soil pore volumes.

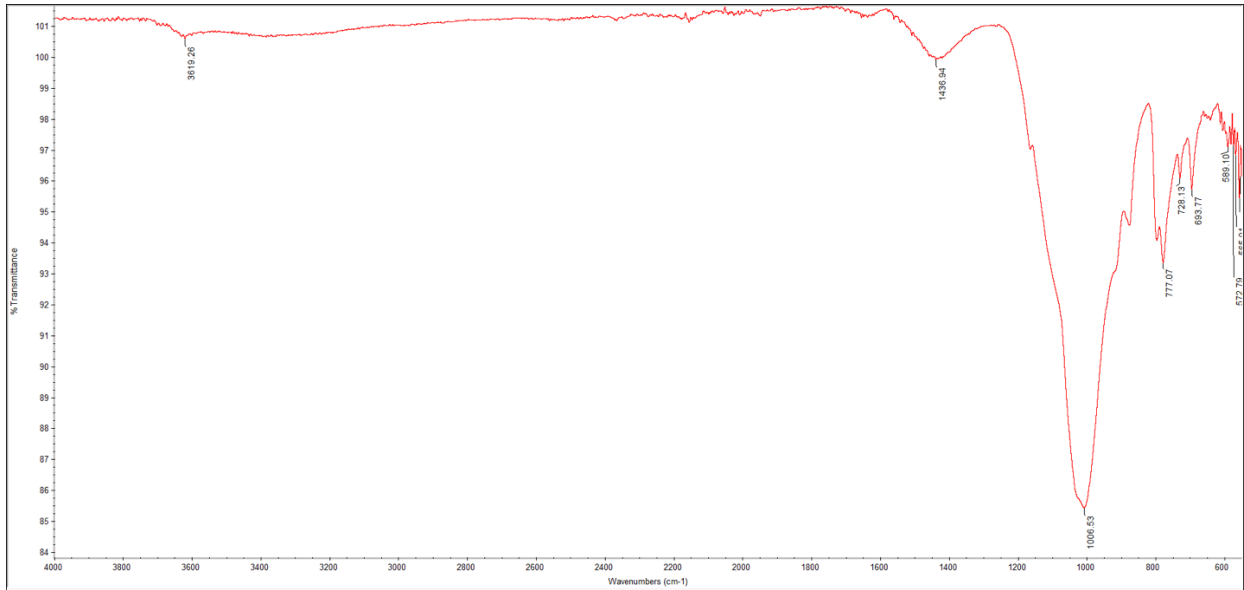


Figure A-5. FT-IR result of raw SW soil.

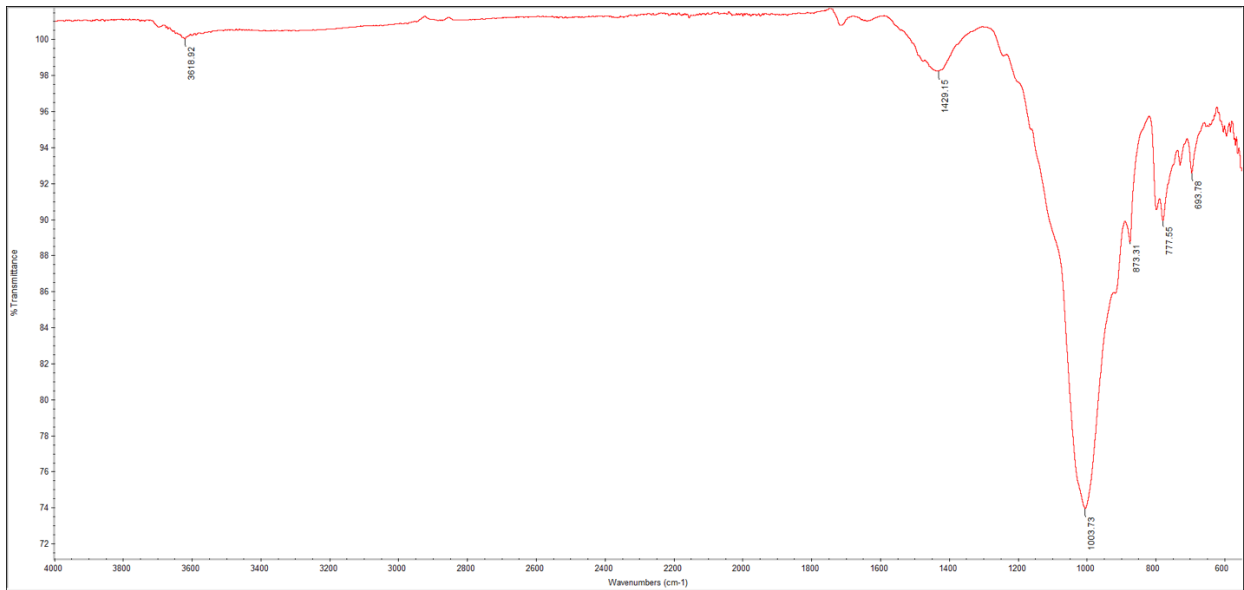


Figure A-6. FT-IR result of post-adsorption SW soil for PFOAaMS.

Table A-2. Predicted PFAS concentrations in the solid phase for adsorption (q_e^s)

PFASs		UND	SW	NF	BS	CE
PFOA (μM)	0.01	0.0514	0.0871	0.0414	0.0717	0.159
	0.1	0.491	1.02	0.414	0.805	1.63
	1	4.69	12.0	4.14	9.03	16.7
	10	44.8	141	41.4	101	171
PFOAB (μM)	0.01	159	57.2	269	87.8	259
	0.1	332	154	512	124	440
	1	693	415	973	175	747
	10	1448	1116	1851	247	1268
PFOAAmS (μM)	0.01	4500	9128	619	272	1268
	0.1	5797	23464	1003	473	2361
	1	7468	60311	1627	823	4396
	10	9621	155023	2639	1430	8186

Table A-3. Predicted PFAS concentrations in the solid phase for desorption (q_e^d)

PFASs		UND	SW	NF	BS	CE
PFOA (μM)	0.01	0.207	0.363	0.375	0.397	1.18
	0.1	0.947	2.76	1.88	2.81	4.90
	1	4.33	20.9	9.41	19.9	20.4
	10	19.8	159	47.2	141	85.2
PFOAB (μM)	0.01	158	869	662	172	664
	0.1	346	4887	1258	344	1522
	1	756	27479	2390	686	3486
	10	1654	154526	4539	1369	7986
PFOAAmS (μM)	0.01	2515	17274	591	326	1900
	0.1	4371	30019	937	504	3152
	1	7596	52167	1485	781	5232
	10	13200	90656	2354	1210	8683

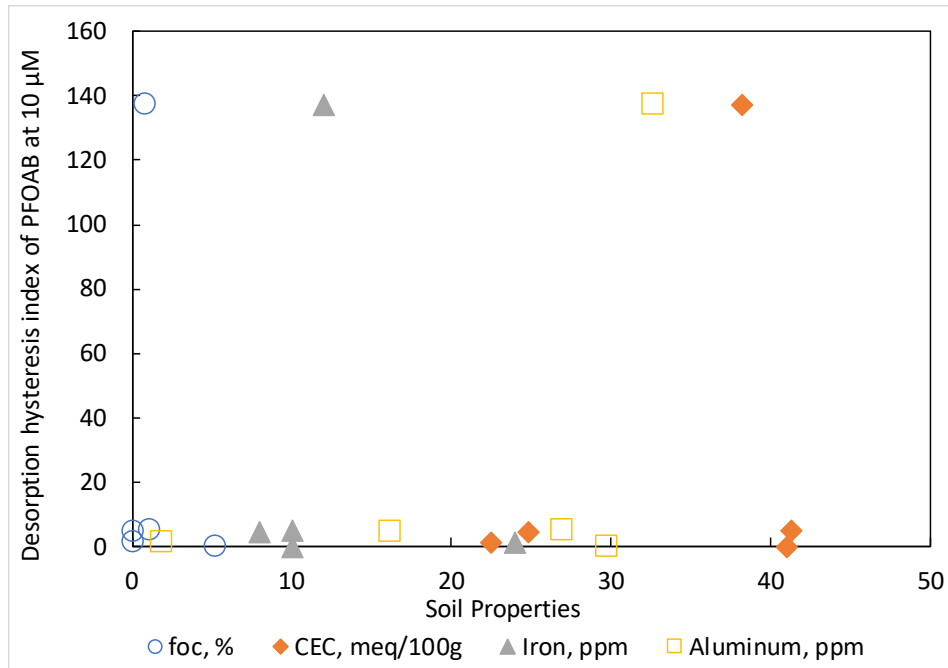


Figure A-7. The desorption hysteresis index of PFOAB at 10 µM versus the fraction of soil organic matter, CEC, Iron, and Aluminum, respectively.

Appendix B

Table B-1. Paired Samples t-Test for all six PFASs

		Paired Differences					t	df	Sig. (2-tailed)
		Mean	Std. Deviation	Std. Error Mean	95% Confidence Interval of the Difference				
					Lower	Upper			
Pair 1	Head - Tail	2.42809	5.31169	1.25198	-.21335	5.06953	1.939	17	.069

Table B-2. Paired Samples t-Test for four poly-PFASs

		Paired Differences					t	df	Sig. (2-tailed)
		Mean	Std. Deviation	Std. Error Mean	95% Confidence Interval of the Difference				
					Lower	Upper			
Pair 1	Head - Tail	3.86685	5.63373	1.62632	-.28735	7.44635	2.378	11	.037

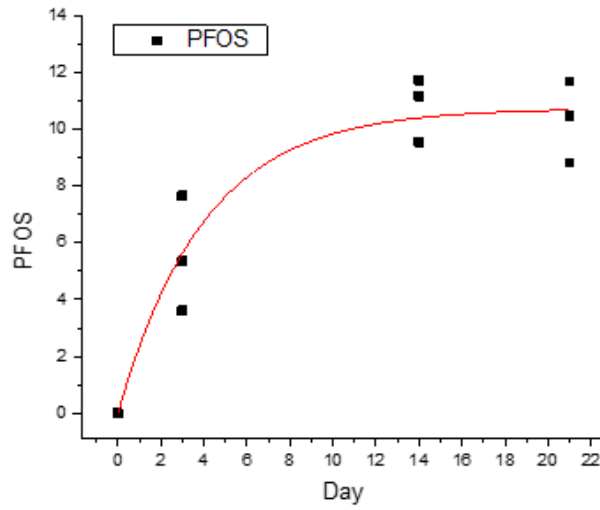
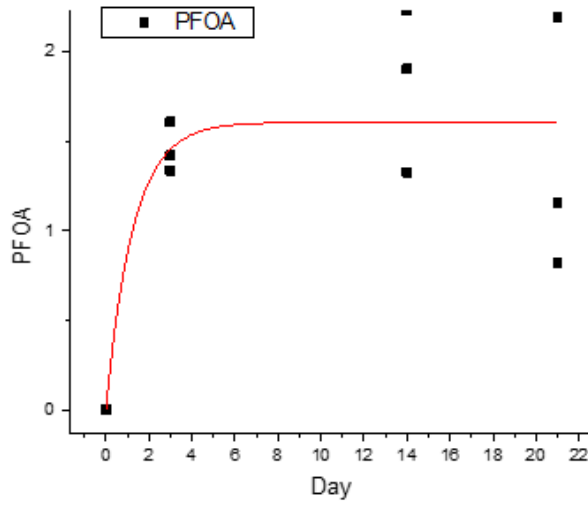


Figure B-1. Uptake fitting curves of PFOA and PFOS in the second experiment.

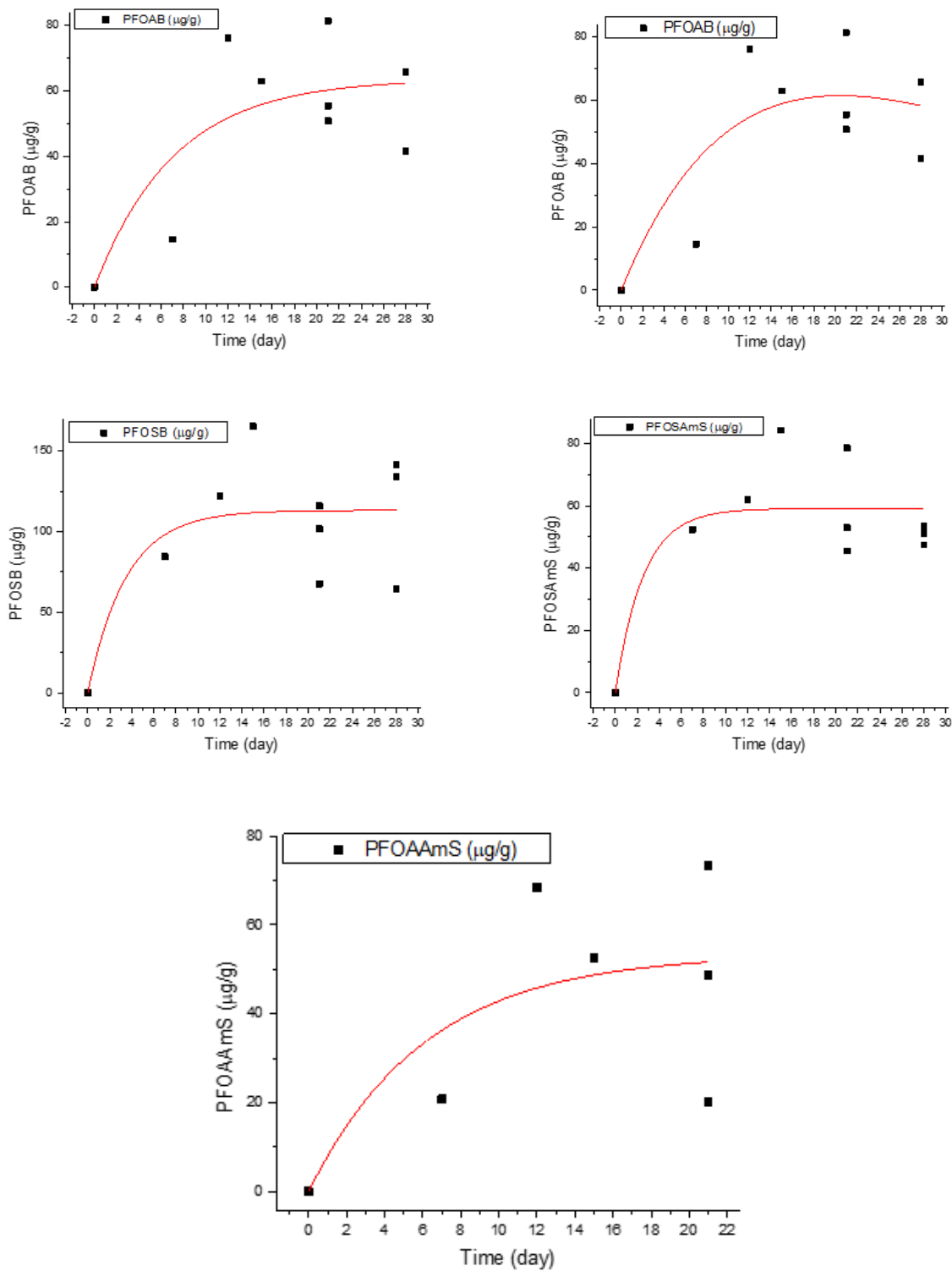


Figure B-2. Uptake fitting curves of four poly-PFASs in the first experiment.

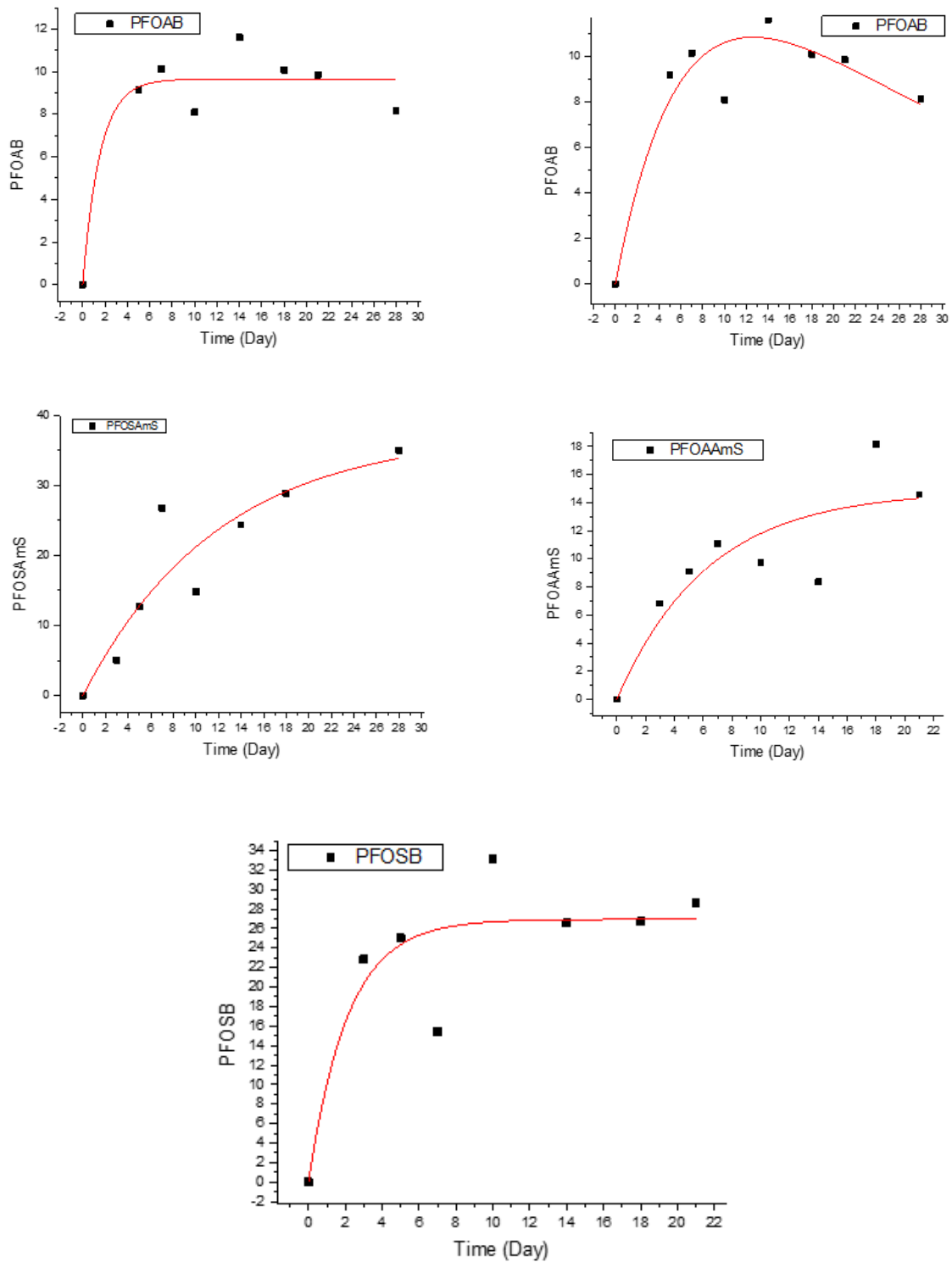


Figure B-3. Uptake fitting curves of four poly-PFASs in the second experiment.

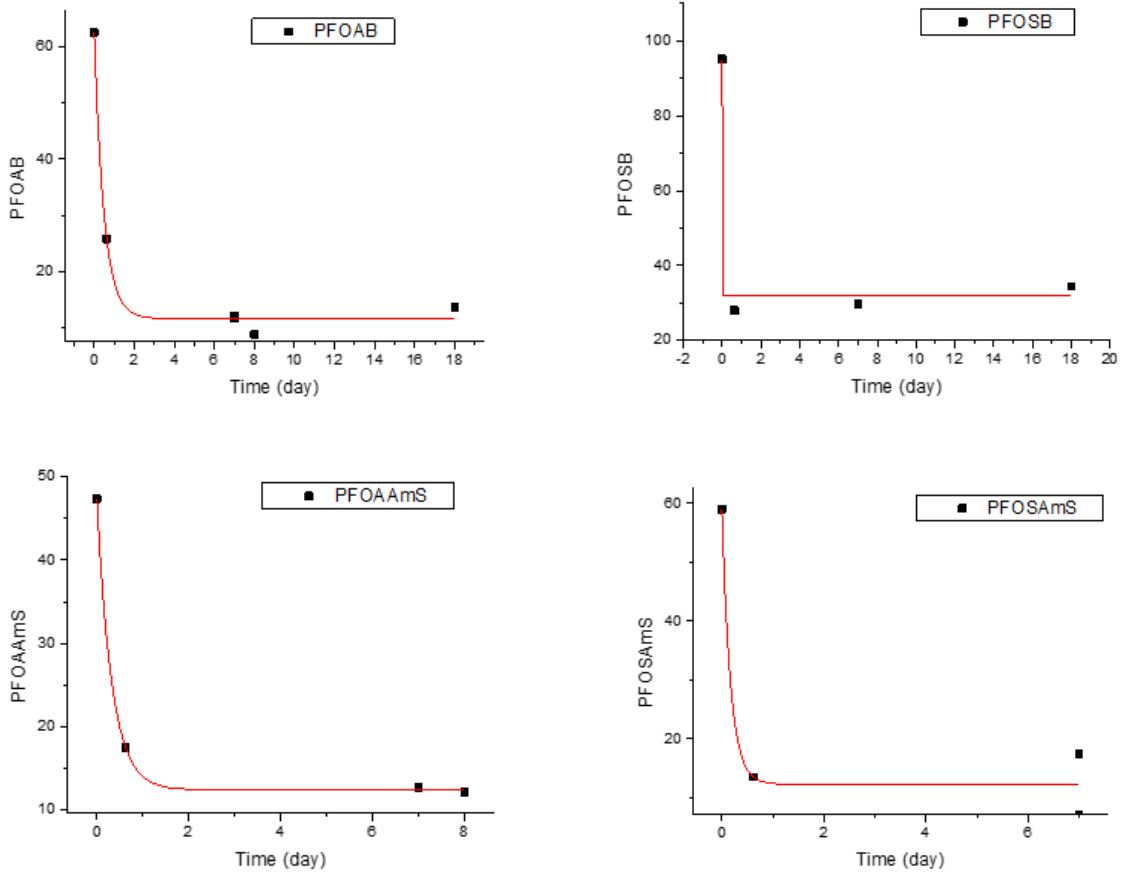


Figure B-4. Elimination fitting curves of four poly-PFASs in the first experiment.

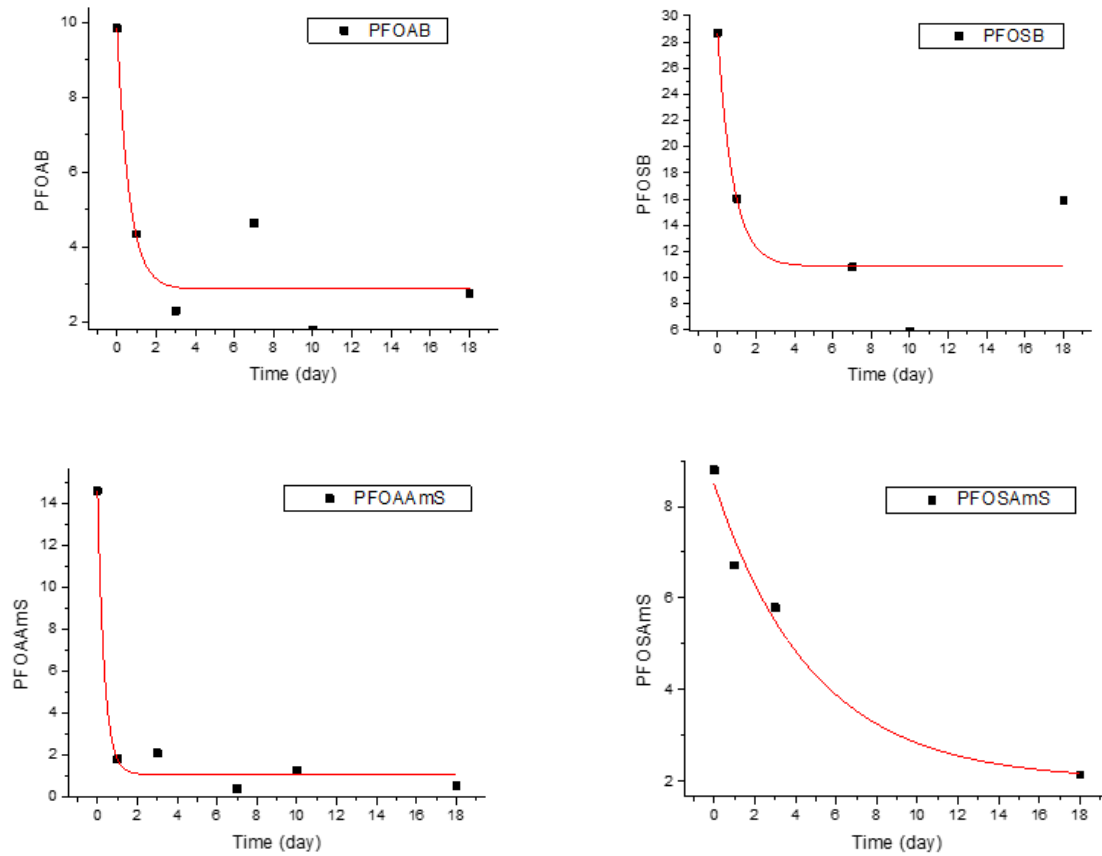


Figure B-5. Elimination fitting curves of four poly-PFASs in the second experiment.

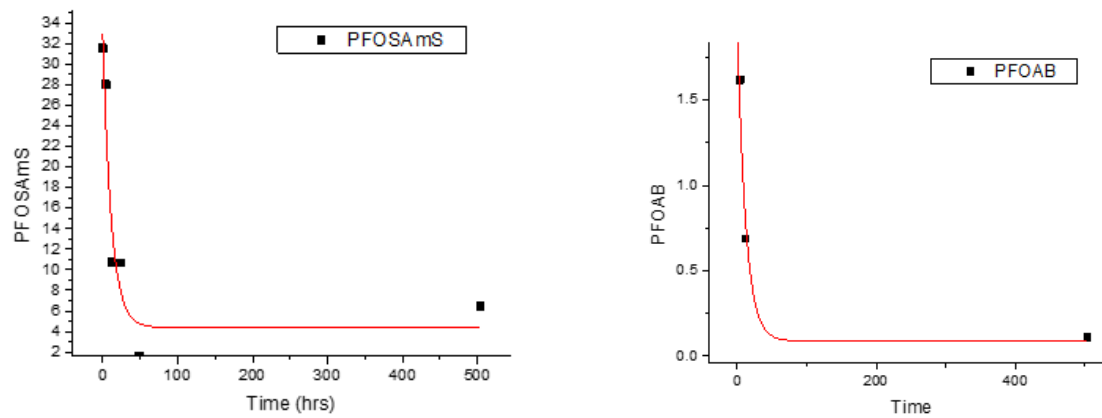


Figure B-6. Elimination fitting curves of PFOAB and PFOSAmS in the additional experiment.

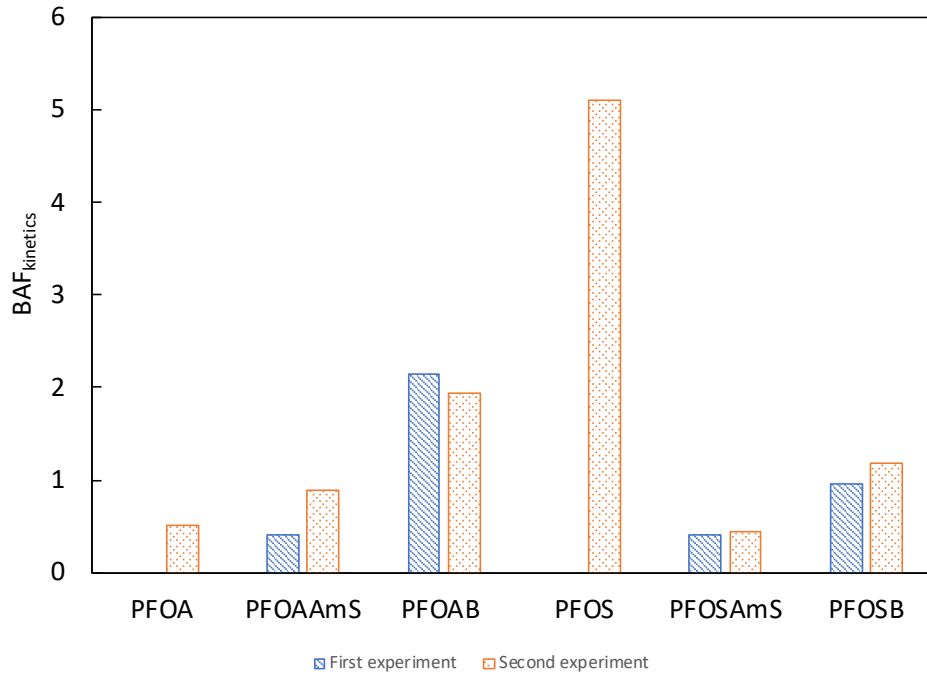


Figure B-7. Kinetic BAF values in the first and the second bioaccumulation experiment.